Cosa è la Spintronica?

Valentin Alek Dediu

Consiglio Nazionale Delle Ricerche
ISMN, via Gobetti 101, Bologna, ITALY

ISMN-CNR

People from ISMN involved

Spintronic Dev. Lab

<u>V. Alek Dediu</u>

I. Bergenti

L. Hueso

E. Lunedei

A. Riminucci

P. Graziosi (Ph. D)

C. Newby

F. Bona

S. Rose (tecn)

Nanotechnology Lab

F. Biscarini
M. Cavallini

Spectroscopy Lab

G. Ruani
M. Murgia
P. Nozar

Strong support from

Prof. Carlo TALIANI

Nobel prize 2007 in Physics

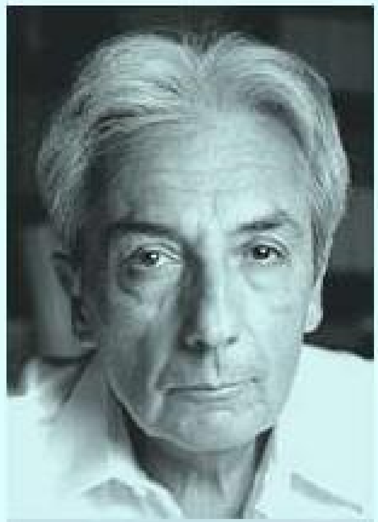

Photo: B. Fert, Invisuphoto

Albert Fert

1/2 of the prize

France

Université Paris-Sud;
Unité Mixte de Physique
CNRS/THALES
Orsay, France

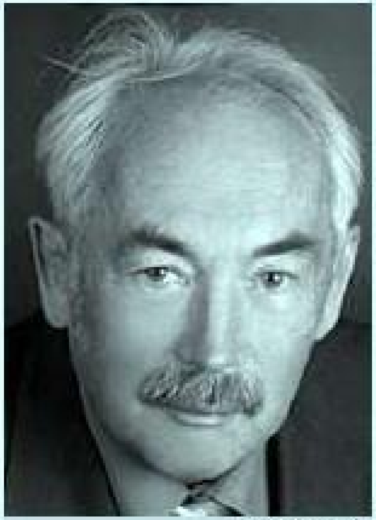

Photo: ©
Forschungszentrum Jülich

Peter Grünberg

1/2 of the prize

Germany

Forschungszentrum Jülich
Jülich, Germany

L’elettrone: la carica e lo spin

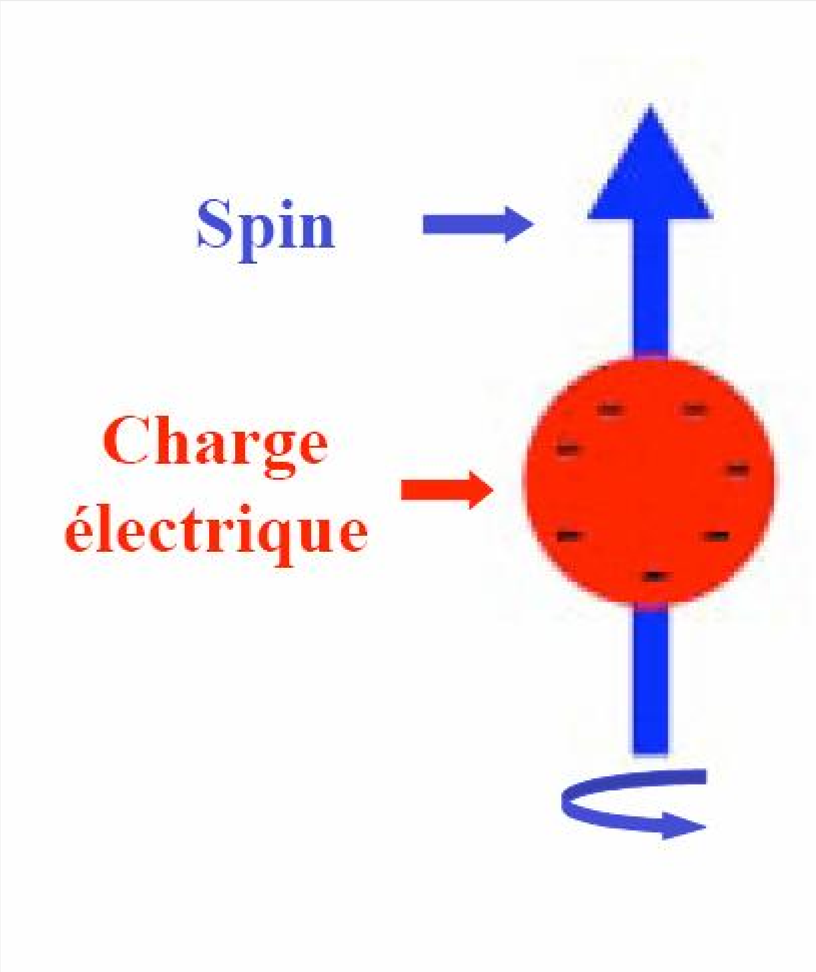

What is Spintronics?

Spintronics is a new branch of electronics based on purely quantum effects, where the information is stored, transmitted and read via electrical carrier spin orientation.
It requires an artificial manipulation of the spins orientation

SI = spin polarized injector
ST = spin polarized transporter
SA = spin analyzer
Ls = spin diffusion length

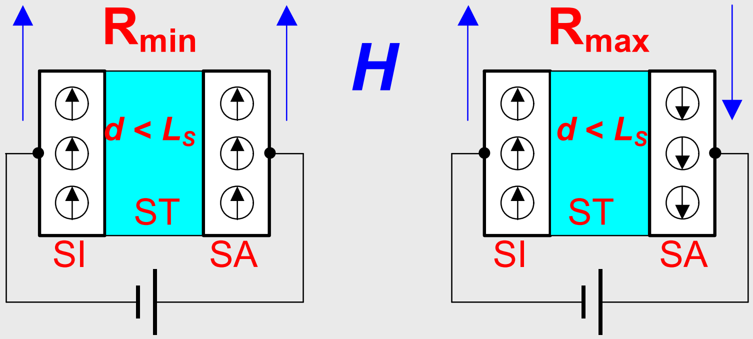

Spin valve

Is Spin Polarized injection POSSIBLE?

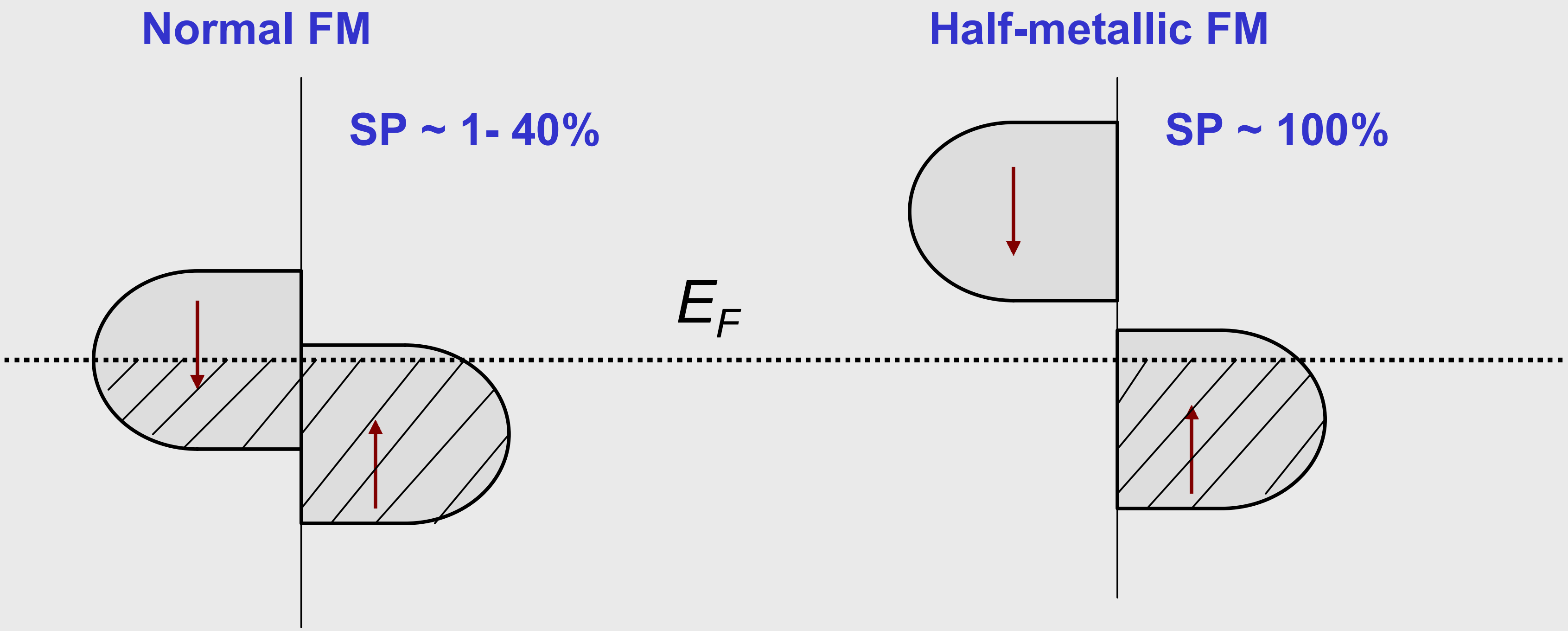

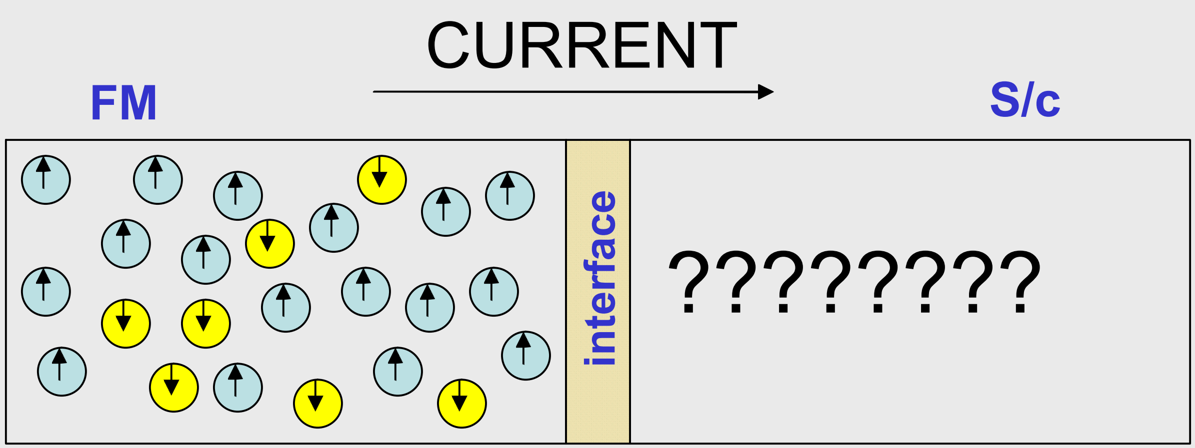

Anysotropic Magnetoresistance (AMR): William Thomson, 1856

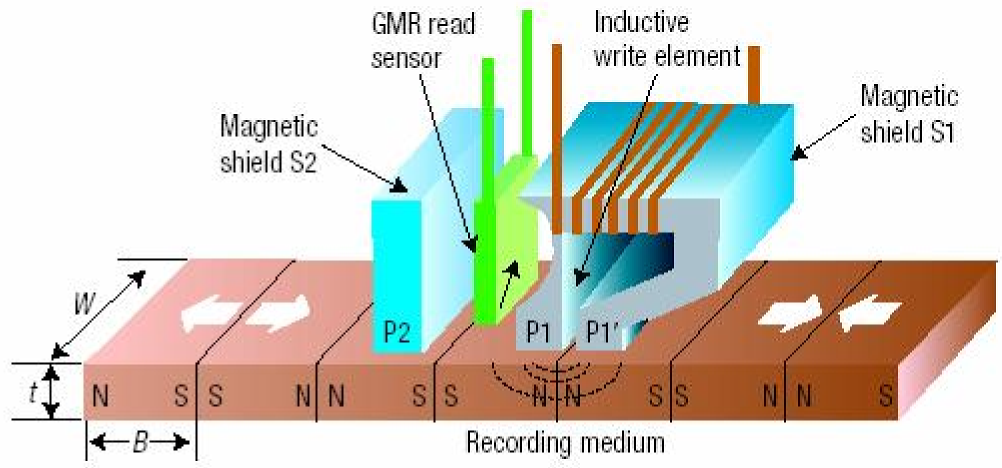

Figure 1 Magnetoresistive head for hard-disk recording. Schematic structure of the magnetoresistive head introduced by IBM for its hard disk drives in 1991. A magnetic sensor based on anisotropic magnetoresistance (left) is added to the inductive 'ring-type' head (right) still used for writing. The distances P1–P1′ and P1–P2 between the pole pieces of the magnetic shields S1 and S2 define respectively the 'write' and 'read' gaps, on which depends the minimum length *B* of the magnetic domains. *W* is the track width and *t* is the thickness of the recording medium. Note that in today's hard disk recording, *W* and *B* are of the order of 100 nm and 30 nm respectively, but with a different arrangement of head and domains in 'perpendicular recording'[1].

Anysotropic Magnetoresistance (AMR): the nature

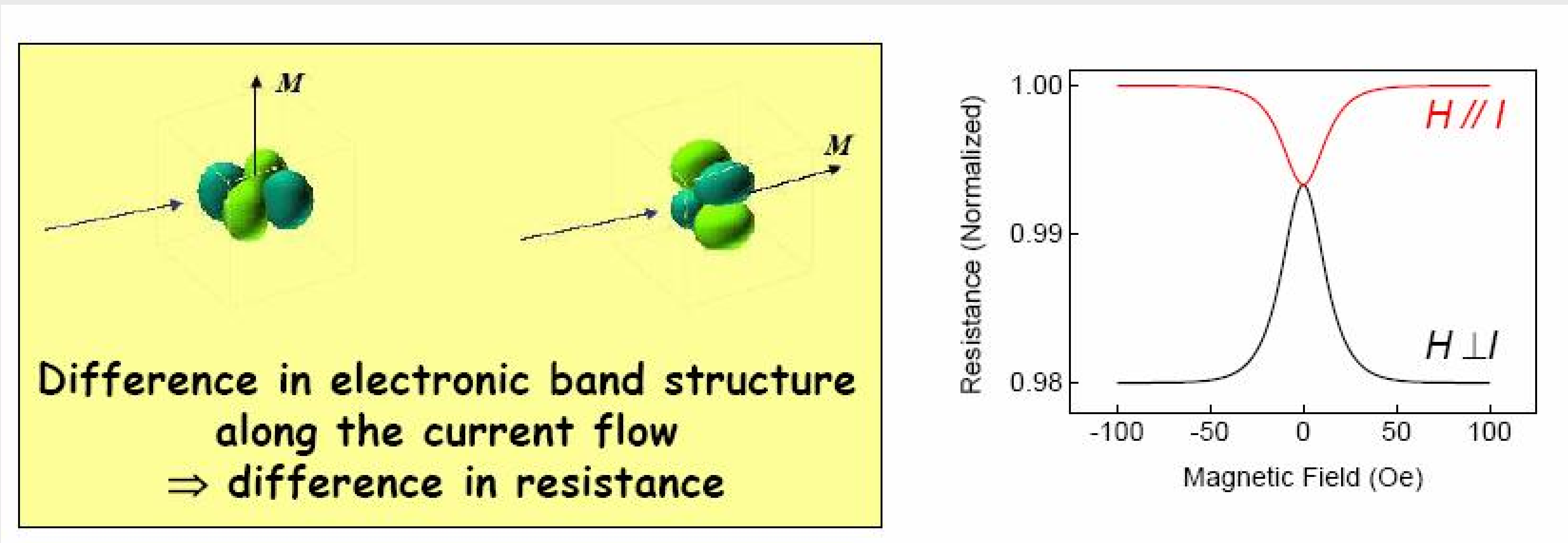

Non è basato sulla polarizzazione degli spin

Comincia l'era dello spin polarizzato

RAPID COMMUNICATIONS

PHYSICAL REVIEW B VOLUME 39, NUMBER 7 1 MARCH 1989

Enhanced magnetoresistance in layered magnetic structures with antiferromagnetic interlayer exchange

G. Binasch, P. Grünberg, F. Saurenbach, and W. Zinn

Institut für Festkörperforschung, Kernforschungsanlage Jülich G.m.b.H., Postfach 1913, D-5170 Jülich, West Germany

(Received 31 May 1988; revised manuscript received 12 December 1988)

Enhanced magnetoresistance in layered magnetic structures with antiferromagnetic interlayer exchange

G. Binasch, P. Grünberg, F. Saurenbach, and W. Zinn

Institut für Festkörperforschung, Kernforschungsanlage Jülich G.m.b.H., Postfach 1913, D-5170 Jülich, West Germany

(Received 31 May 1988; revised manuscript received 12 December 1988)

The electrical resistivity of Fe-Cr-Fe layers with antiferromagnetic interlayer exchange increases when the magnetizations of the Fe layers are aligned antiparallel. The effect is much stronger than the usual anisotropic magnetoresistance and further increases in structures with more than two Fe layers. It can be explained in terms of spin-flip scattering of conduction electrons caused by the antiparallel alignment of the magnetization.

Currently there is much interest in layered magnetic structures, which is partly due to the prospect that layering can be used to modify the material properties or to obtain new properties, uncharacteristic for the bulk materials. In the past few years we have concentrated our research on exploration of the exchange coupling between different magnetic films and on the coupling of ferromagnetic films across nonmagnetic or antiferromagnetic interlayers. For practical reasons we have restricted the work to the most simple structure where this question can be investigated, i.e., a magnetic double layer consisting of two ferromagnetic films interspaced by a film of another material. A very interesting case which we found during the course of this work was double layers of Fe interspaced by Cr as sketched in Fig. 1. If these films are of reasonably good monocrystalline quality and if the thickness d_0 of the Cr film is approximately 1 nm, then we observed that the effective exchange coupling of the Fe layers across the Cr is antiferromagnetic (AF). This happens for epitaxial growth of the layered Fe-Cr-Fe structure both along the [100] and [110] crystallographic directions.[1-3]

Although the microscopic origin of this AF coupling up to now remains somewhat unclear, we found that such structures display some novel and unique magnetic properties both in their static and dynamic behavior.[1,2] The new feature we report on here and which also comes as a result of the AF coupling is a strong increase of the magnetoresistance effect. Usually magnetoresistance refers to the so-called anisotropic effect, i.e., the difference in resistivity $\Delta R = R_\parallel - R_\perp$ for currents flowing parallel ($R_\parallel$) and perpendicular ($R_\perp$) to the magnetization. As we show here, in layered structures with AF coupling a change in resistivity due to antiparallel alignment of the magnetizations in the ferromagnetic films can be observed. In the investigated cases it is much stronger than the anisotropic effect. It is clear that this is an attractive aspect for applications, such as magnetoresistive field sensors.

We have two methods available to recognize AF coupling, namely hysteresis curves measured via the magneto-optic Kerr effect (MOKE) and light scattering (LS) from spin waves. A more extensive description has been given elsewhere.[4] Here we will exploit the peculiar behavior of spin waves in the antiparallel aligned state as shown in Fig. 1. The spectra we show can be obtained only in this state and therefore can be used as a signature of it. The scattering geometry is also of importance because the observed waves have to propagate perpendicular to the sample magnetization J. Since the propagation direction is determined by the plane of incidence of the probing laser light this fact can be used to determine the direction of J. The direction of the externally applied field B_0 of course, is known. We will encounter two important cases: J is collinear with B_0 in the one and perpendicular to it in the other.

In order to be able to measure magnetoresistance of such samples, they were made in the shape of thin strips. The strip width was 1 mm, with a length of 10 mm. This is large enough to focus a laser beam onto the sample, which is necessary to apply the methods described above.

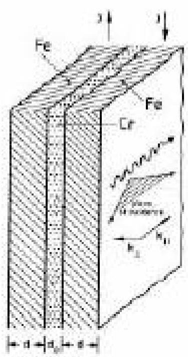

FIG. 1. Ferromagnetic double layer with antiparallel alignment of the magnetizations. Also indicated is the plane of incidence of the laser light for the observation of light scattering from spin waves and hysteresis curves via MOKE.

Resistance was measured with the usual four-point method with current and voltage leads on both ends of the strip. The samples were grown epitaxially on [110]-oriented GaAs by the well-established method[3] and hence the film plane is parallel to a (110) atomic plane. For the thickness d of the individual Fe films, we chose $d = 12$ nm and confirmed that the easy axis (EA) was along [100]. For smaller values of d one has to be careful because the EA can switch to a [110] direction.[4] In our case the [110] direction was the in-plane hard axis (HA). The long axis of the strip was parallel to a [100] direction and hence the EA of the sample. The Cr thickness was $d_0 = 1$ nm, which leads to AF coupling in agreement with previous results.[2,3] As a reference sample we also made a single Fe film with thickness $d = 25$ nm in order to measure, for comparison only, the anisotropic magnetoresistance (MR) effect. Morphology and composition during growth of the samples were monitored by means of spin-polarized low-energy electron-diffraction and Auger analysis.

In Figs. 2(a) and 2(b) we see the MOKE hysteresis loops from the double layers with AF coupling for B_0 along the EA and HA. The directions of the magnetization are indicated by the encircled pairs of arrows. This information is obtained from the MOKE intensities and the displayed LS spectra. Let us discuss as an example the hysteresis loop shown in Fig. 2(a) in more detail. The field B_0 is applied along the EA, which is the long axis of the strip. It is clear that for large enough B_0 the samples saturate in the field direction (parallel alignment). If we start with parallel alignment in the positive field direction and reduce B_0 then at a certain, but still positive value of B_0, the magnetization of one film reverses via domain-wall motion (point 1). Hence in small fields we have antiparallel alignment. In a negative field, at point 2, the other film also reverses, and we have saturation. Points 3 and 4 mark the magnetization reversals when B_0 is scanned back. From the size of the MOKE signal at points 1–4 one learns which of the two films reverses the magnetization. The larger change is due to the upper film. We see that in Fig. 2(a) the lower film always reverses first, independent of the direction of the field scan. We also had samples where the upper film always reversed first. Obviously, this is caused by slightly different coercive fields of the two Fe films. In the low-field regime, light scattering from spin waves has been performed and the spectra are also displayed. A typical feature of these spectra is the fact that Stokes and anti-Stokes scattering is observed at different frequencies. As has been explained in more de-

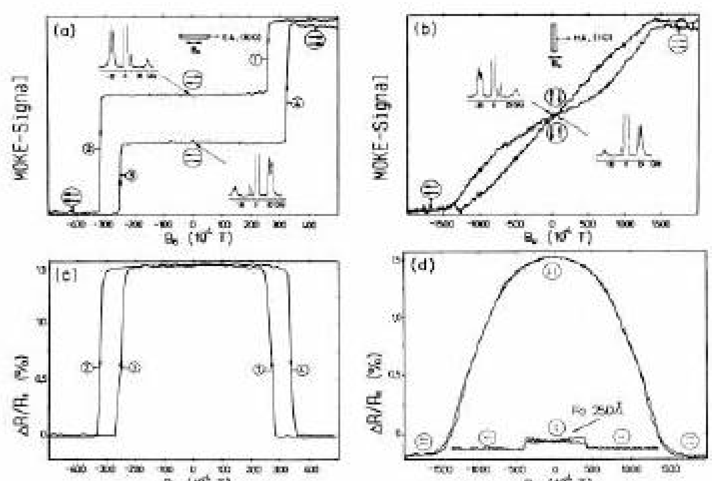

FIG. 2. (a)–(b) MOKE hysteresis curves and (c)–(d) magnetoresistance $\Delta R/R_s = (R - R_s)/R_s$ from Fe double layers with antiferromagnetic coupling. Also, (d) displays the anisotropic MR effect of a 250-Å-thick Fe film.

Comincia l'era dello spin polarizzato

VOLUME 61, NUMBER 21 PHYSICAL REVIEW LETTERS 21 NOVEMBER 1988

Giant Magnetoresistance of (001)Fe/(001)Cr Magnetic Superlattices

M. N. Baibich,[a] J. M. Broto, A. Fert, F. Nguyen Van Dau, and F. Petroff
Laboratoire de Physique des Solides, Université Paris-Sud, F-91405 Orsay, France

P. Eitenne, G. Creuzet, A. Friederich, and J. Chazelas
Laboratoire Central de Recherches, Thomson CSF, B.P. 10, F-91401 Orsay, France

(Received 24 August 1988)

VOLUME 61, NUMBER 21

Giant Magnetoresistance of (001)Fe/(001)Cr Magnetic Superlattices

M. N. Baibich,[a] J. M. Broto, A. Fert, F. Nguyen Van Dau, and F. Petroff
Laboratoire de Physique des Solides, Université Paris-Sud, F-91405 Orsay, France

P. Eitenne, G. Creuzet, A. Friederich, and J. Chazelas
Laboratoire Central de Recherches, Thomson CSF, B.P. 10, F-91401 Orsay, France
(Received 24 August 1988)

We have studied the magnetoresistance of (001)Fe/(001)Cr superlattices prepared by molecular-beam epitaxy. A huge magnetoresistance is found in superlattices with thin Cr layers. For example, with $t_{Cr} = 9$ Å, at $T = 4.2$ K, the resistivity is lowered by almost a factor of 2 in a magnetic field of 2 T. We ascribe this giant magnetoresistance to spin-dependent transmission of the conduction electrons between Fe layers through Cr layers.

PACS numbers: 75.50.Rr, 72.15.Gd, 75.70.Cn

There is now considerable interest in the study of multilayers composed of magnetic and nonmagnetic metals and great advances have been obtained in the understanding of their magnetic properties.[1-4] Recently the transport properties of magnetic multilayers and thin films have been investigated and have revealed interesting properties resulting from the interplay between electron transport and magnetic behavior.[5-7] In this Letter we present magnetoresistance measurements on (001)Fe/(001)Cr superlattices prepared by molecular-beam epitaxy (MBE). In superlattices with thin Cr layers, the magnetoresistance is very large (a reduction of the resistivity by a factor of about 2 is observed in some samples). This giant magnetoresistance raises exciting questions and moreover is promising for applications.

The (001)Fe/(001)Cr bcc superlattices have been grown by MBE on (001) GaAs substrates under the following conditions: The residual pressure of the MBE chamber was 5×10^{-11} Torr, the substrate temperature was generally around 20 °C, the deposition rate was about 0.6 Å/s for Fe and 1 Å/s for Cr. This deposition rate was obtained by use of specially designed evaporation cells in which a crucible of molybdenum is heated by electron bombardment. The individual layer thicknesses range from 9 to 90 Å and the total number of bilayers is generally around 30. The growth of the superlattices and their characterization by reflection high-energy electron diffraction, Auger-electron spectroscopy, x-ray diffraction, and scanning-transmission-electron microscopy have been described elsewhere.[8] Note that the Cr (Fe) Auger line disappears during the growth of a Fe (Cr) layer. This, as well as the main features of the scanning-transmission-electron-microscopy cross sections, rules out a deep intermixing of Fe and Cr.[8] However, the Auger effect, which averages the concentrations over a depth of about 12 Å, cannot probe the interface roughness at the atomic scale. Surface extended x-ray-absorption fine-structure experiments have been started to probe this roughness more precisely.

The magnetic properties of the Fe/Cr superlattices have been investigated by magnetization and torque measurements.[9] The magnetization is in the plane of the layers and an antiferromagnetic (AF) coupling between the adjacent Fe layers is found when the Cr thickness t_{Cr} is smaller than about 30 Å.[9] A signature of this AF interlayer coupling is shown in Fig. 1: As the Cr thickness decreases below 30 Å, the hysteresis loop is progressively tilted. For example, with $t_{Cr} = 9$ Å, a field $H_S \approx 2$ T is needed to overcome the antiferromagnetic coupling and to saturate the magnetization at about the bulk Fe value. When the applied field is decreased to zero, the AF coupling brings the magnetization back to about zero. As can be seen from the variation of the low-field slopes in Fig. 1, the AF coupling steeply increases when t_{Cr} decreases from 30 to 9 Å. The existence of such AF couplings has already been found in Fe/Cr sandwiches by the light-scattering and magneto-optical measurements

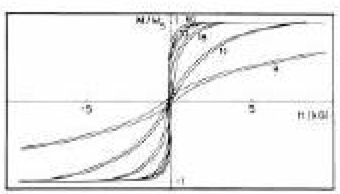

FIG. 1. Hysteresis loops at 4.2 K with an applied field along [110] in the layer plane for several (001)Fe/(001)Cr superlattices: [(Fe 60 Å)/(Cr 60 Å)]$_5$, [(Fe 30 Å)/(Cr 30 Å)]$_{10}$, [(Fe 30 Å)/(Cr 18 Å)]$_{30}$, [(Fe 30 Å)/(Cr 12 Å)]$_{30}$, [(Fe 30 Å)/(Cr 9 Å)]$_{40}$, where the subscripts indicate the number of bilayers in each sample. The number beside each curve represents the thickness of the Cr layers.

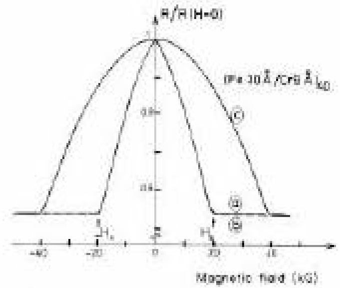

FIG. 2. Magnetoresistance of a [(Fe 30 Å)/(Cr 9 Å)]$_{40}$ superlattice at 4.2 K. The current is along [110] and the field is in the layer plane along the current direction (curve a), in the layer plane perpendicular to the current (curve b), or perpendicular to the layer plane (curve c). The resistivity at zero field is 54 μΩ cm. There is a small difference between the curves in increasing and decreasing field (hysteresis) that we have not represented in the figure. The superlattice is covered by a 100-Å Ag protection layer. This means that the magnetoresistance of the superlattice alone should be slightly higher.

of Grünberg *et al.*[1] and by the spin-polarized low-energy electron-diffraction experiments of Carbone and Alvarado.[10] The AF coupling between the Fe layers has been ascribed to indirect exchange interactions through the Cr layers, but a theoretical model of these interactions is still lacking.[4,9]

The magnetoresistance of the Fe/Cr superlattices has been studied by a classical ac technique on small rectangular samples. Examples of magnetoresistance curves at 4.2 K are shown in Figs. 2 and 3. The resistance decreases during the magnetization process and becomes practically constant when the magnetization is saturated. The curves *a* and *b* in Fig. 2 are obtained for applied fields in the plane of layers in the longitudinal and transverse directions, respectively. The field H_S is the field needed to overcome the AF couplings and to saturate the magnetization (compare with Fig. 1). In contrast, fields applied perpendicularly to the layers (curve *c*) have to overcome not only the AF coupling but also the magnetic anisotropy, so that the magnetoresistance is saturated at a field higher than H_S.

The most remarkable result exhibited in Figs. 2 and 3 is the huge value of the magnetoresistance. For $t_{Cr} = 9$ Å and $T = 4.2$ K, see Fig. 2, there is almost a factor of 2 between the resistivities at zero field and in the saturated state, respectively (in absolute value, the resistivity change is about 23 μΩ cm). By comparison of the results for three different samples in Fig. 3, it can be seen

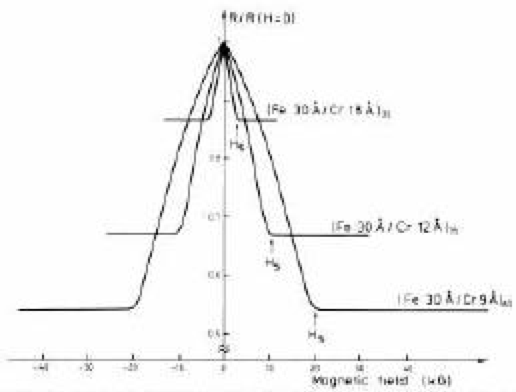

FIG. 3. Magnetoresistance of three Fe/Cr superlattices at 4.2 K. The current and the applied field are along the same [110] axis in the plane of the layers.

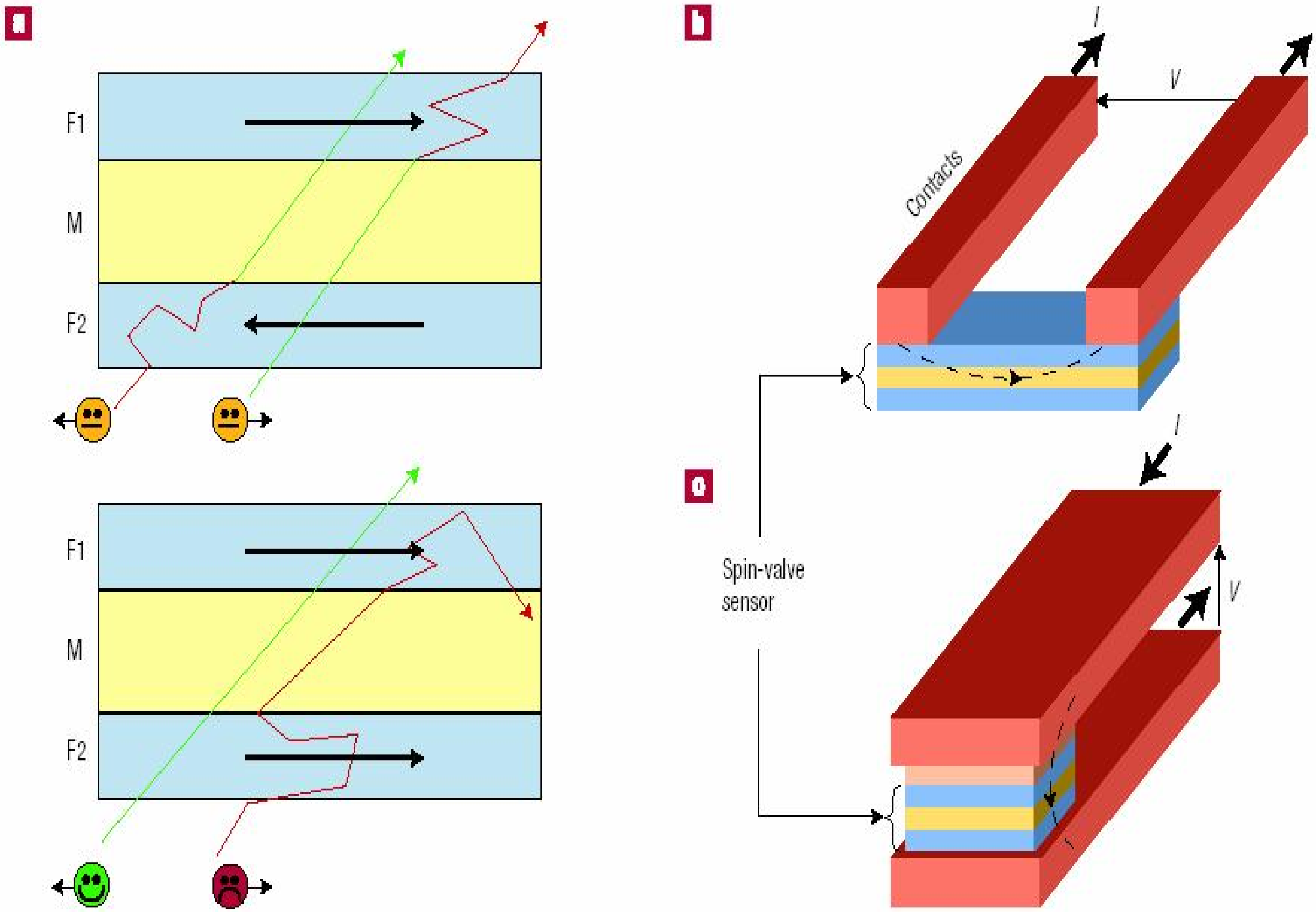

Figure 2 The spin valve. **a**, Schematic representation of the spin-valve effect in a trilayer film of two identical ferromagnetic layers F1 and F2 sandwiching a n
metal spacer layer M, the current circulating in plane. When the two magnetic layers are magnetized parallel (lower scheme), the spin-up electrons (spin antip
magnetization) can travel through the sandwich nearly unscattered, providing a conductivity shortcut and a low resistance. In contrast, in the antiparallel case
both spin-up and spin-down electrons undergo collisions in either F1 or F2, giving rise to a higher overall resistance. **b**, Schematic arrangement of the 'curren
valve sensor in a read head. **c**, Schematic arrangement of the 'current perpendicular to plane' spin-valve sensor in a read head. In both configurations, the rec
travels parallel to the front face of the sensor.

Giant Magnetoresistance metallic multilayers

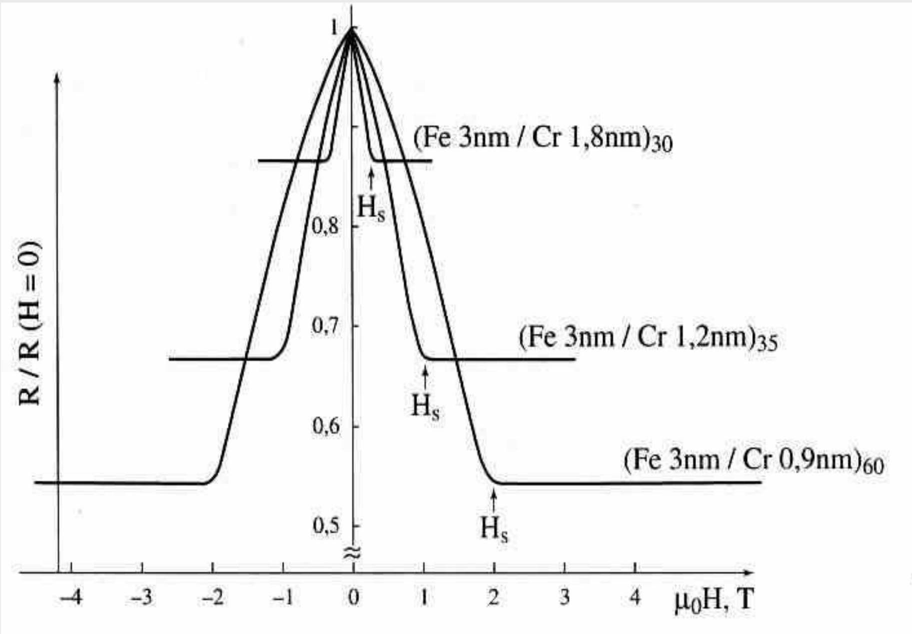

M. Baibich et al., PRL (1988)
FNVD et al., J. Phys. (1988)

- Original GMR effects were not directly usable :
  - –The MR effect is spread over a too large field (low sensitivity)
  - –Need for a biasing field

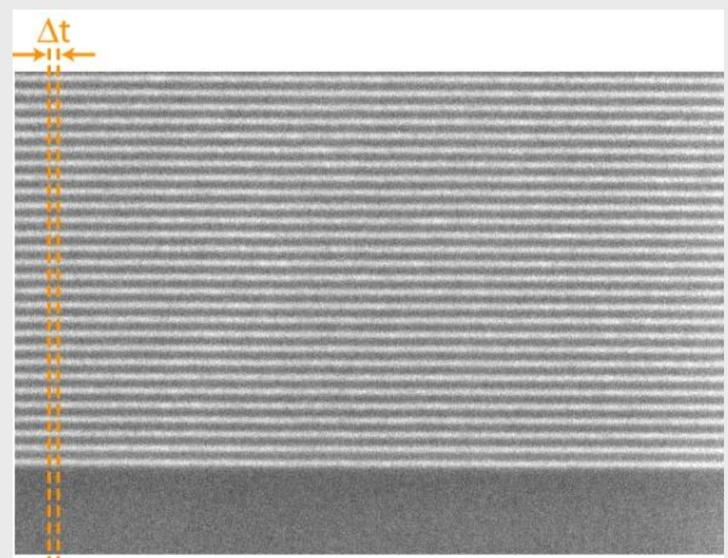

Grünberg

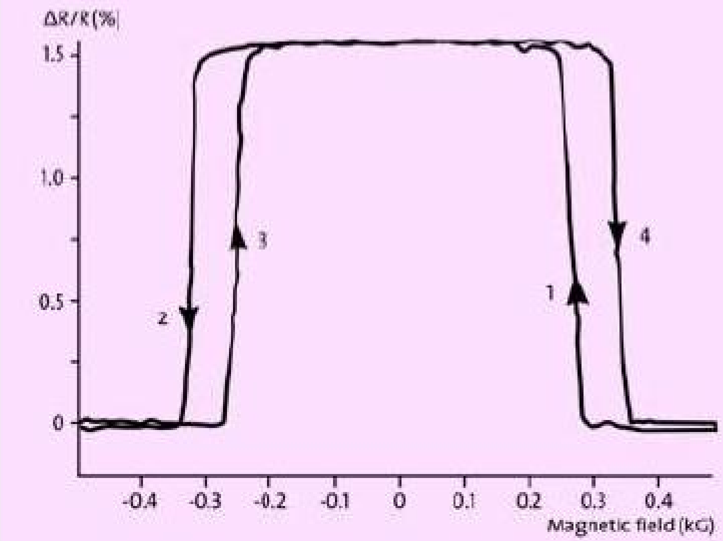

Fert

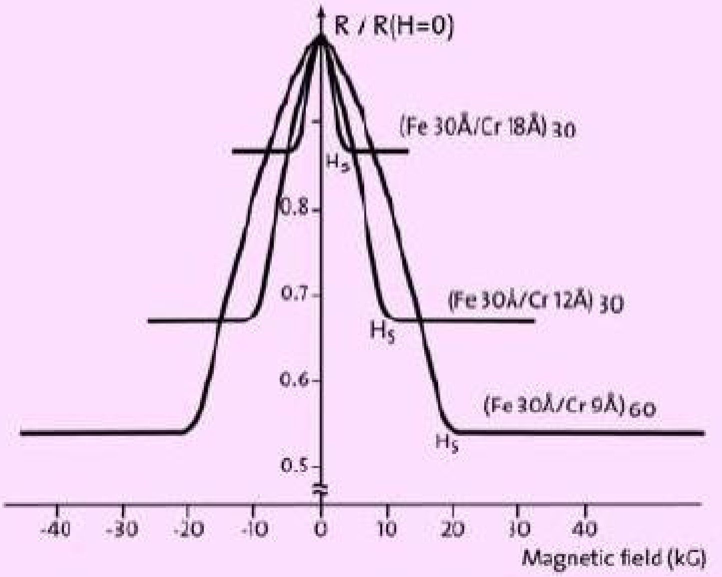

Fe/Cr/Fe trilayer
(~1.5 % @ RT)

$(Fe/Cr)_{60}$ multilayer
(~ 50 % @ 4.2 K)

Evolution of read/write sensor technology

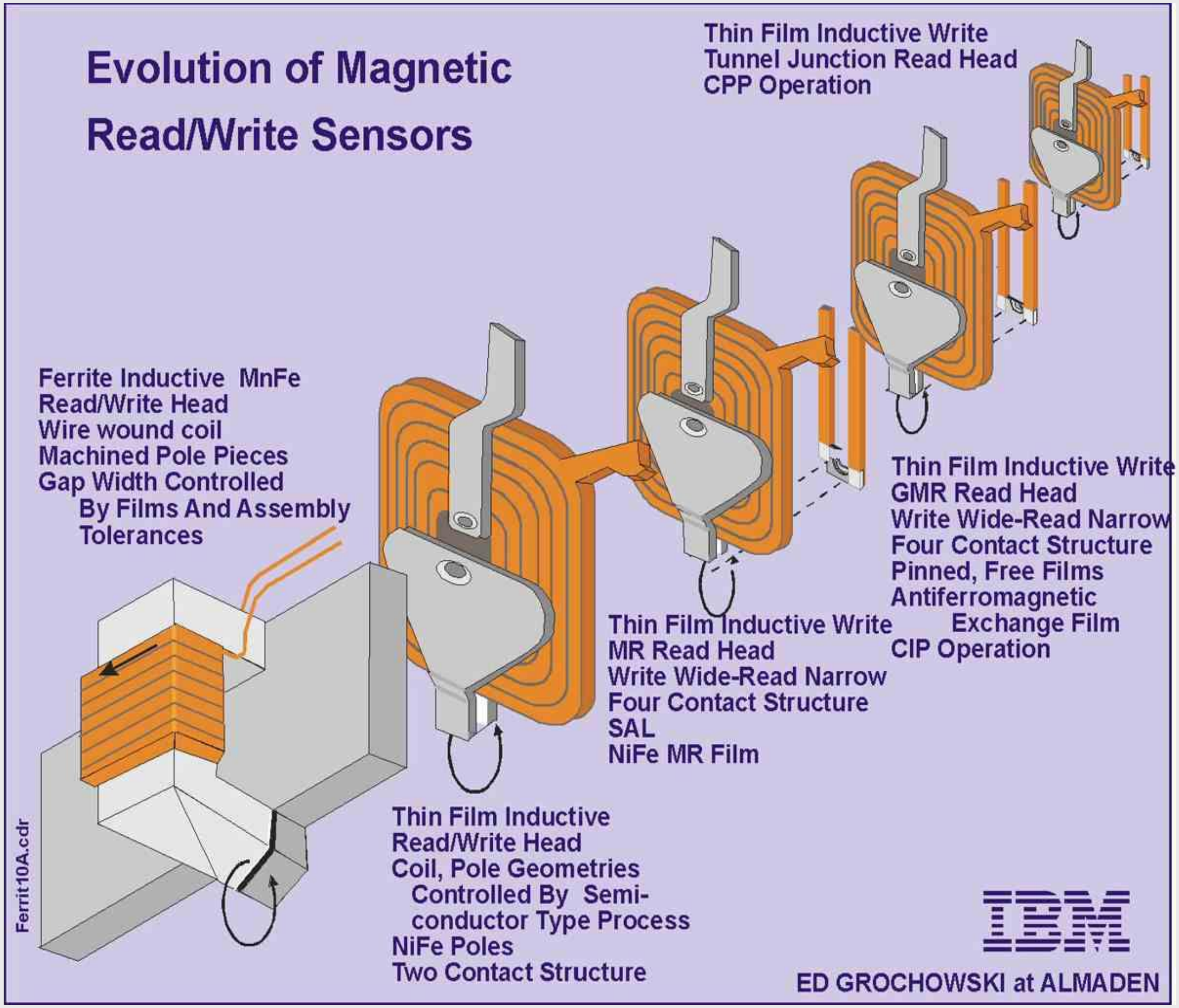

Impact of the introduction of GMR heads

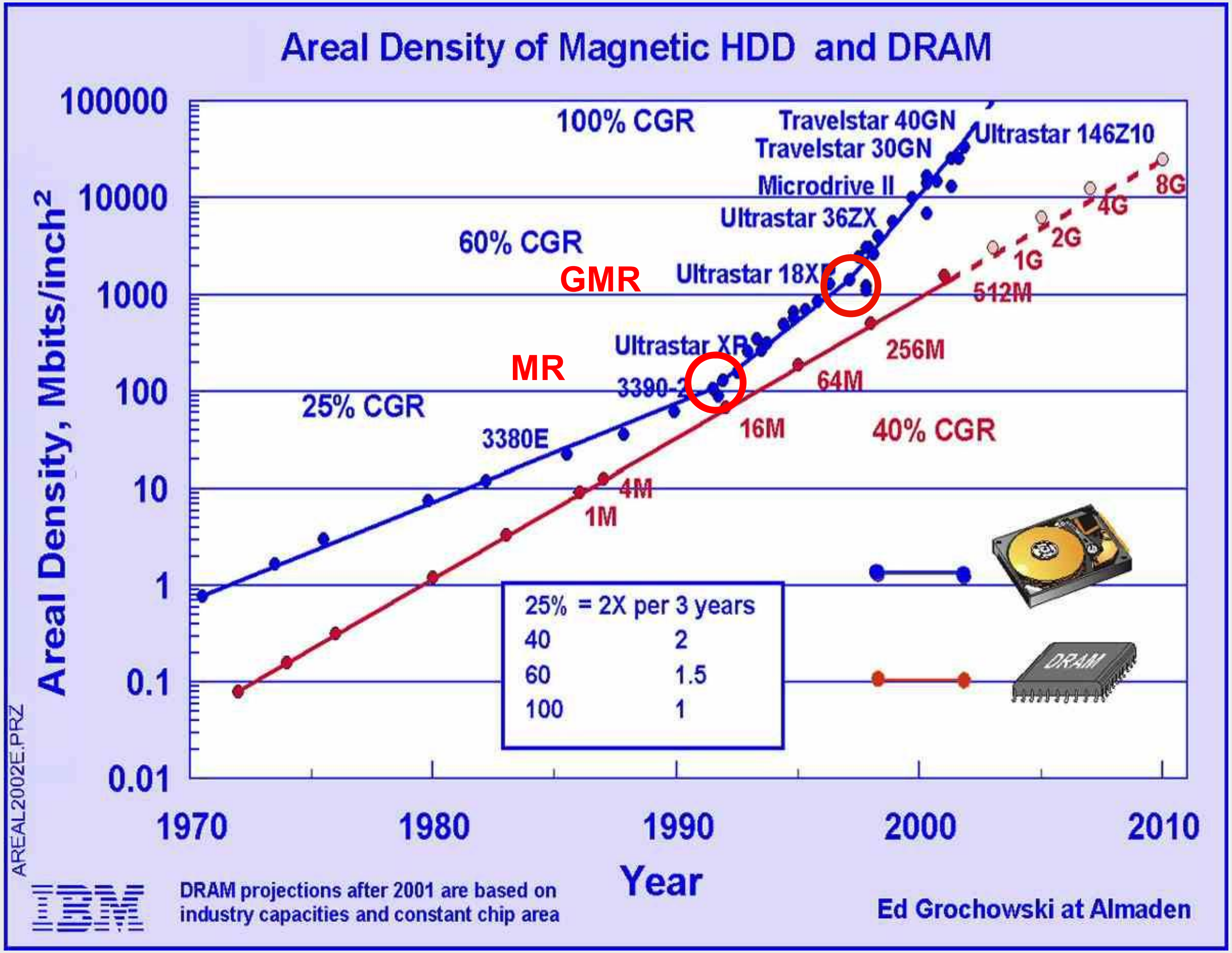

L'effetto Spin Valve

La resistenza del dispositivo cambia drasticamente tra gli stati di magnetizzazione parallela e antiparallela

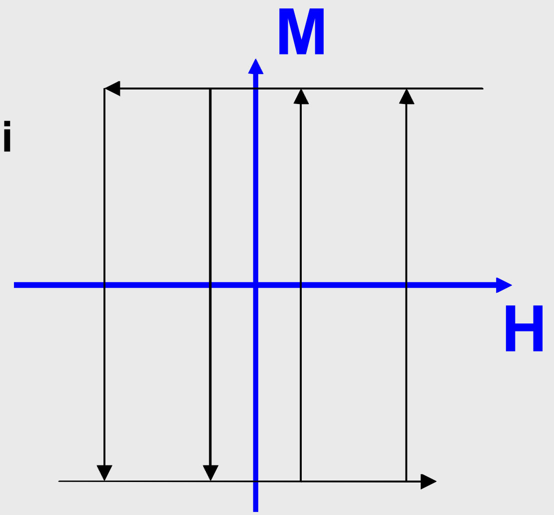

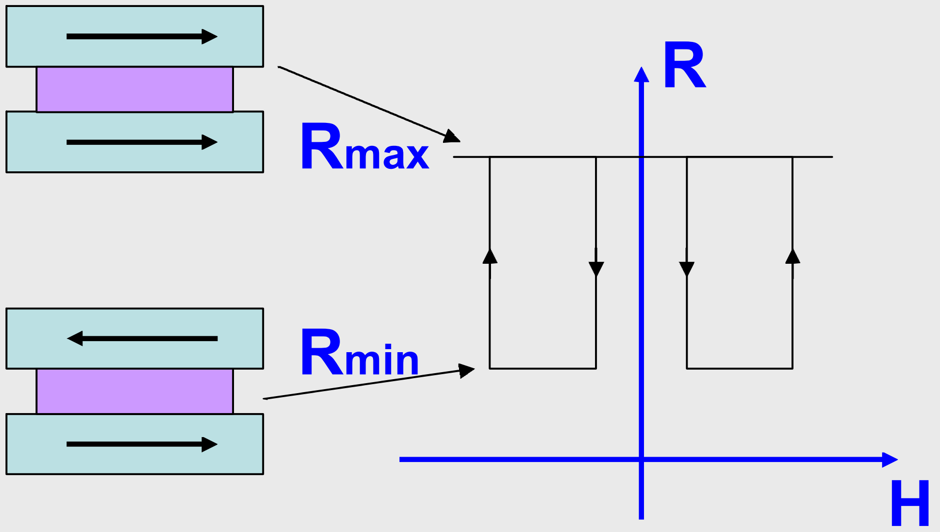

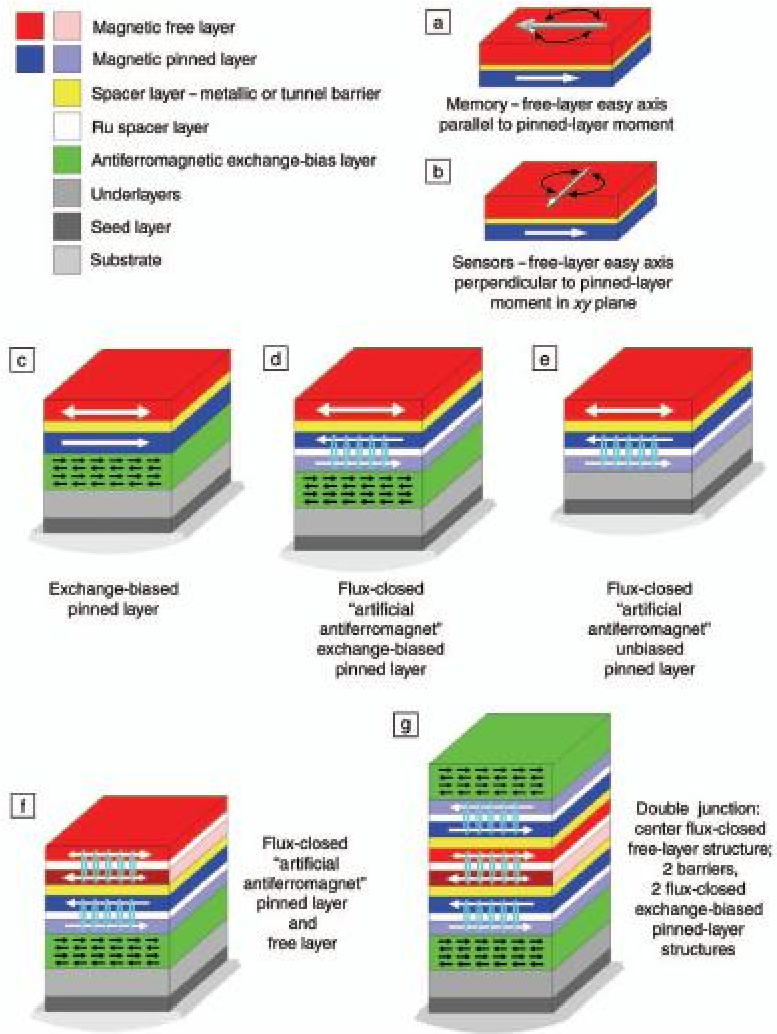

Figure 1. Spin-engineered magnetic devices. (a), (b) The easy axis of the "free" ferromagnetic layer in a magnetoresistive (MR) device is oriented based on the purpose for which it is engineered. Field sensor devices such as read heads rely on a free layer with an easy axis at right angles to the moment of the "pinned" layer. Impinging magnetic fields will rotate the moment away from this middle position and the sensor resistance changes. On the other hand, MR devices designed for use in memory applications will have a free-layer easy axis parallel to that of the pinned layer. (c) A very basic giant magnetoresistance/tunneling magnetoresistance (GMR/TMR) stack consisting of (1) a pinned ferromagnetic layer magnetically locked by exchange bias to the interfacial field of an antiferromagnetic (AF) layer and (2) a simple ferromagnetic free layer. The spin valve is such a stack using a conducting spacer layer between the ferromagnetic layers. (d) In this case, the pinned layer is in fact an element consisting of a pair of ferromagnetic layers antiferromagnetically coupled through a ruthenium spacer layer; the lower layer in this artificial antiferromagnet is pinned via exchange bias as in (c). This flux closure (light blue ellipses) increases the magnetic stability of the pinned layer and reduces coupling to the free layer. (e) Pinned element consisting of an AF-coupled pair of ferromagnetic layers acting as a single "hard" layer, with no exchange-bias layer to discourage rotation of the pinned element. (f) Both the pinned and free elements consist of AF-coupled pairs. (g) A double tunnel junction. All ferromagnetic elements consist of AF-coupled pairs. There are two pinned ferromagnets, both exchange-biased by AF layers. Spin-filtering occurs both as current tunnels from the first pinned layer to the free element and again as it tunnels from the free element to the second pinned element. (From Reference 13.)

Magnetic tunnel junctions

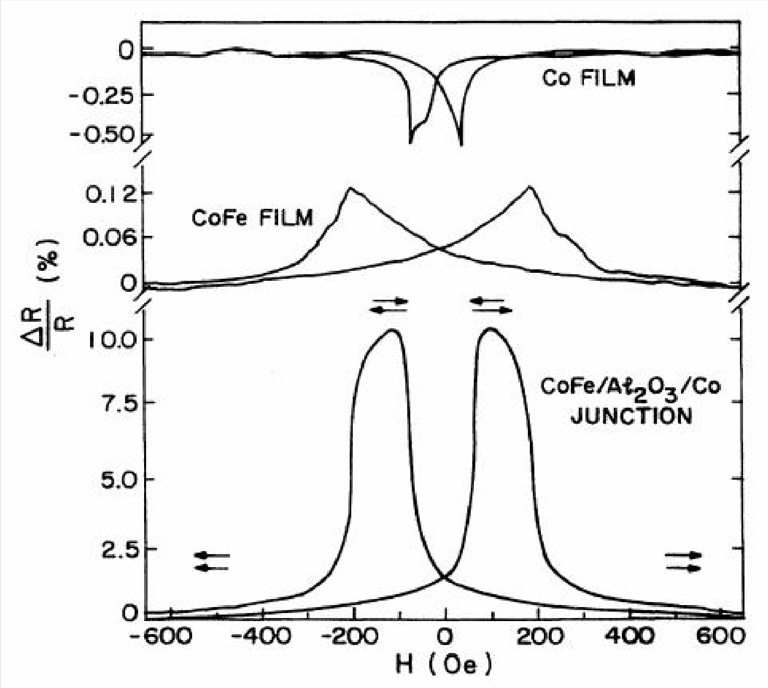

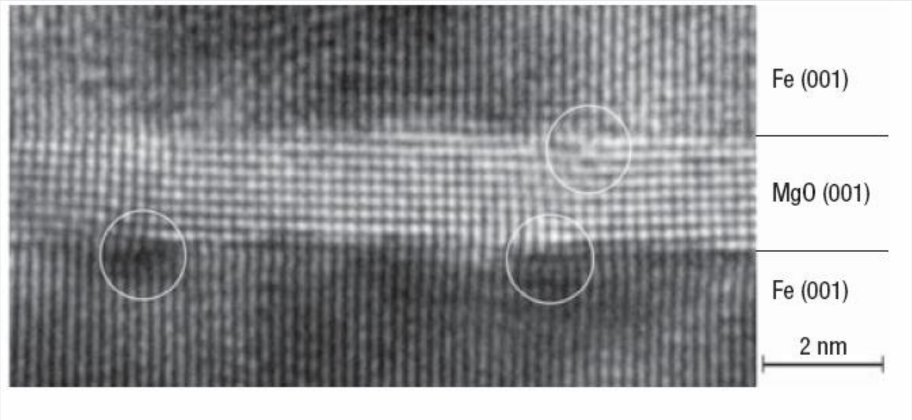

J.S. Moodera *et al*., Phys. Rev. Lett. **74**, 3273 (1995)

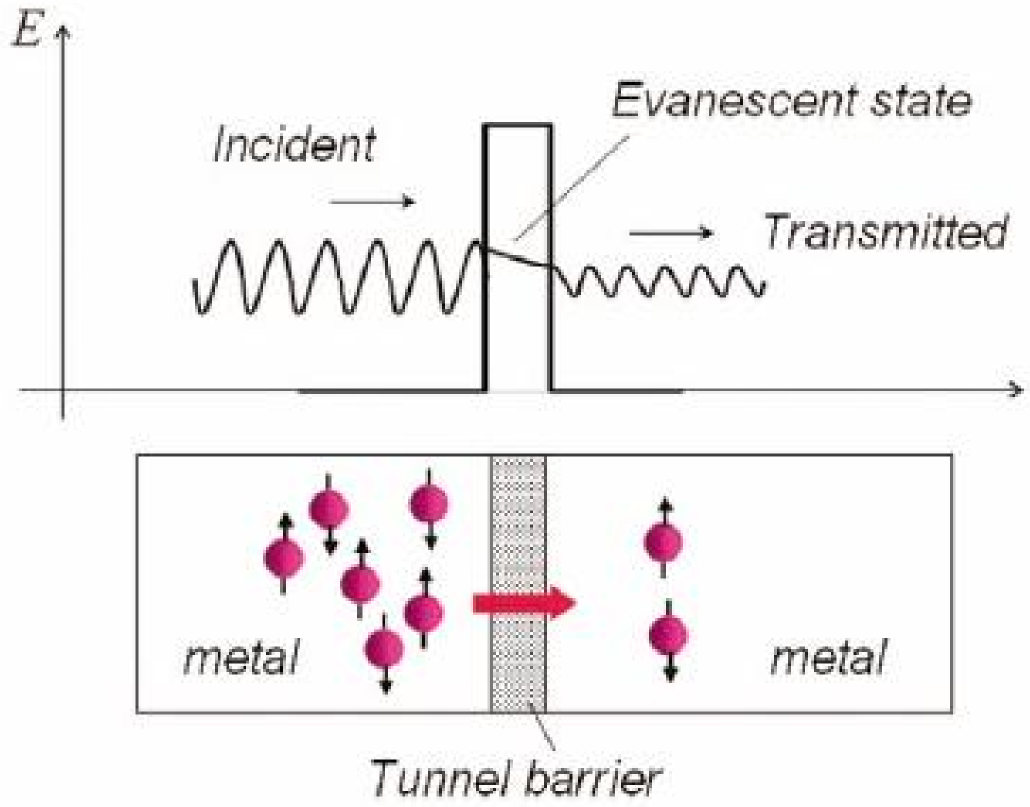

Fig. 1 Electron tunneling through a thin tunnel barrier layer. (Top) The wave nature picture of the tunneling of the electrons. A traveling wave approaching from the left of the barrier. When the barrier height is greater than the energy of the electron, the electron wave inside the barrier layer becomes evanescent as its amplitude decreases exponentially through the barrier. If the barrier layer is thin enough so that the amplitude of the evanescent wave does not completely diminish at the other side of the barrier, a traveling wave reemerges again with the residual amplitude and continues to propagate. (Bottom) The corresponding particle view of the tunneling effect. The amplitude ratio between the transmitted and incident waves determines the probability of an electron tunneling through the barrier.

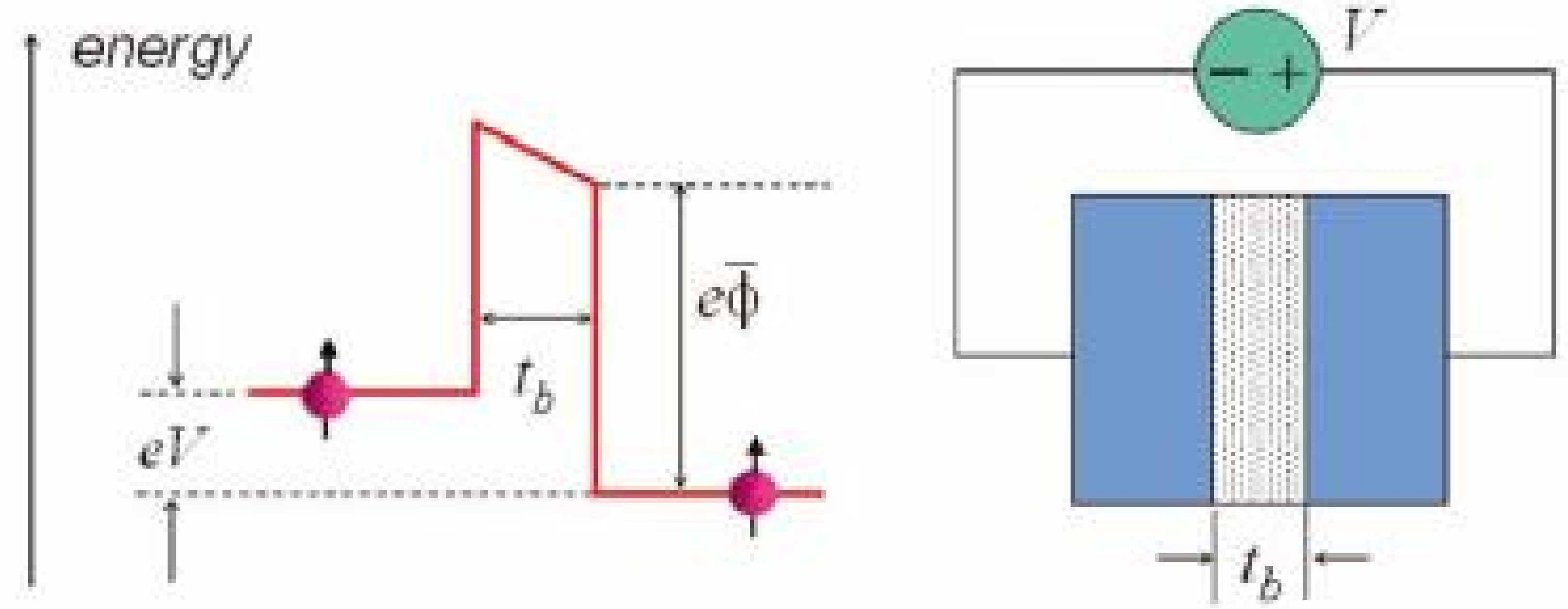

Fig. 2 Illustration of the bias of a tunnel junction and Simmon's I-V relation.

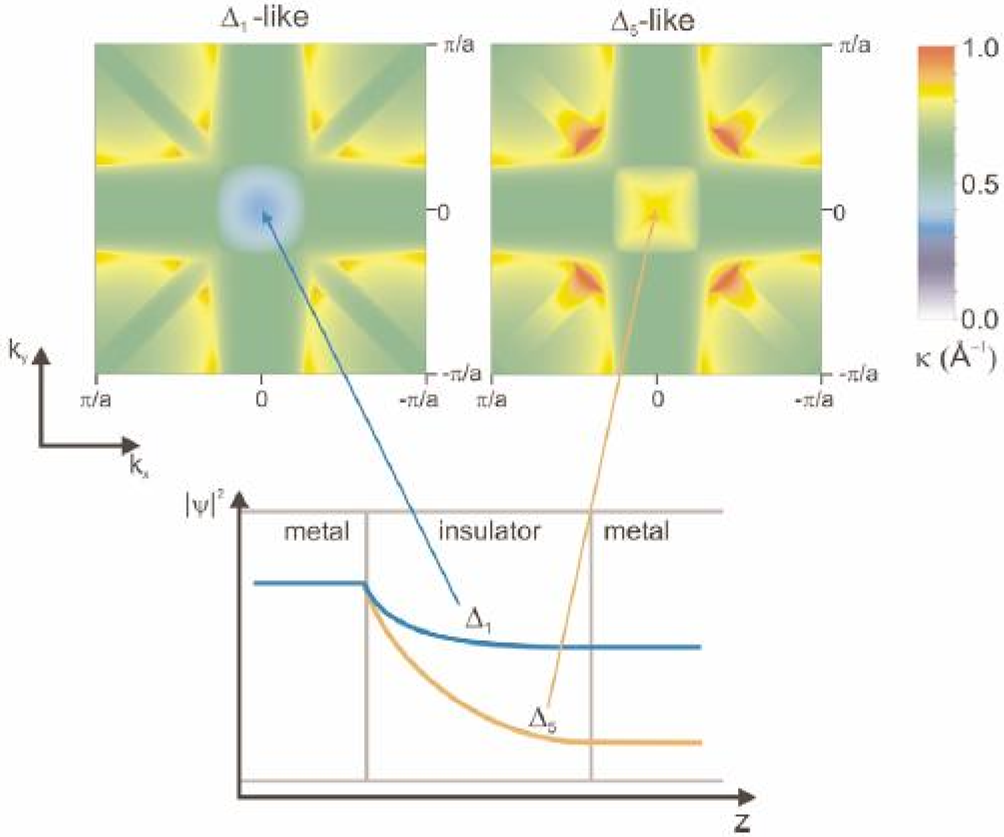

Fig. 6 (Top) Imaginary part κ of the complex wave vector in the surface Brillouin zone at the Fermi level for the two bands of MgO with the smallest κ. (Bottom) Schematic of the probability amplitudes at the $\bar{\Gamma}$ point with Δ_1 and Δ_5 symmetry. (Reprinted with permission from[73]. © 2006 American Physical Society.)

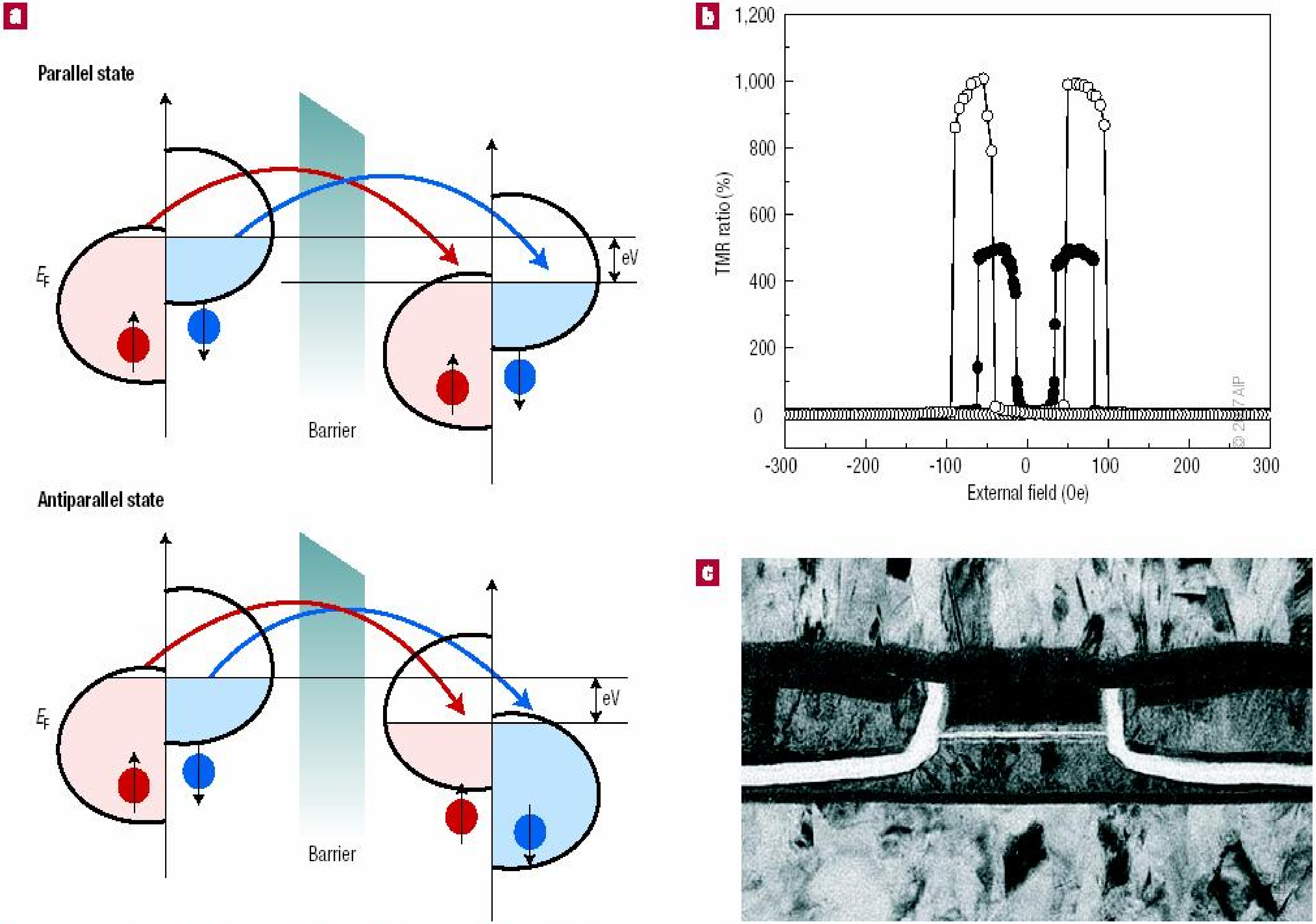

Figure 4 The magnetic tunnel junction. **a**, Schematic representation of the tunnel magnetoresistance in the case of two identical ferromagnetic metal layers separated by a non-magnetic amorphous insulating barrier such as Al_2O_3. The tunnelling process conserves the spin. When electron states on each side of the barrier are spin-polarized, then electrons will more easily find free states to tunnel to when the magnetizations are parallel (top picture) than when they are antiparallel (bottom picture). **b**, Record high magnetoresistance TMR = $(R_{max} - R_{min})/R_{min}$ for the magnetic stack $(Co_{25}Fe_{75})_{80}B_{20}$ (4 nm)/MgO (2.1 nm)/$(Co_{25}Fe_{75})_{80}B_{20}$ (4.3 nm) annealed at 475 °C after growth, measured at room temperature (filled circles) and at 5 K (open circles). Reprinted with permission from ref. 31. **c**, Transmission electron microscope cross-section of a TMR read head from Seagate. Reprinted with permission from ref. 32. The tunnel junction stack appears vertically at the centre of the picture, with the tunnel barrier at the level of the thin white horizontal line. The thick bent lines on both sides are the insulating layers between top and bottom contacts. The two thick light grey layers on top and bottom are the magnetic pole pieces (see Fig. 1). The track width of the TMR element is typically 90–100 nm.

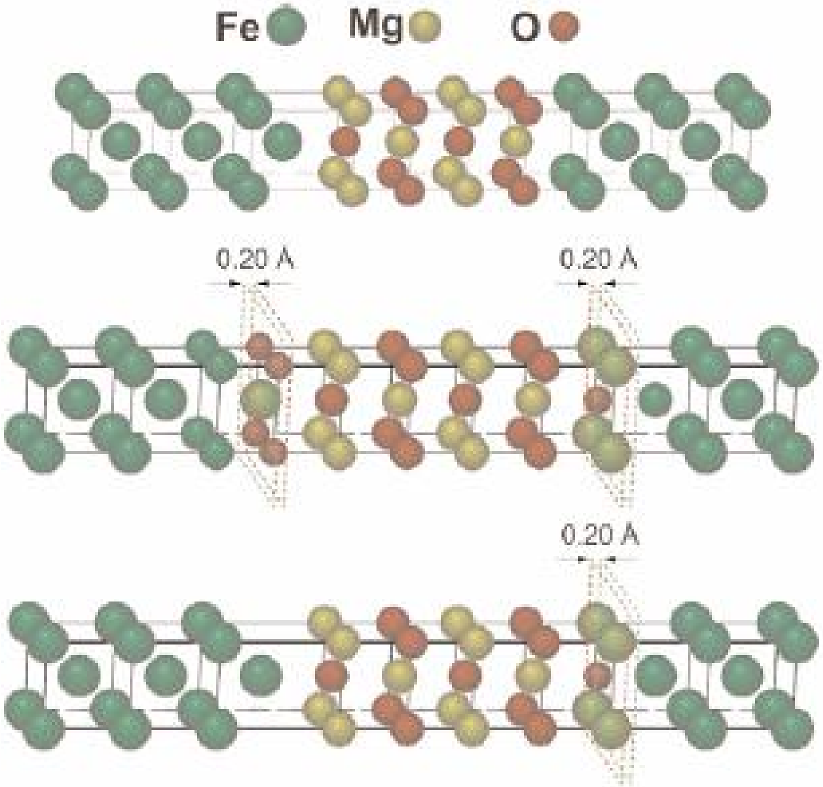

Fig. 9 Considered interface geometries with and without FeO layer: ideal junction (top), symmetric junction (middle), and asymmetric junction (bottom). (Reprinted with permission from[80]. © 2005 American Physical Society.)

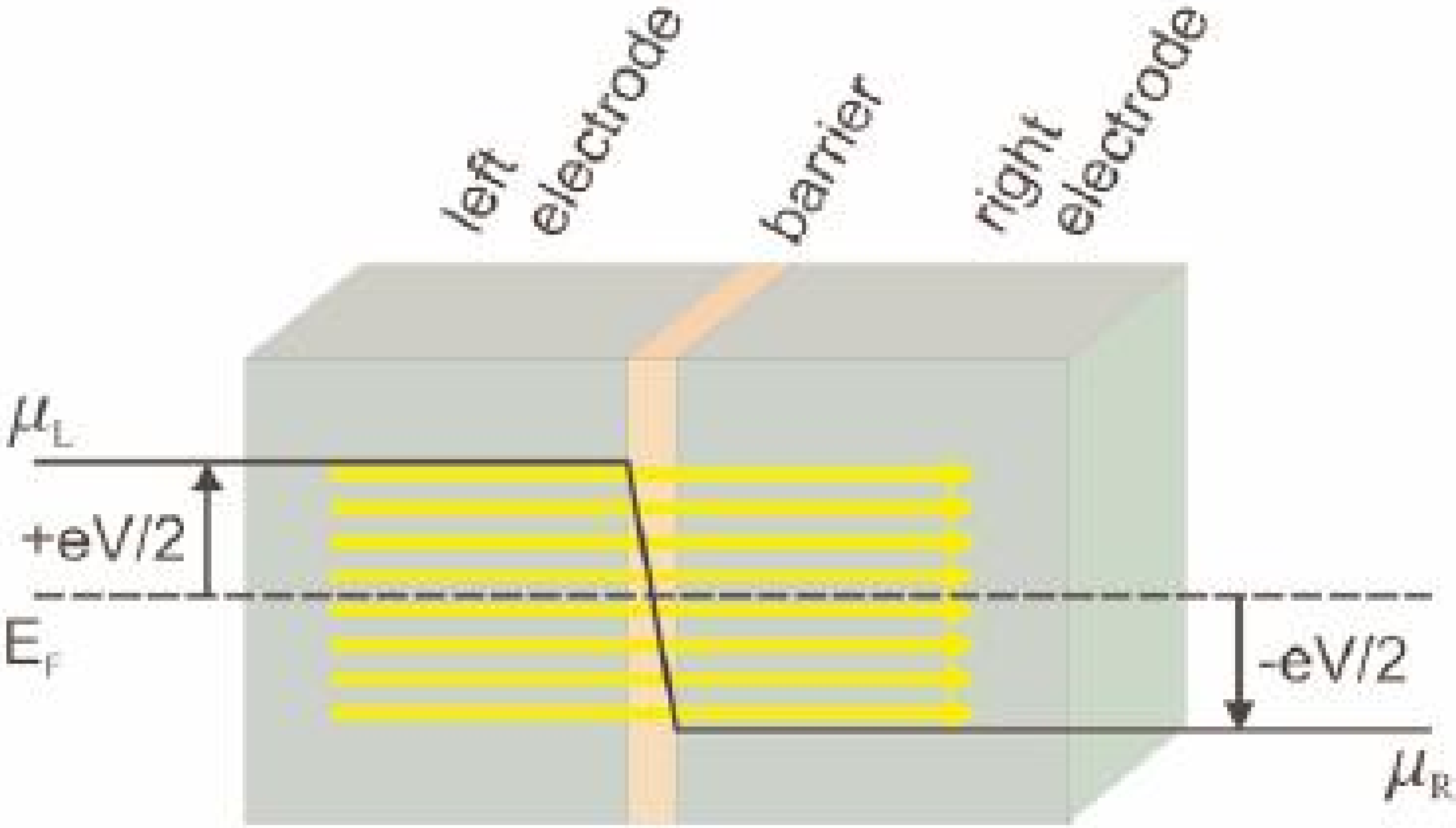

Fig. 5 Spatial variation of the electrochemical potential under an applied bias voltage V. The tunneling states (yellow arrows) in the energy window between μ_R and μ_L contribute to the current.

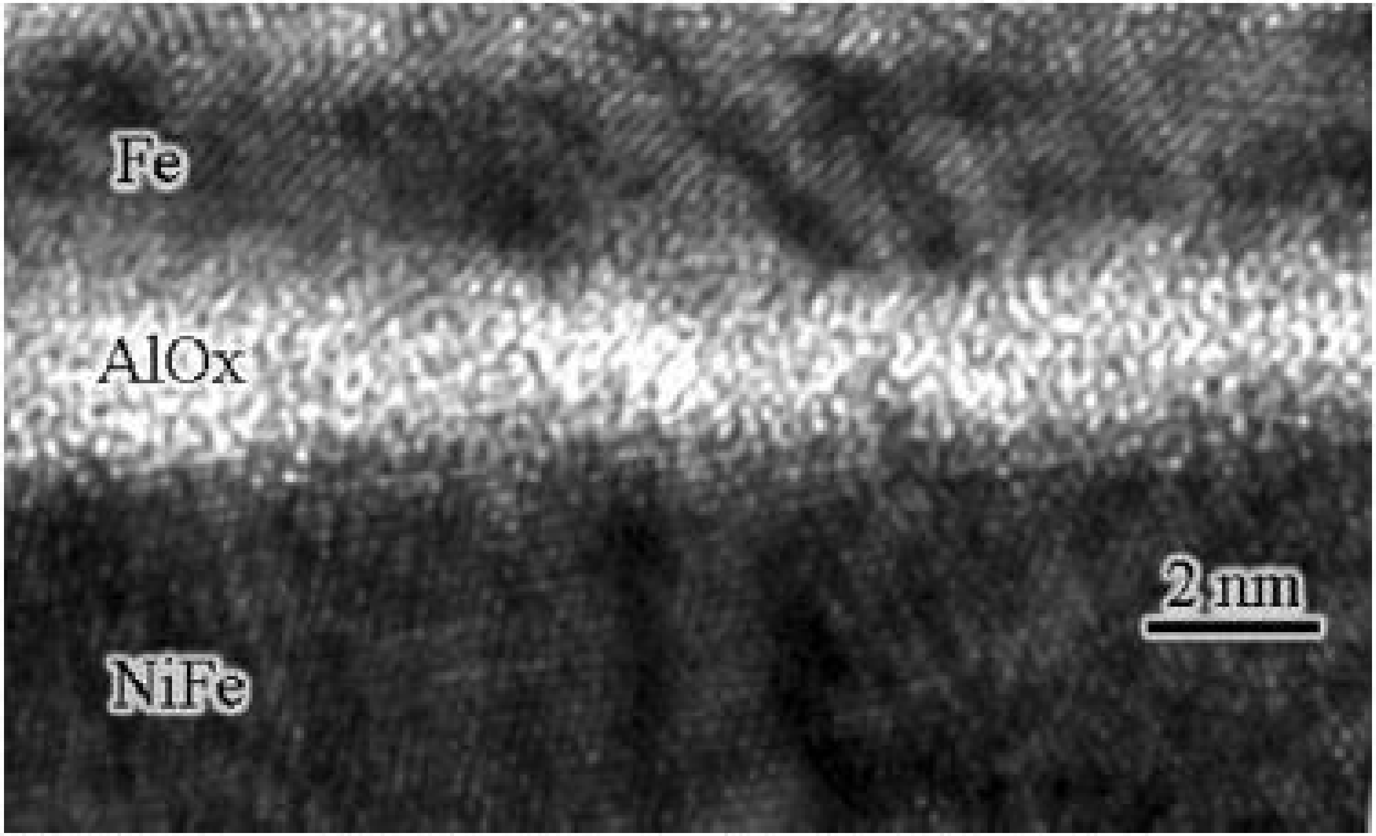

Fig. 7 TEM image of a Fe/AlO_x/NiFe tunnel junction fabricated using a sputtering technique. The AlO_x tunnel barrier is formed by depositing Al followed by a plasma-enhanced oxidation process.

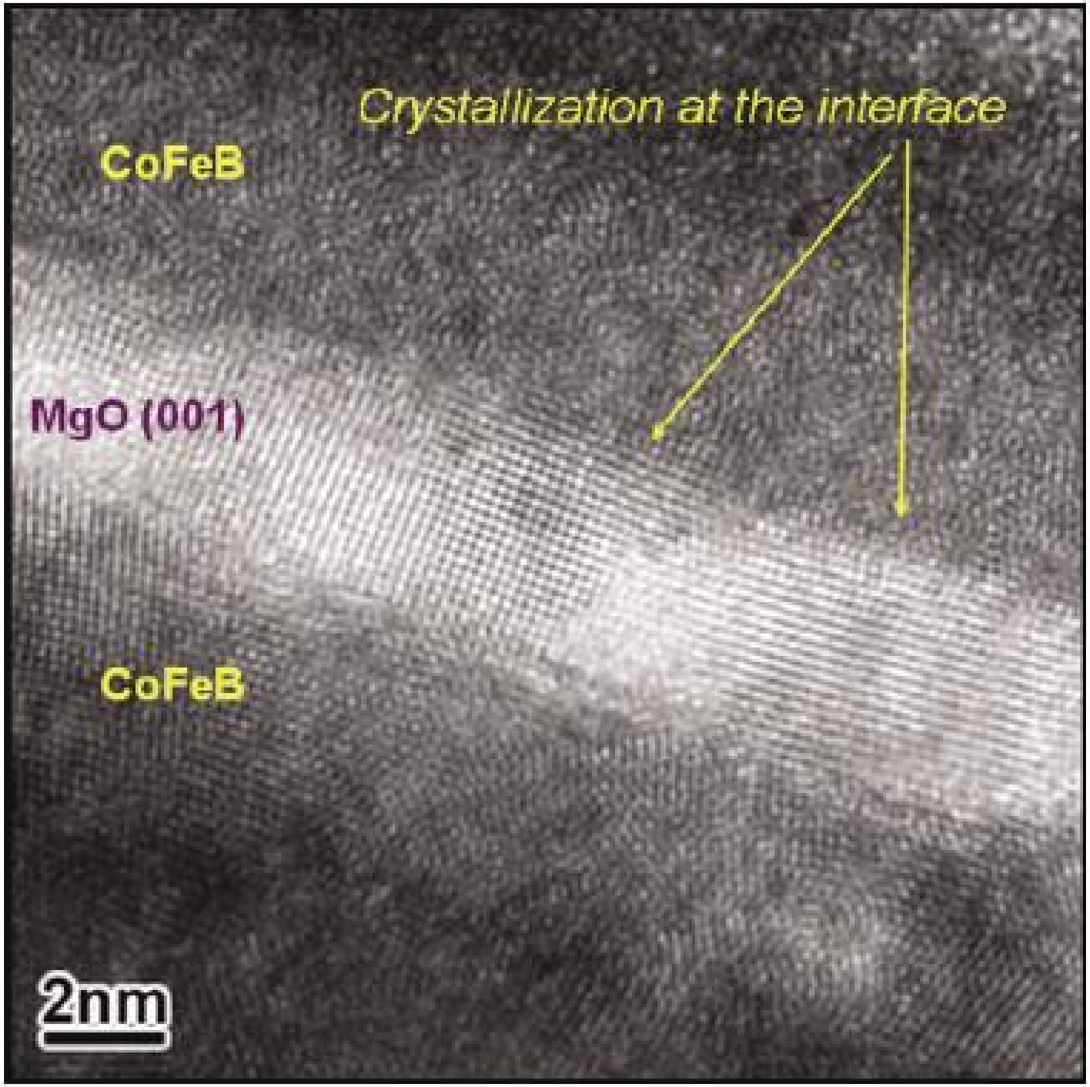

Fig. 9 TEM image of a CoFeB/MgO/CoFeB MTJ deposited using a sputtering technique followed by postannealing at 270°C. The as-deposited CoFeB is purely amorphous while the directly deposited MgO layer clearly shows a well-oriented (001) texture. After the annealing process, the two CoFeB layers form a bcc crystalline structure epitaxially from the interface with the MgO lattice. The measured room-temperature TMR ratio of this particular MTJ is ~110%[34].

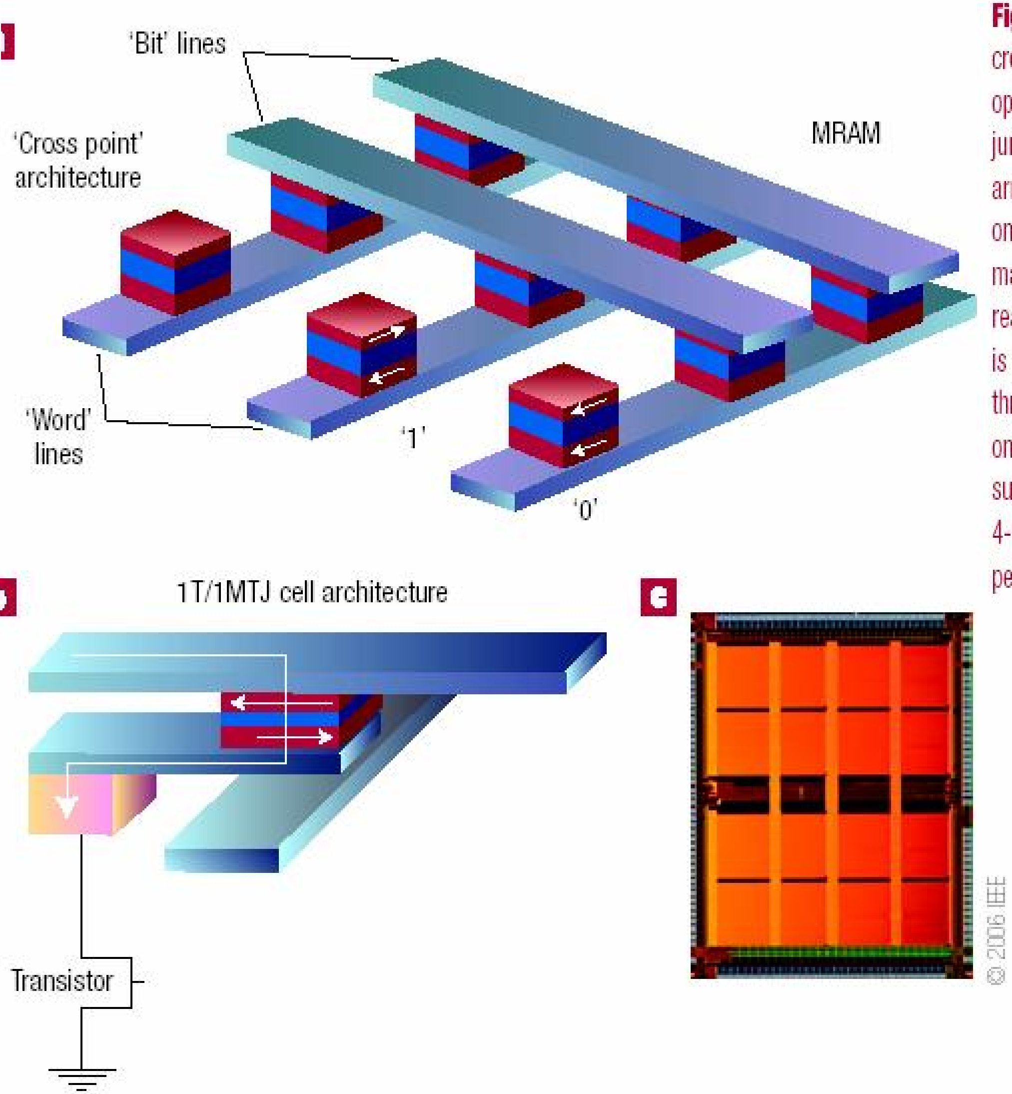

Figure 5 Magnetic random access memory. **a**, Principle of MRAM, in the basic cross-point architecture. The binary information 0 and 1 is recorded on the two opposite orientations of the magnetization of the free layer of magnetic tunnel junctions (MTJ), which are connected to the crossing points of two perpendicular arrays of parallel conducting lines. For writing, current pulses are sent through one line of each array, and only at the crossing point of these lines is the resulting magnetic field high enough to orient the magnetization of the free layer. For reading, the resistance between the two lines connecting the addressed cell is measured. **b**, To remove the unwanted current paths around the direct one through the MTJ cell addressed for reading, the usual MRAM cell architecture has one transistor per cell added, resulting in more complex 1T/1MTJ cell architecture such as the one represented here. **c**, Photograph of the first MRAM product, a 4-Mbit stand-alone memory commercialized by Freescale in 2006. Reprinted with permission from ref. 33.

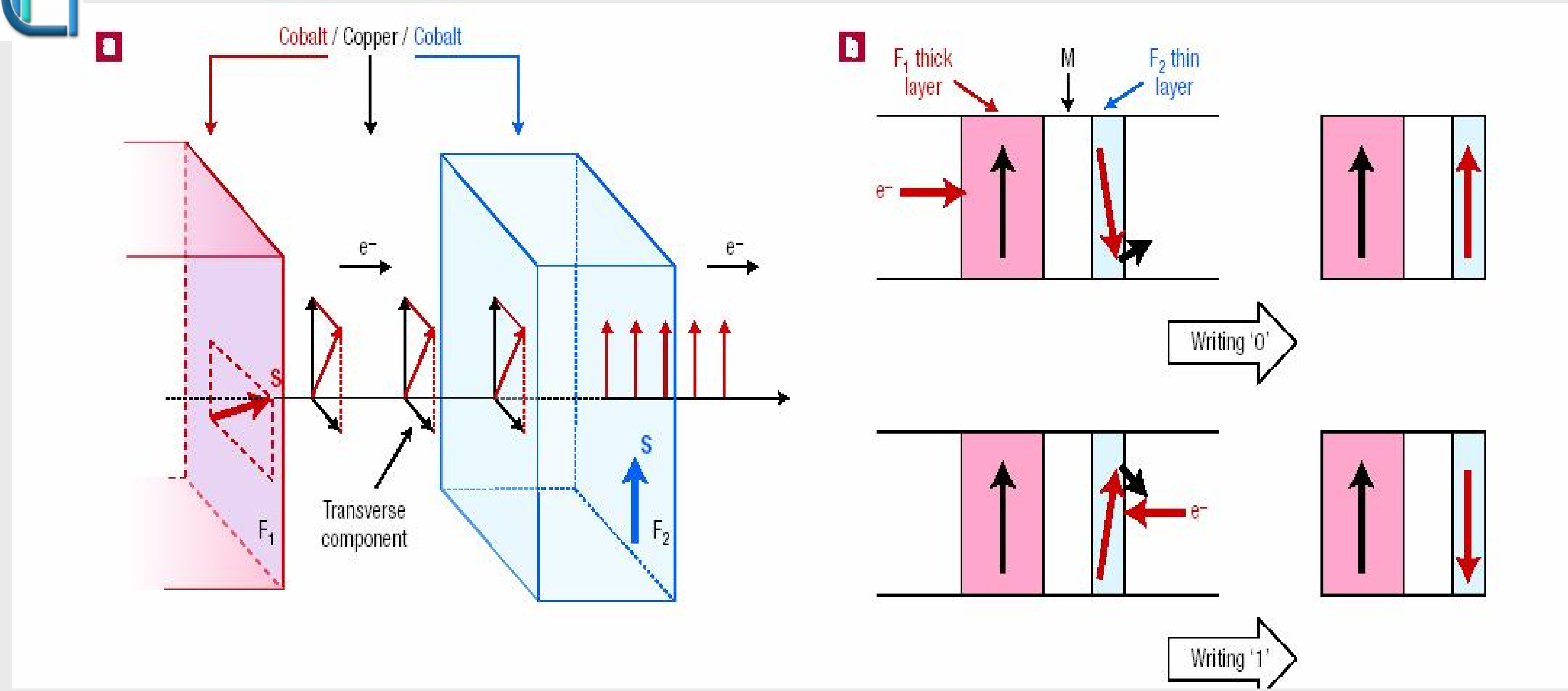

Figure 6 Spin-transfer switching. **a**, Principle of the STT effect, for a typical case of a Co(F1)/Cu/Co(F2) trilayer pillar. A current of *s* electrons flowing from left to right will acquire through F1 (assumed to be thick and acting as a spin polarizer) an average spin moment along the magnetization of F1. When the electrons reach F2, the *s*–*d* exchange interaction quickly aligns the average spin moment along the magnetization of F2. To conserve the total angular momentum, the transverse spin angular momentum lost by the electrons is transferred to the magnetization of F2, which senses a resulting torque tending to align its magnetization towards F1. **b**, Principle of STT writing of a MRAM cell: reversing the current flowing through the cell will induce either parallel or antiparallel orientation of the two ferromagnetic layers F1 and F2.

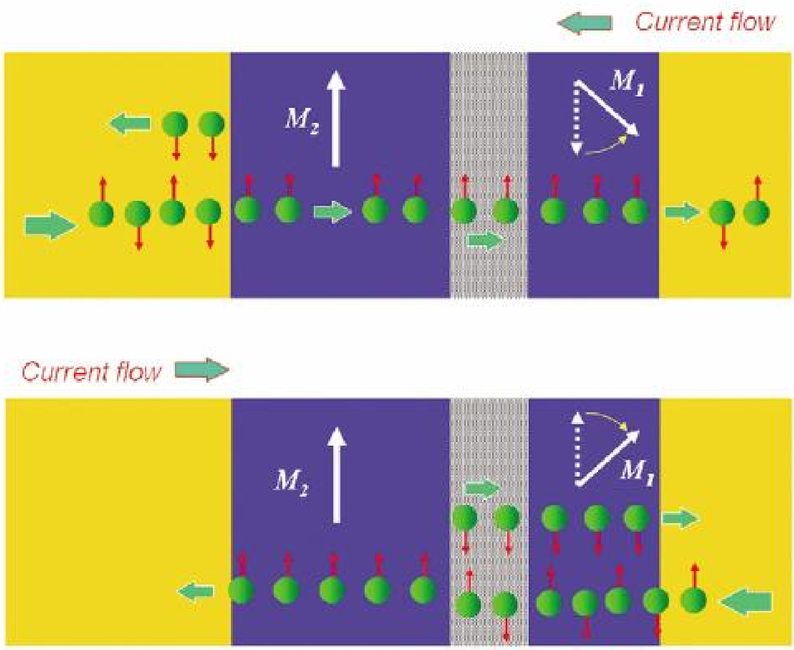

Fig. 17 The spin torque effect, also known as spin momentum transfer. Reversing the current direction reverses the spin polarization direction of the tunneling current. If the electrons flow from layer 2 to layer 1, the effect of spin torque is to rotate the magnetization of layer toward the parallel state. In reversing the direction of tunneling current, the antiparallel state is preferred.

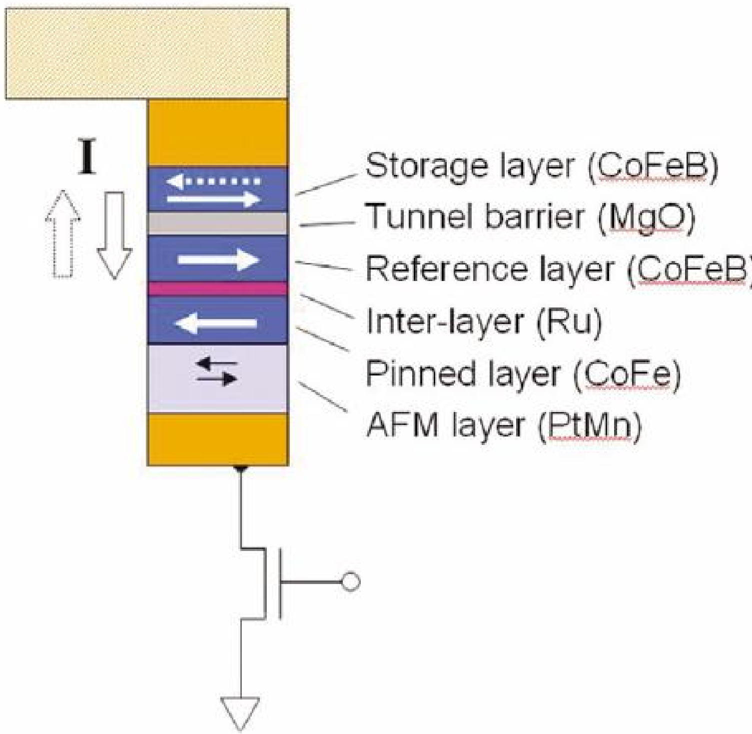

Fig. 18 Schematic of Sony's spin-RAM memory element with direct current injection in which spin torque is used to perform the magnetic switching of the storage layer[56].

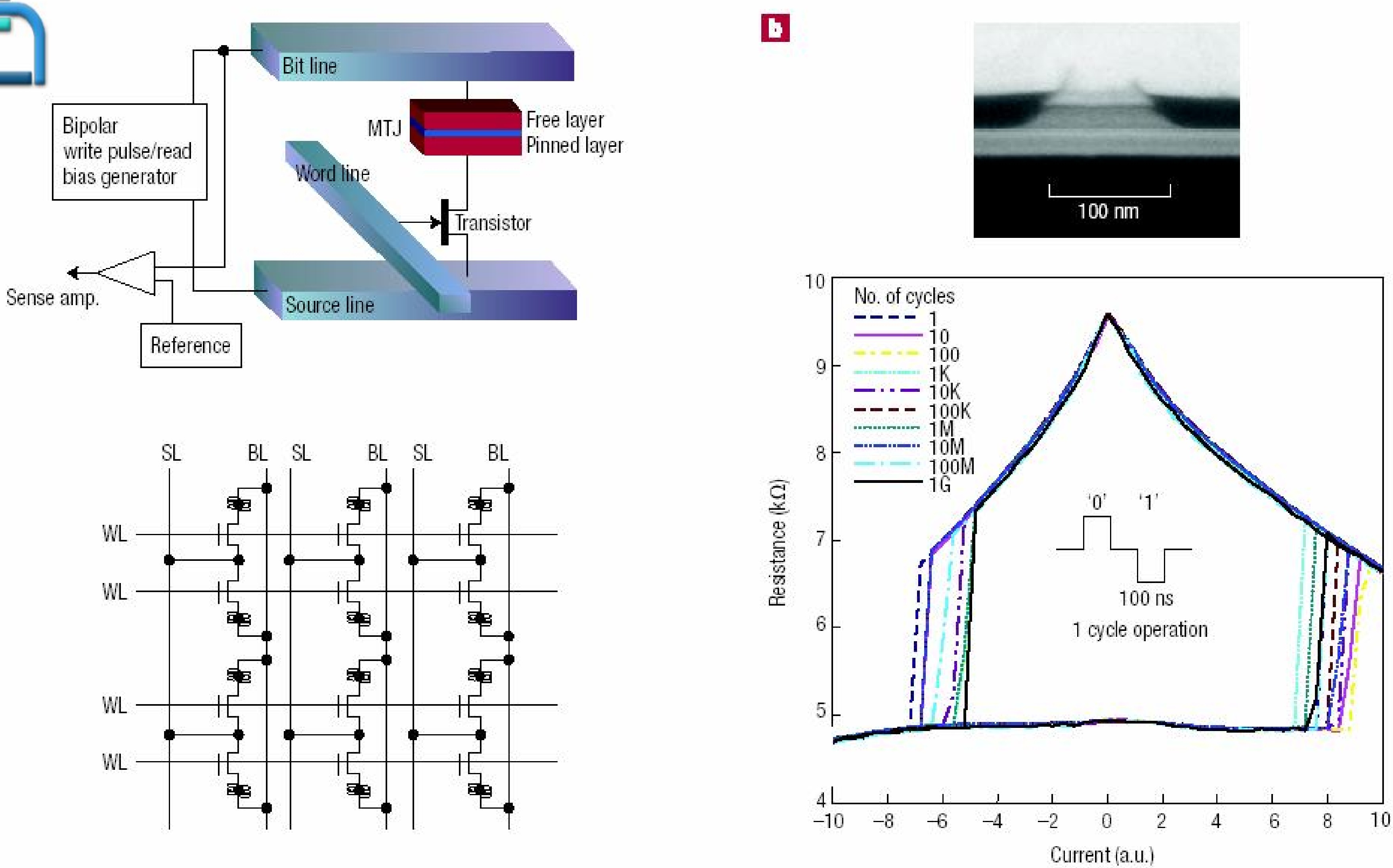

Figure 7 The spin-RAM. **a**, Schematic architecture of a spin-RAM; upper panel, scheme of the memory cell, and lower panel, tentative architecture of the cell array. Reprinted with permission from ref. 70. **b**, Resistance versus current hysteresis loop of a spin-RAM cell. Reprinted with permission from ref. 71. The different colours show the evolution of the loop after an increasing number (up to 1 G = 10^9) of writing cycles (100 ns pulses of successively positive and negative currents, see image). This demonstrates excellent stability. TEM image: TMR device size 100 nm × 50 nm; free layer CoFe (1.0 nm) / NiFe (2.0 nm); tunnel barrier MgO (1.0 nm).

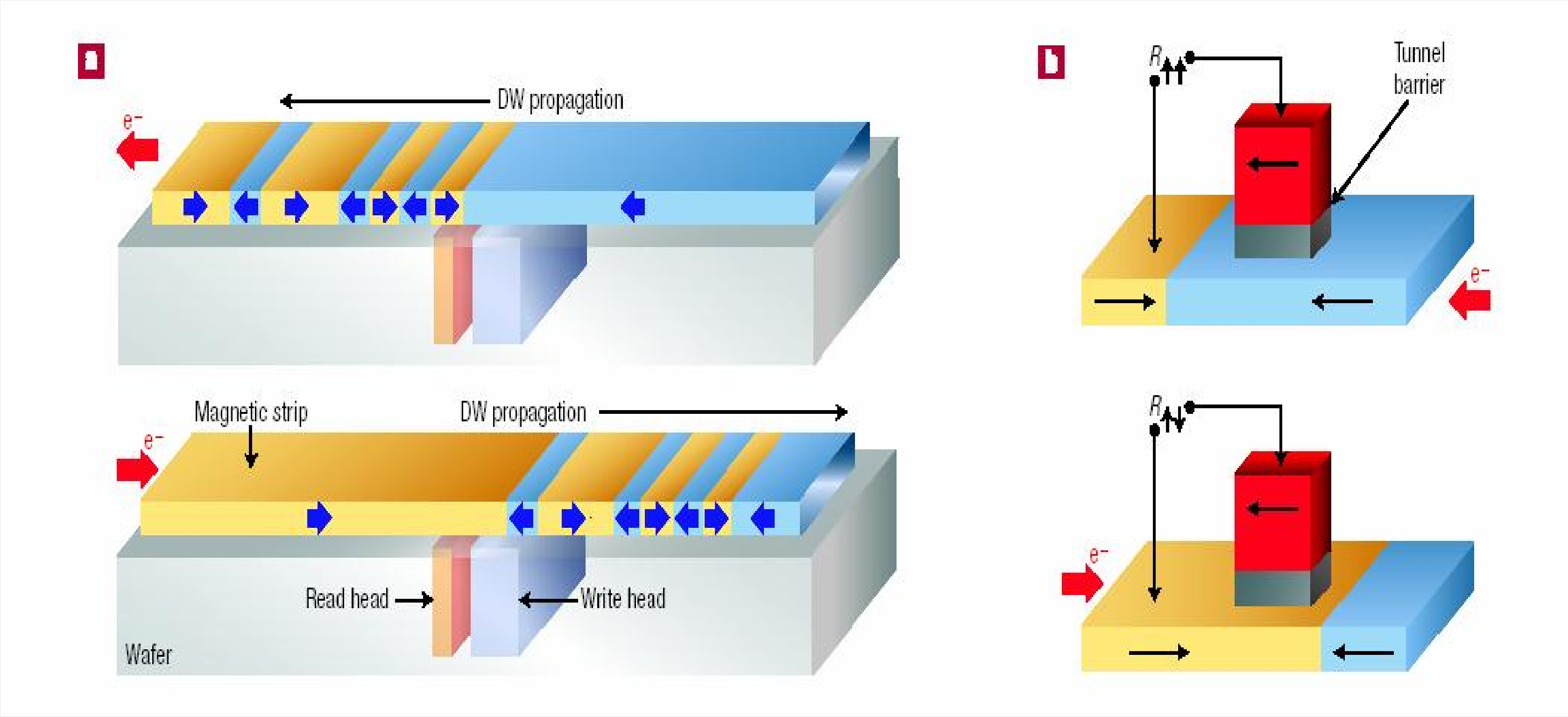

Figure 8 Domain wall storage devices. Examples of storage devices using current-induced domain wall (DW) propagation. **a**, In the concept first proposed by Parkin[94], the binary information is stored by a chain of domain walls in a magnetic stripe. An electrical current in the stripe, by applying the same pressure to all the domain walls, moves them simultaneously at the same speed for a sequential reading (or writing) at fixed read and write heads. A reverse current can move the domain walls in the opposite direction for resetting, or in an alternative solution the domain walls might turn on a loop. This mimics the fast passing of bits in front of the head in HDD recording, but here there is no moving part and addressing a sector would be done by CMOS electronics at microsecond access times. The initial scheme[94] proposes to store data in vertical stripes: this would open the way to very compact high capacity 'storage track memory devices'. Other schemes now propose multilayers of in-plane domain tracks, which would be easier to fabricate. **b**, Scheme of a MRAM cell using domain wall propagation from one stable position to another on either side of a magnetic tunnel junction (ref. 95).

From CIP to CPP sensors : TMR vs GMR

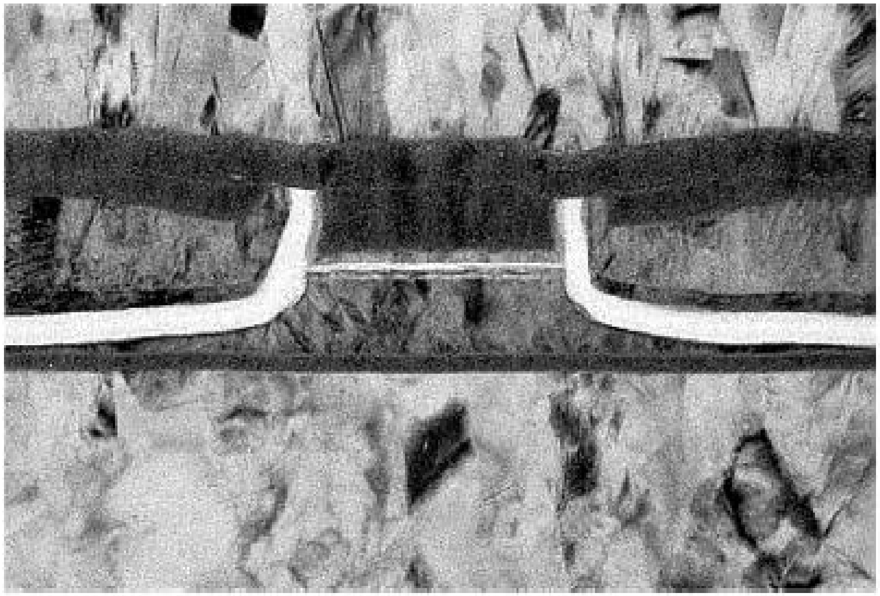

Fig. 2. TEM image of ABS view of a commercial TMR head with permanent magnet longitudinal hard bias layer. Seagate unique design with metal to seed the top shield.

Fig. 1. Industry first 120 GB 2.5-in Seagate Momentus II high capacity mobile drive using TMR reading element.

Commercial product with TMR read-head
S. Mao et al., IEEE Trans. Magn., 42, 97 (2006)

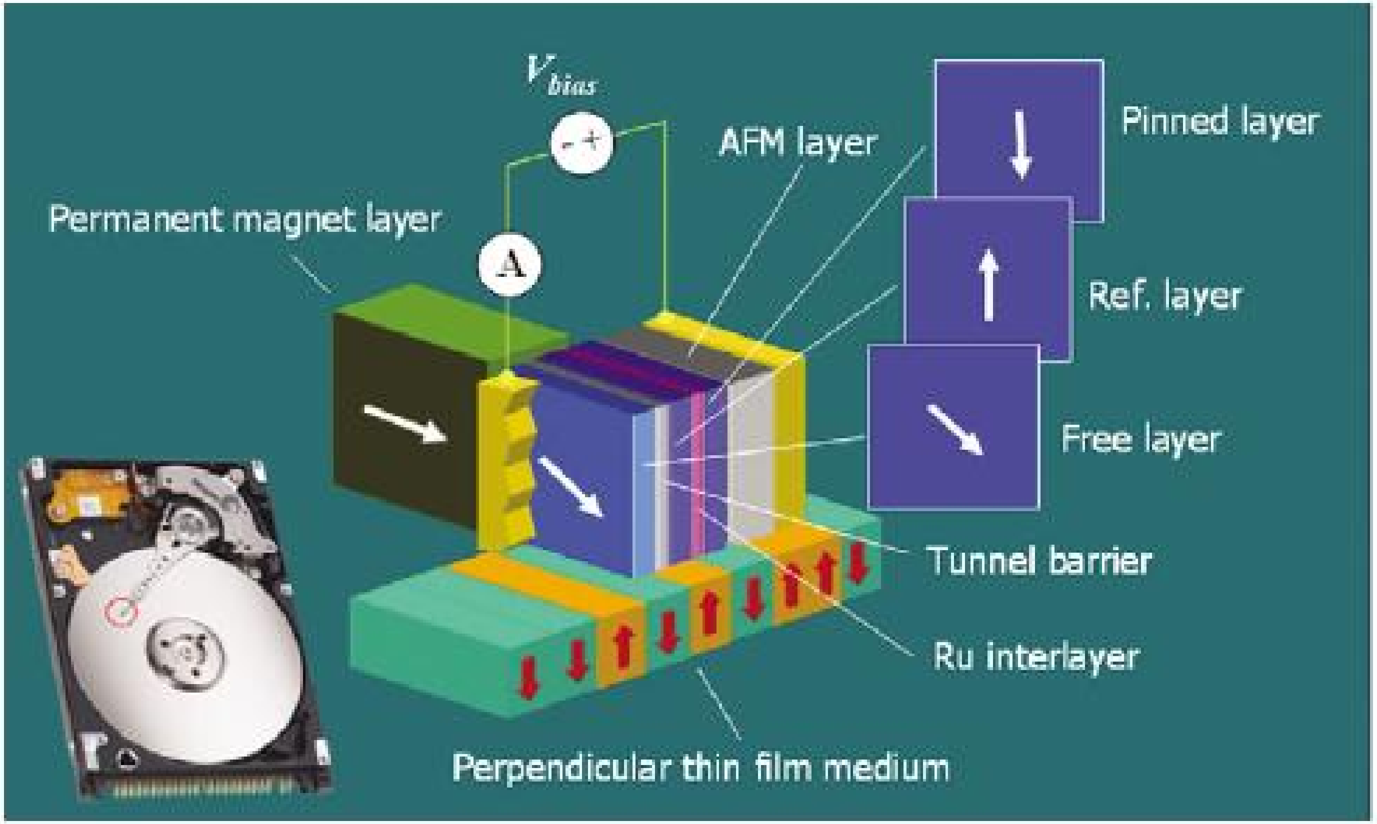

Fig. 12 MTJ read head in an HDD. One magnetic electrode is a free layer, and its magnetization rotates freely in response to the medium signal field. The magnetic moment of the other electrode is 'fixed' through the interlayer magnetic coupling and functions as a reference to the free layer magnetization orientation.

Navigation : use of an attitude detector

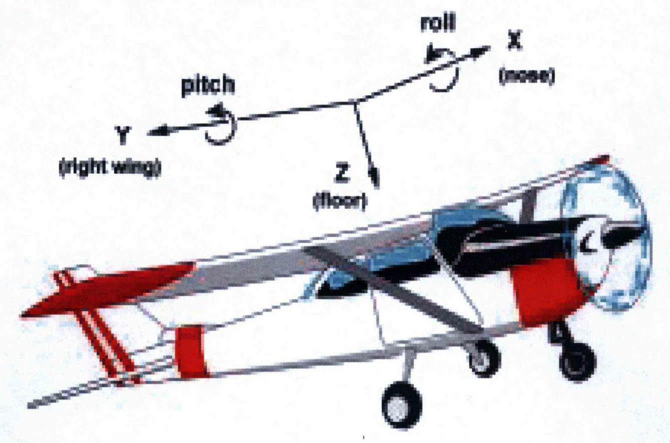

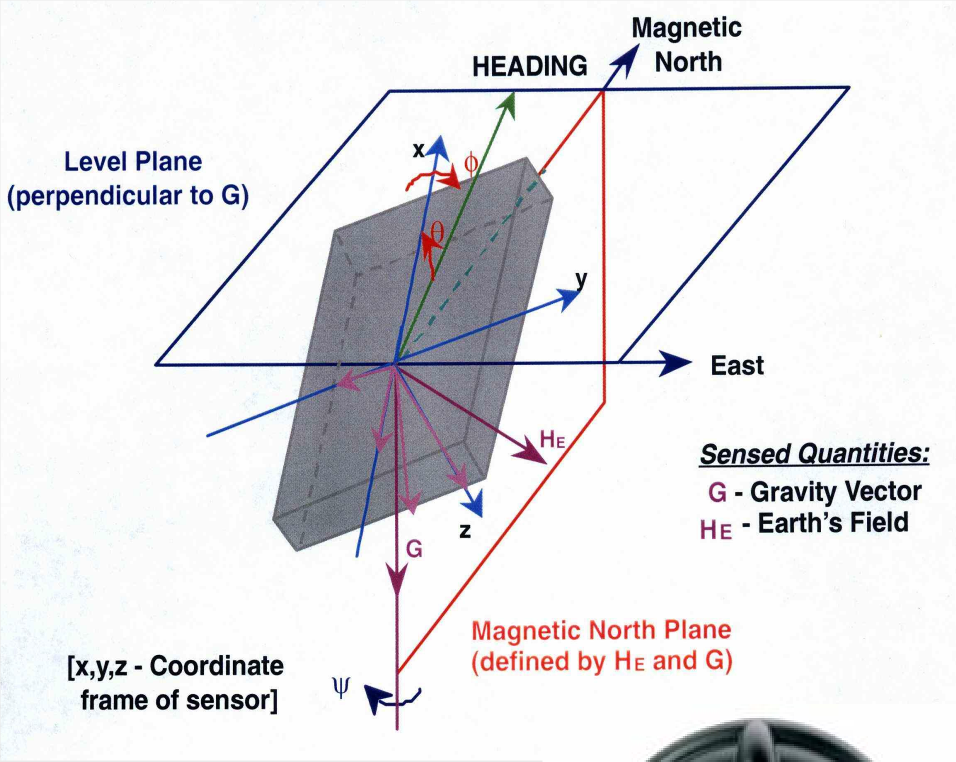

Ref. : www.ssec.honeywell.com

- ➔ 1 triaxial magnetometer → H_E
- ➔ 1 triaxial accelerometer → **G**
- ➔ **G** x H_E = Magnetic East

The simple sailing boat solution →

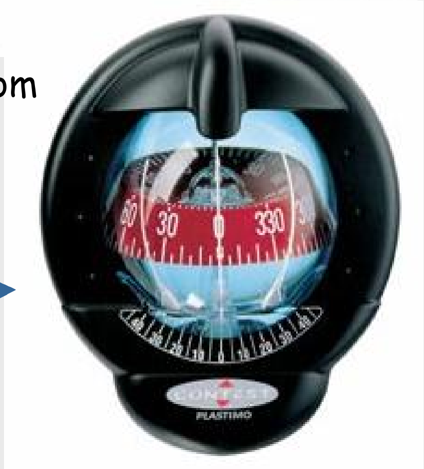

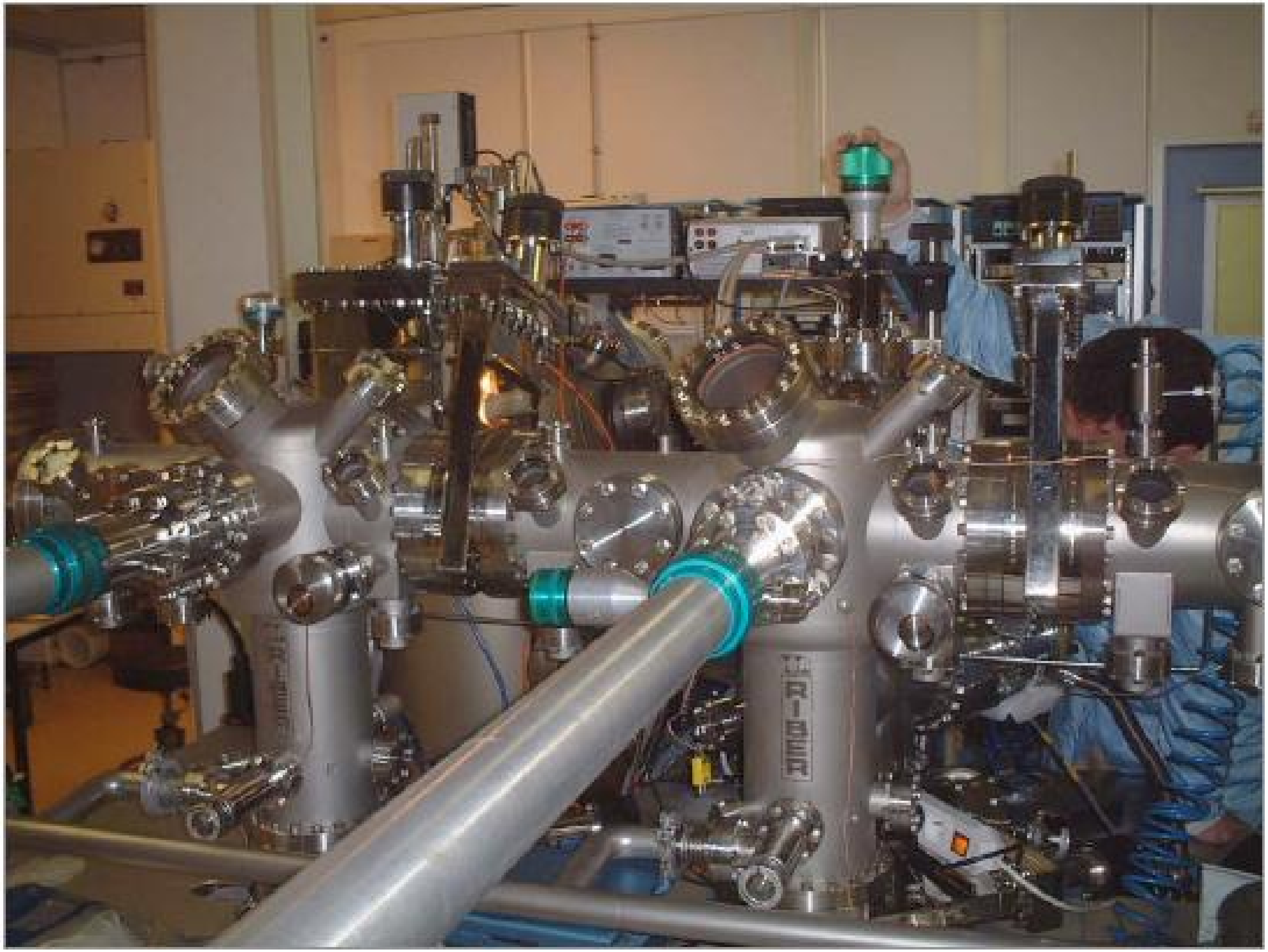
RIBER

Organic spintronics

+

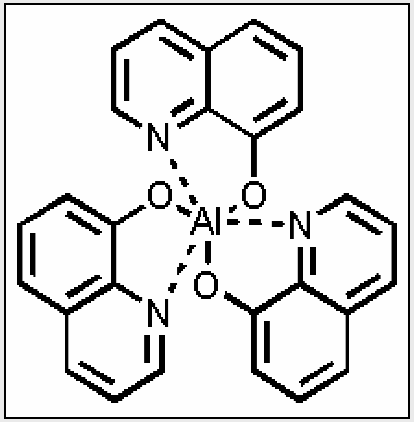

= ?

OS in Spintronics - MOTIVATION

Most organic semiconductors are characterized by very weak spin scattering strength:

- low Spin-Orbit Coupling (low Z values) and
- low Hyperfine Interaction (π-conjugation)

possibility to transport the spin polarized signal to long distances (10^2 nm) even at room temperatures

Technological advantages:

- easy to grow, low sensitivity to impurities
- stable and easily controlable interfaces with many inorganic materials – interface tuning by Self Assembled Monolayers

OUR MAIN APROACH

Direct (current) spin injection in long channels of Organic Semiconductors (>10^2 nm) by using both

conventional - Co, Ni, Fe, …
non-conventional - manganite ($La_{0.7}Sr_{0.3}MnO_3$)

for spin injection and detection

Why manganites –> so far show the best efficiency in applications to Organic Spintronics

easiest way for the investigation of the basic spin physics – still to be understood

Manganites: properties

$R_{1-x}A_xMnO_3$

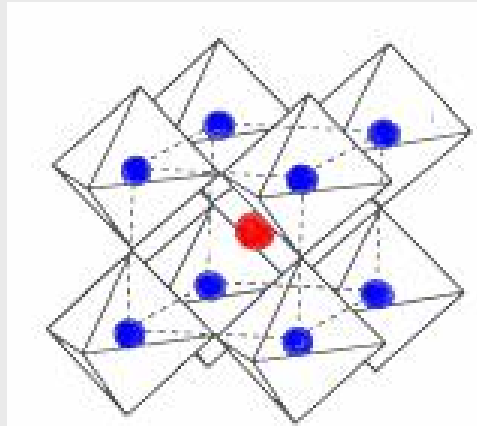

R = La, Pr, Sm..
A = Ca, Sr, Ba…

Mn

Mother system (x=0)

Insulating, AFM

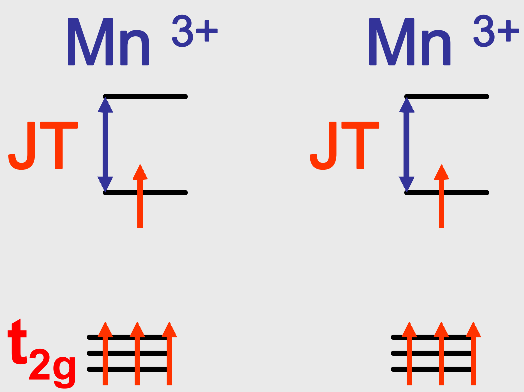

$3t_{2g}$ localized S = 3/2

Mixed valence: Mn^{3+} (1-x), Mn^{4+} (x)

Metallic and FM below Tc

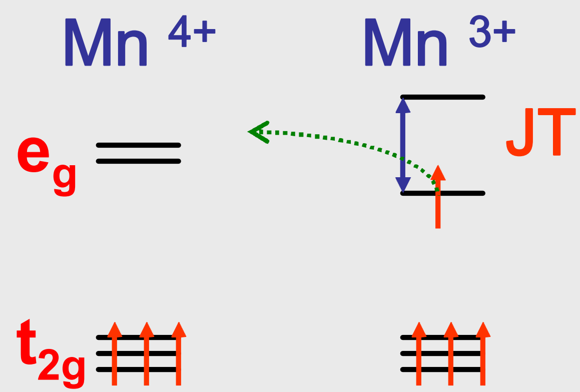

$3t_{2g}$ localized S = 3/2

Phase diagrams of manganites

$La_{1-x}Sr_xMnO_3$

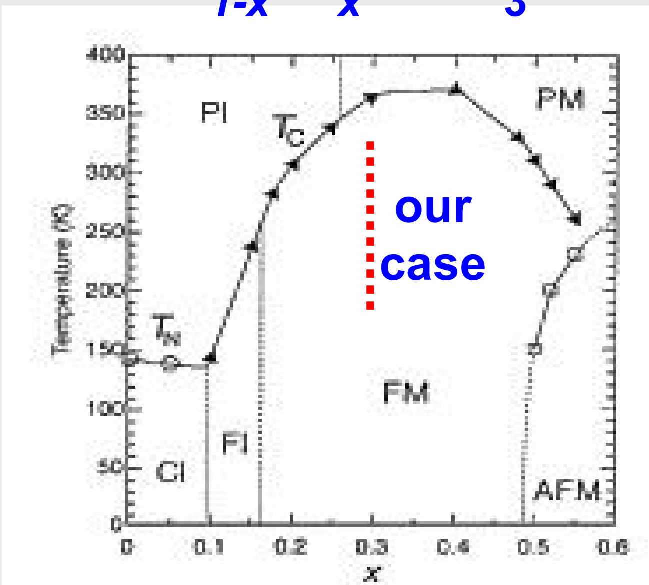

Large bandwidth

Colossal Magnetoresistance

100% spin polarization

$Pr_{1-x}Ca_xMnO_3$

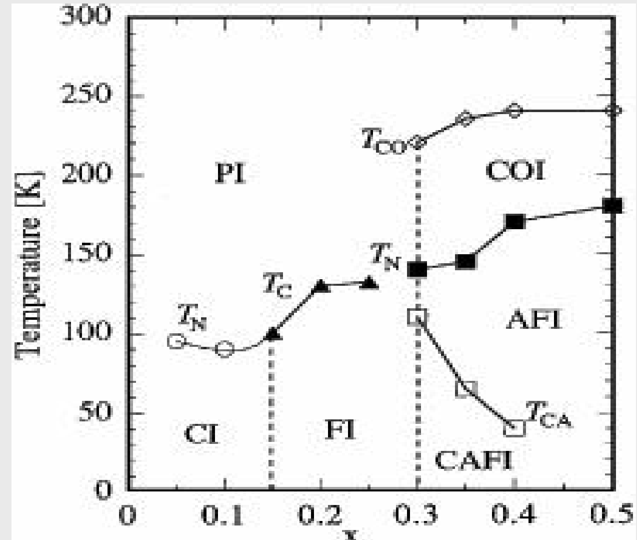

Low bandwidth

Charge-orbital ordering

FM by external stimulation (light, H, E, pressure, X-ray)

FM - ferromagnetic metal,
FI - ferromagnetic insulator,
PM - paramagnetic metal,
PI - paramagnetic insulator,
AFM - antiferromagnetic,
CO - charge ordering
CAFI – canted antiferromagnetic

Magnetic homogeneity in $La_{0.7}Sr_{0.3}MnO_3$ films by SP STM

$T \approx T_C$

4 μm

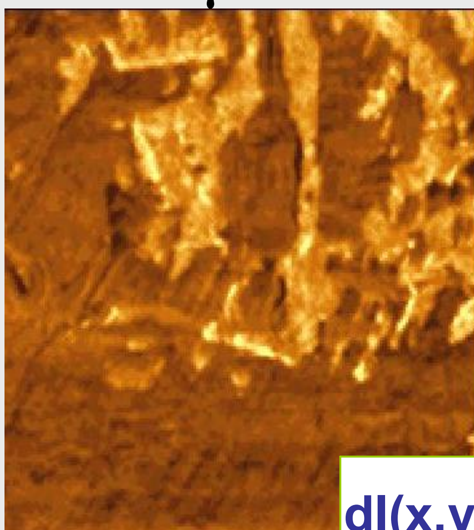

FM ≈ 50%

$T \ll T_C$

4 μm

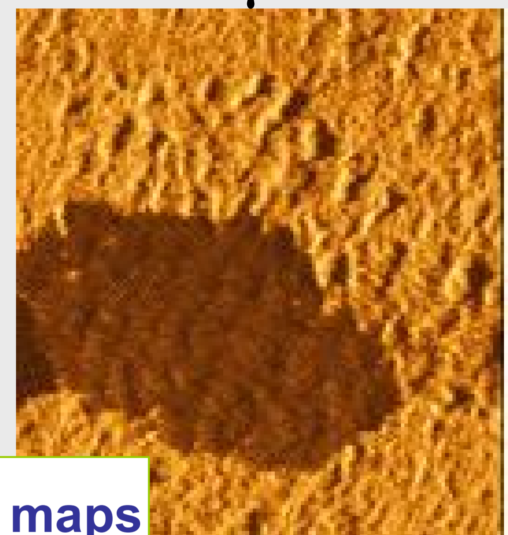

FM ≈ 99%

dI(x,y)/dV maps

High magnetic homogeneity at $T \ll T_C$ results from highly homogeneous oxygen distribution

Facilities involved at ISMN

Film growth:

1. HIGS (Hybrid Integrated Growth System) combining: organic growth chamber (5 + 3 Knudsen cells); Oxide electron beam ablation chamber (4 targets – manganite, magnetite, …); FM metals (3 e-guns); analysing chamber (MR, EL, PL, MOKE)
2. 2 independent PPD (electron beam ablation) for various oxides

Characterizations:

- **Magnetoresistance at low and high magnetic fields (7 T)**
- **MOKE**: 632 nm, temperature 4,2-400 K, up to 1 Tesla
- Time resolved Magneto - **Optical spectroscopy**: EL and PL as function of Field, 100 ps – 1 ms
- **Micro-Raman**
- **STM, AFM + STM spectroscopy with SP tips**

- **Spin Polarized STM** – UHV, variable T (100 –1000K), 0-1000 Oe

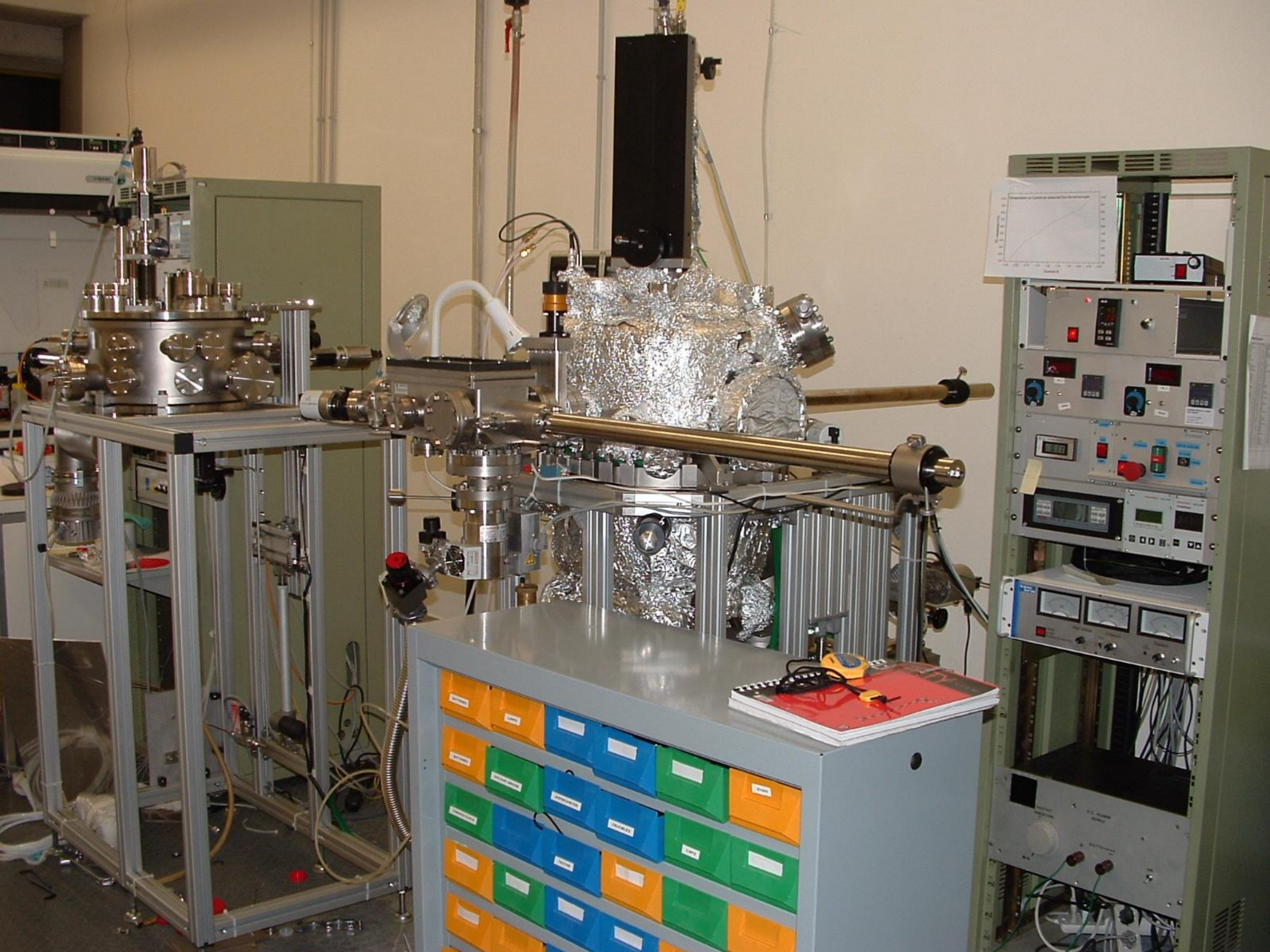

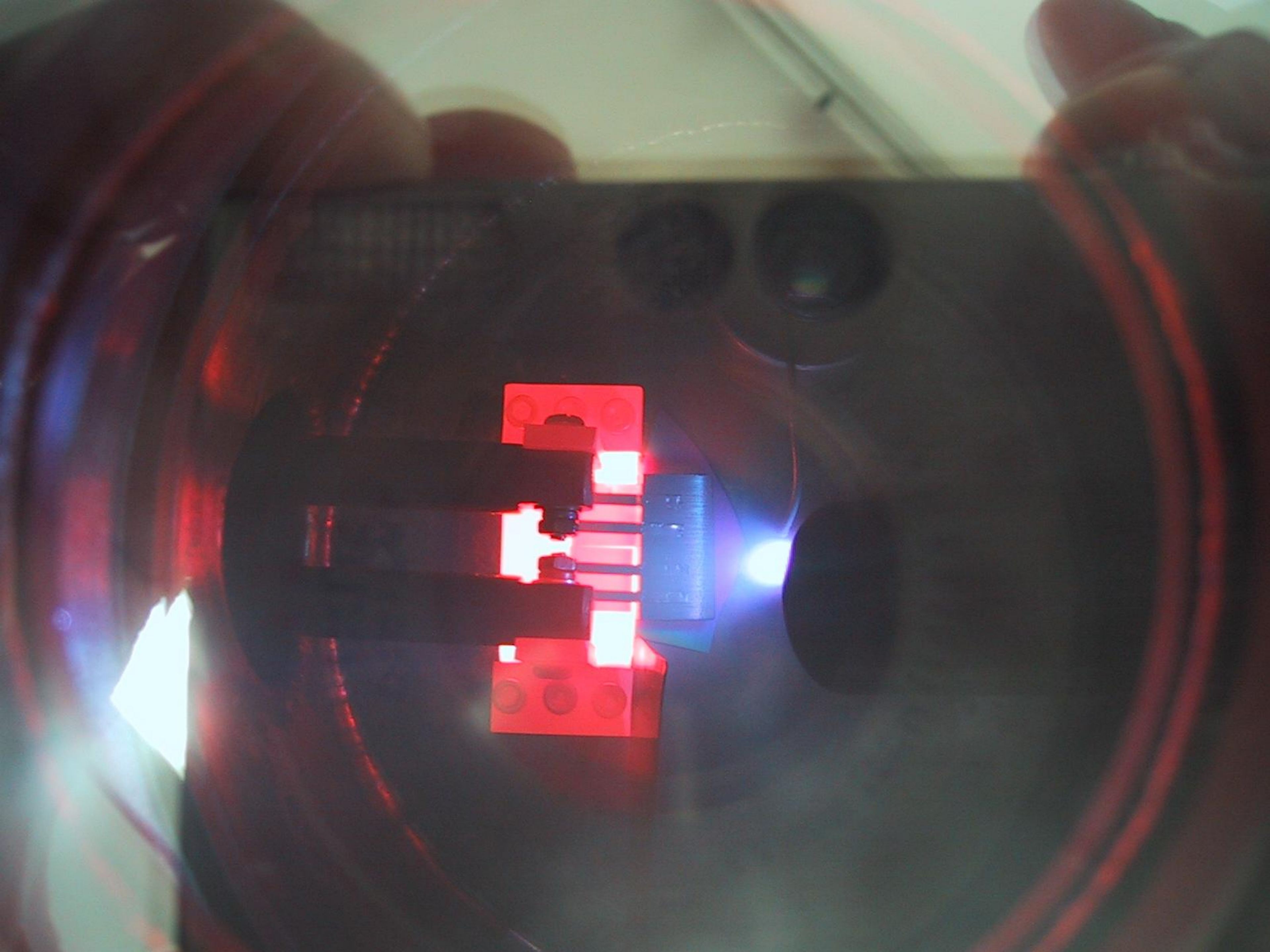

$La_{0.7}Sr_{0.3}MnO_3$ films by electron beam ablation

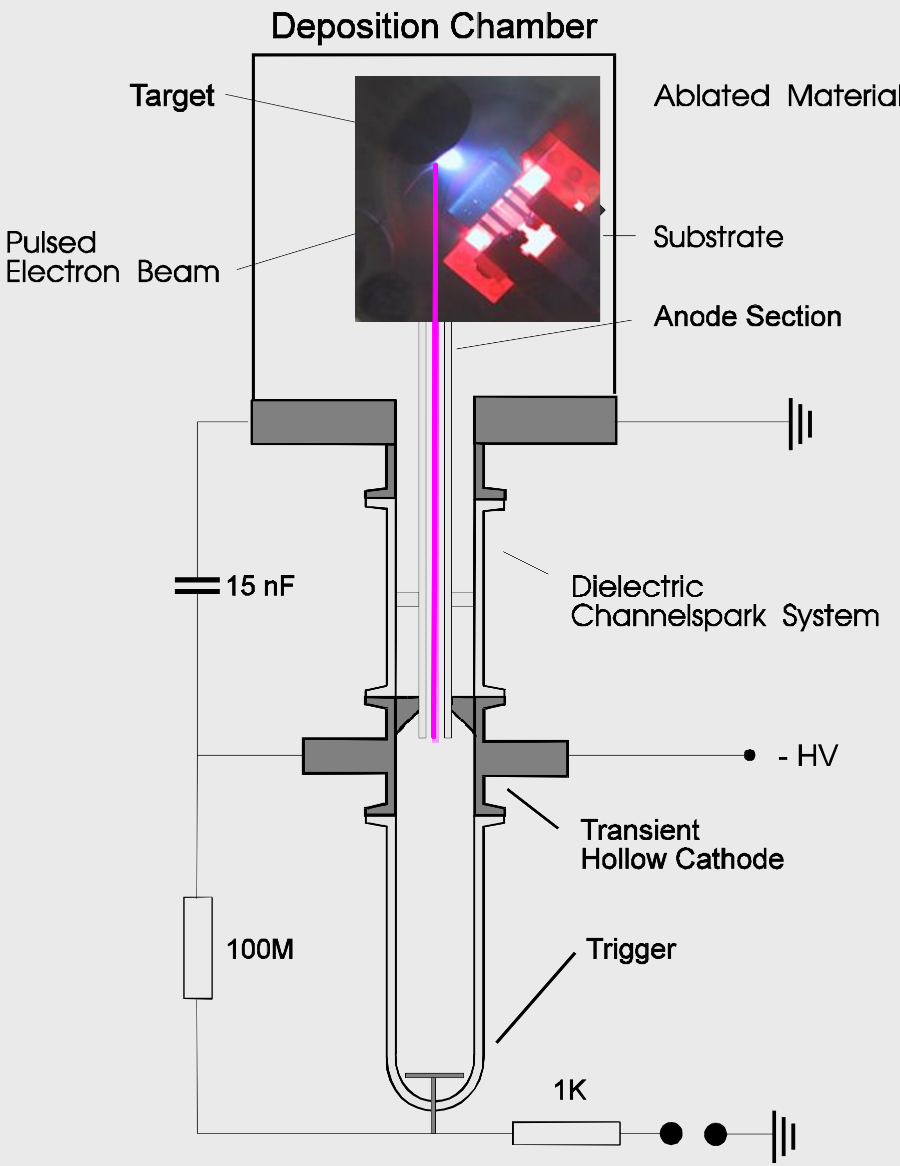

AFM: 50nm LSMO film

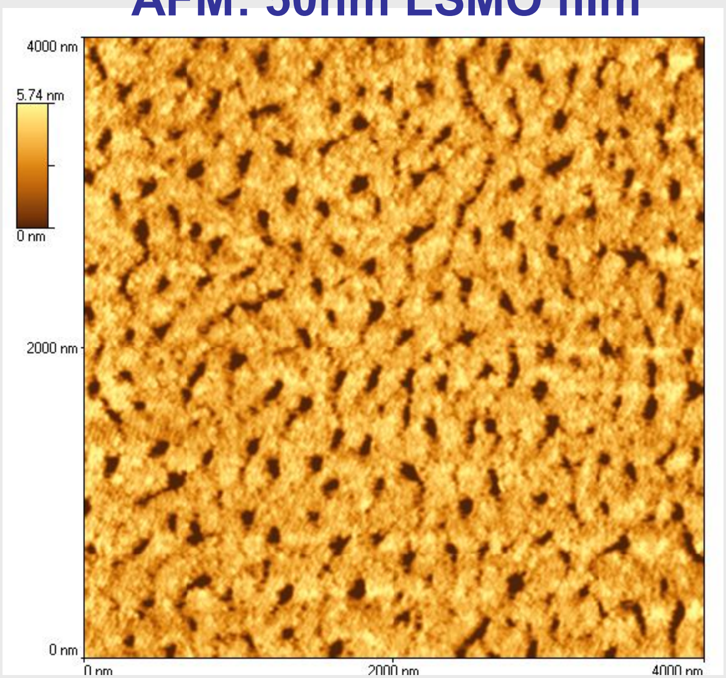

Supercon. Sci. Technol. **8**, 160 (1995)
Phys. Stat. Sol. 215, 1443 (1999)

6T monolayers on LSMO

A) grow a 6T film, desorb multilayers by annealing

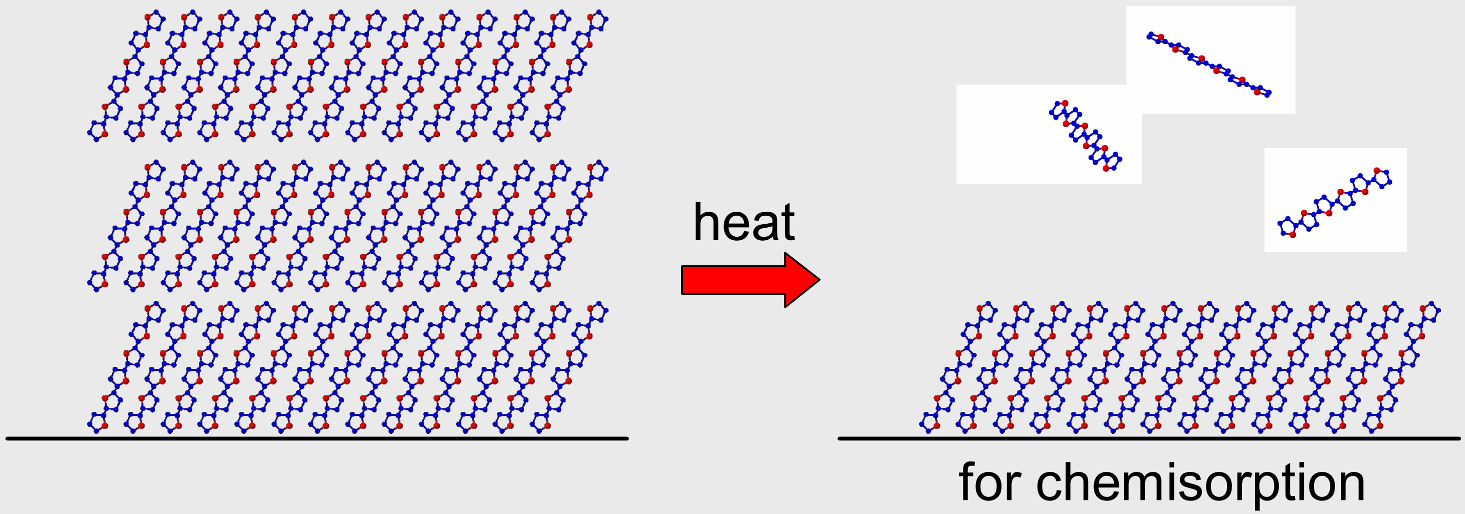

B) gradual deposition

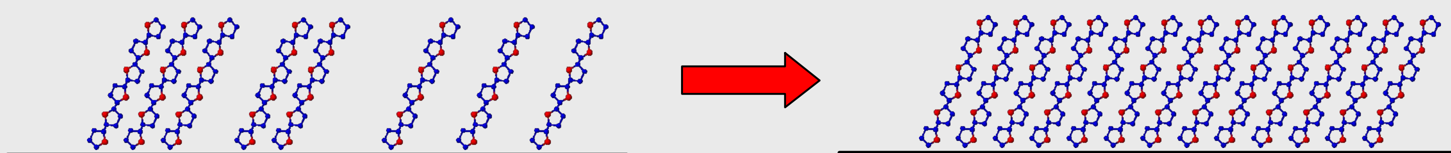

First Organic MR device

V. Dediu, C. Taliani et al.
Sol. St. Comm.122 (2002),181
Patent US6325914

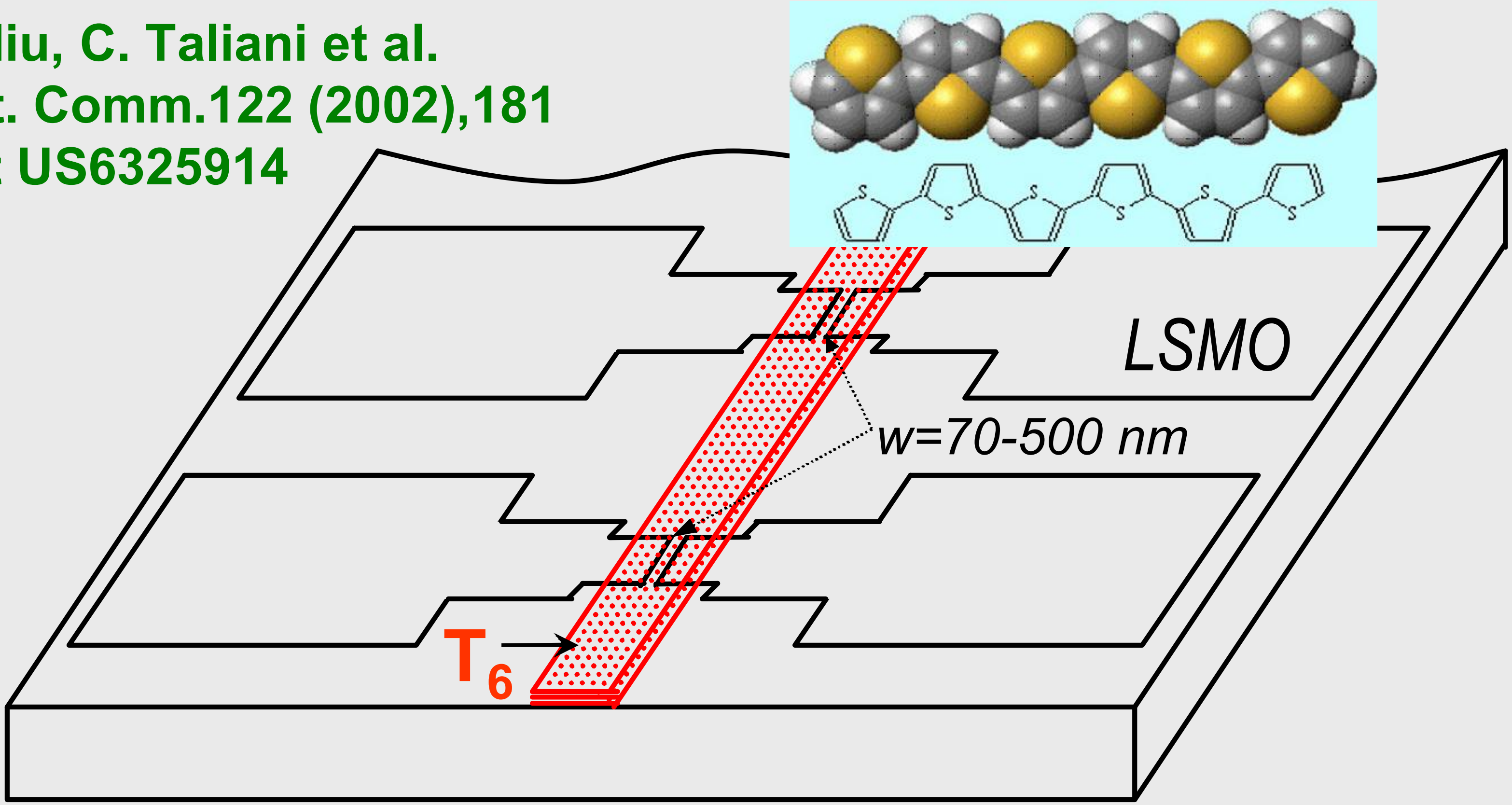

Large negative magnetoresistance measured

Advantage: NO short circuits!

Problem: not possible (at least not at all easy) to reach AP configuration.

Magnetoresistance across LSMO-T_6-LSMO devices

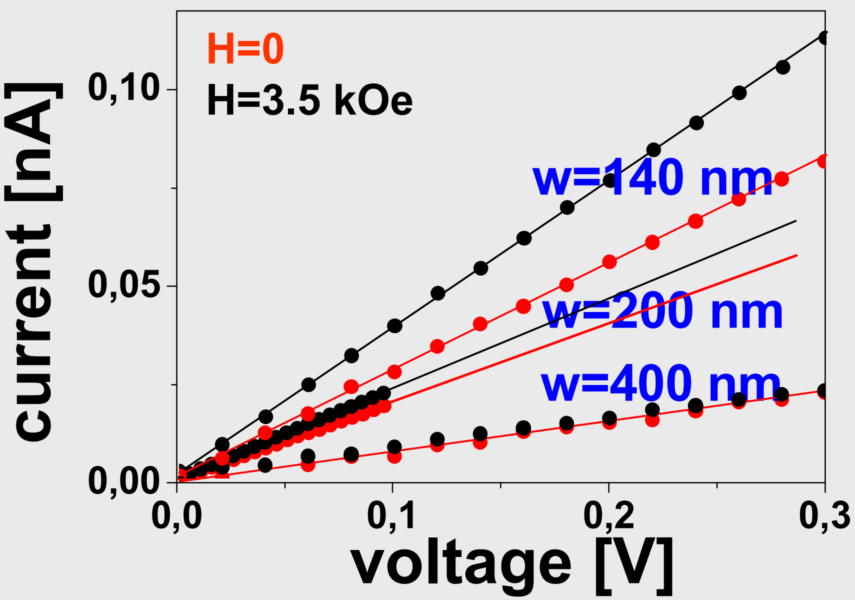

Spin valve effect (negative Magnetoresistance):

a) **Spin polarized injection** at interface

b) **Spin polarized transport** between electrodes

LSMO work function (4.5-4.7 eV) close to T_6 HOMO

V.Dediu,C.Taliani et al. Sol.St.Comm.122,(2002),181

Magnetoresistance vs channel length

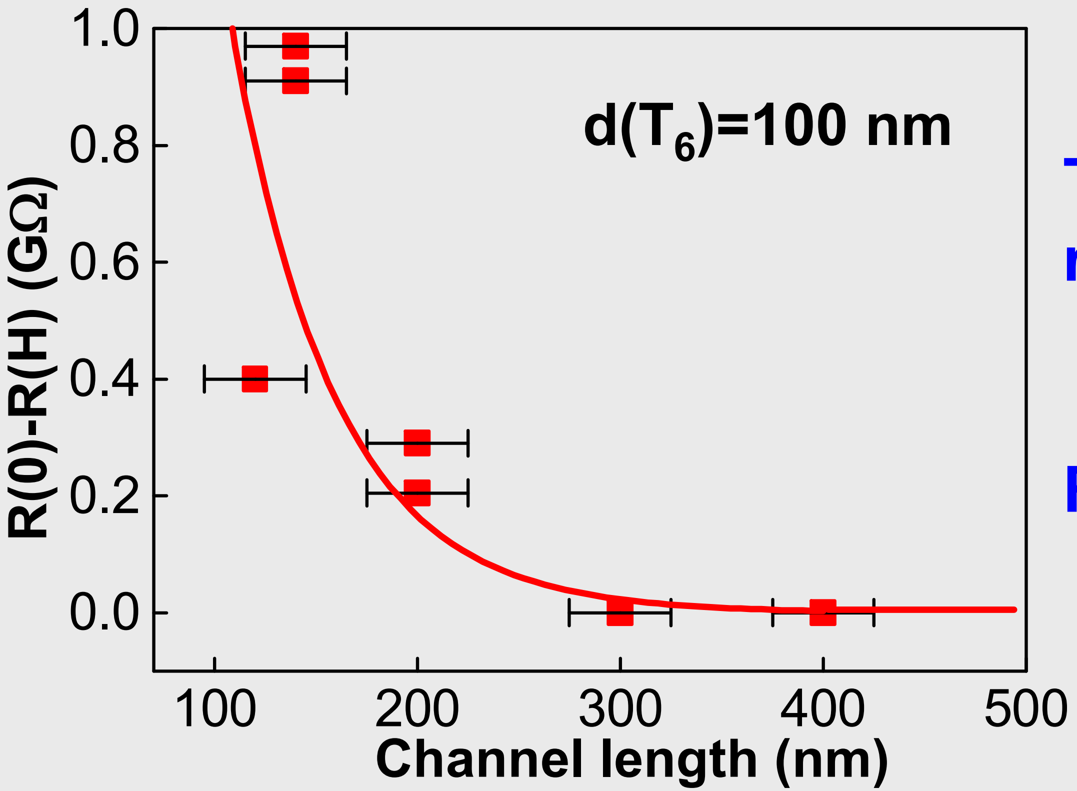

Total LSMO/T6/LSMO resistance scales with *w*

Resistivity $\rho = 10^6\ \Omega$cm

Spin relaxation length $L_S \sim 70$ nm

Spin relaxation time $\tau \sim 10^{-6}$ s

Demonstration of the Spin Valve effect

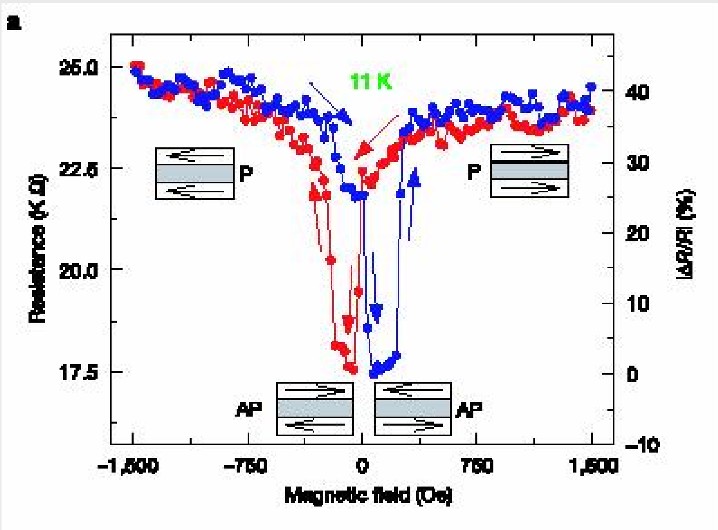

$La_{0.7}Sr_{0.3}MnO_3$/Alq3(130nm)/Co

↓

becomes most used OS in organic spintronics

Z. H. Xiong, V. Vardeny et al.
Nature 427, 821 (2004)

Inverse spin valve effect:

The inverse magnetoresistance was explained by the opposite spin polarizations of the LSMO and of the Co d-bands at the Fermi level

↓

While this explanation looks qualitatively convincing, the detailed mechanism of the inverse spin valve effect is still debating: see the presentation of L. Hueso (Tuesday)

Organic Spintronics - publications

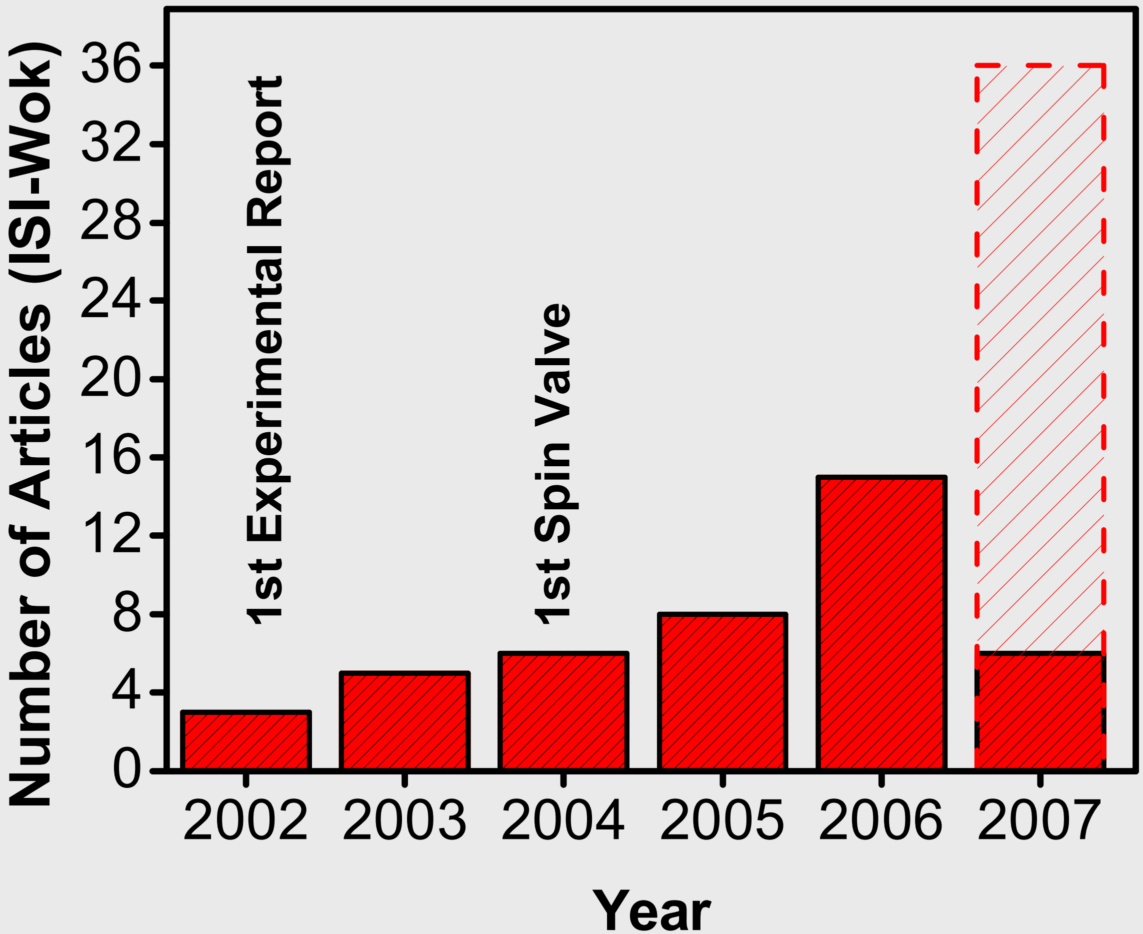

10 nm thick LSMO/NGO film at room temp.

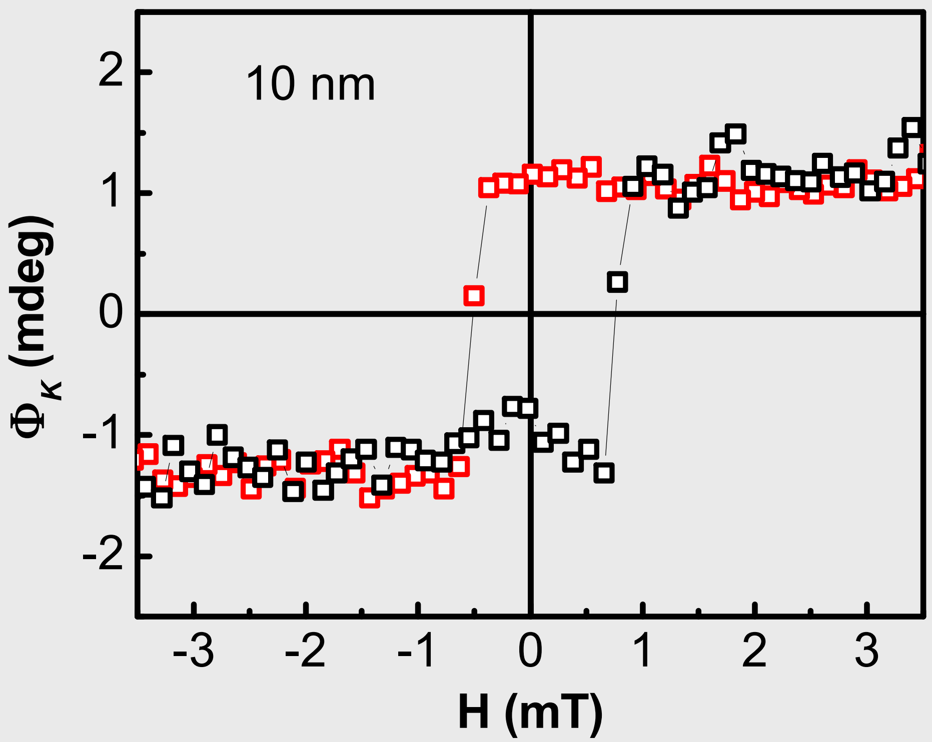

MOKE characterization

MOKE setup built at ISMN by T. Mertelj

4 nm thick LSMO film at room temp.

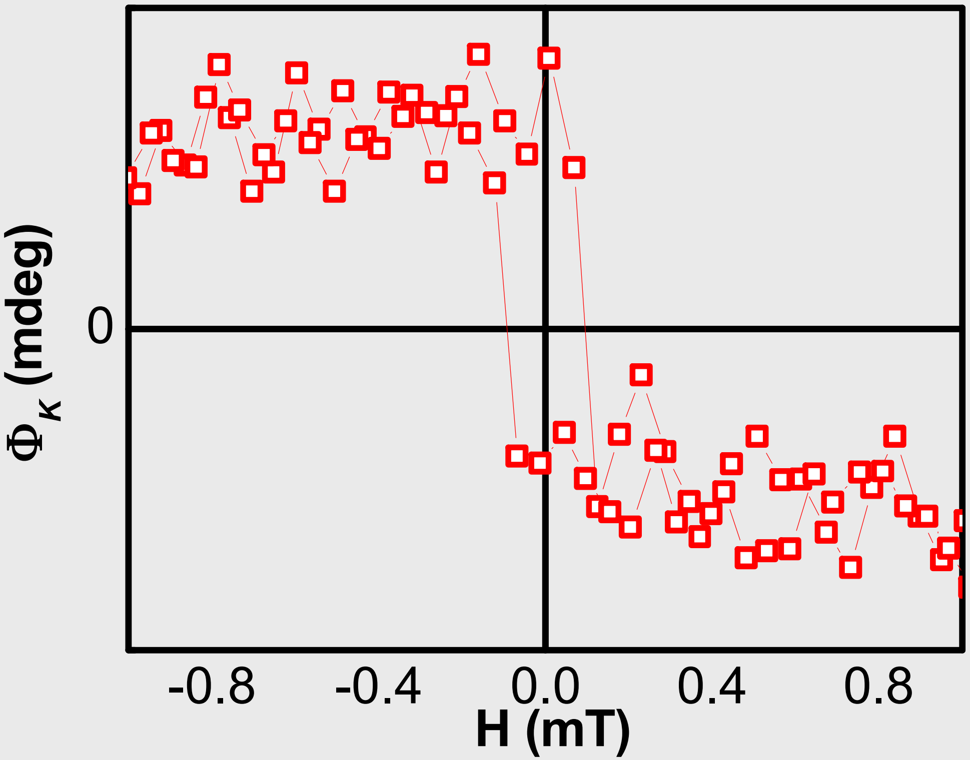

Coercive field
H_C= 5 Oe

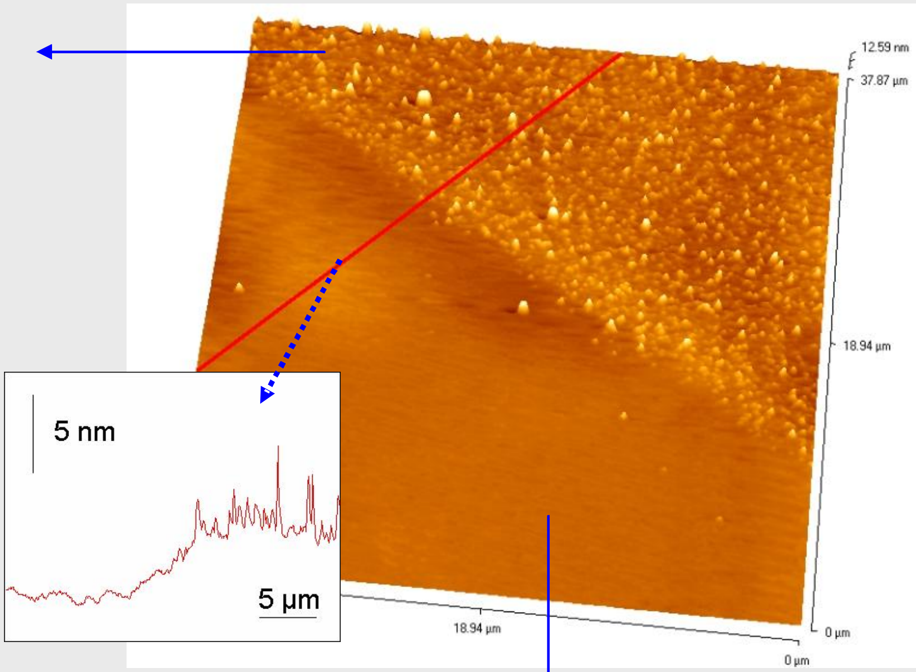

NdGaO$_3$

Film thickness: 4nm

XMCD of LSMO on Si

Element specific, "surface sensitive" magnetic moments

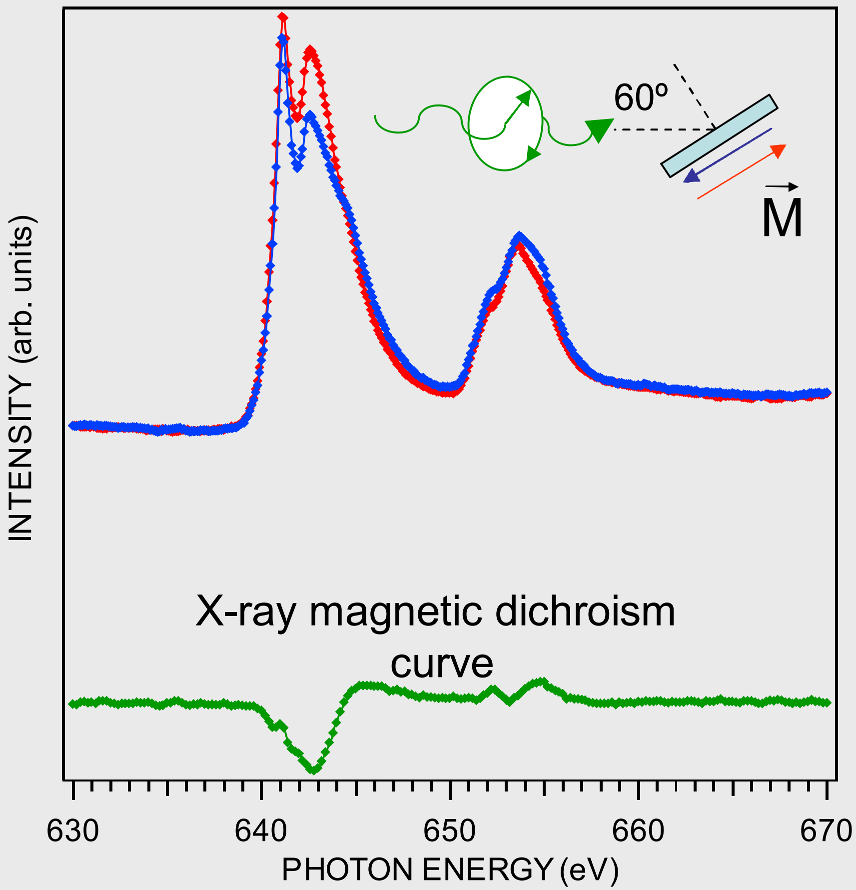

Non-epitaxial LSMO, but clearly ferromagnetic at RT

Vertical Spin Valve geometry

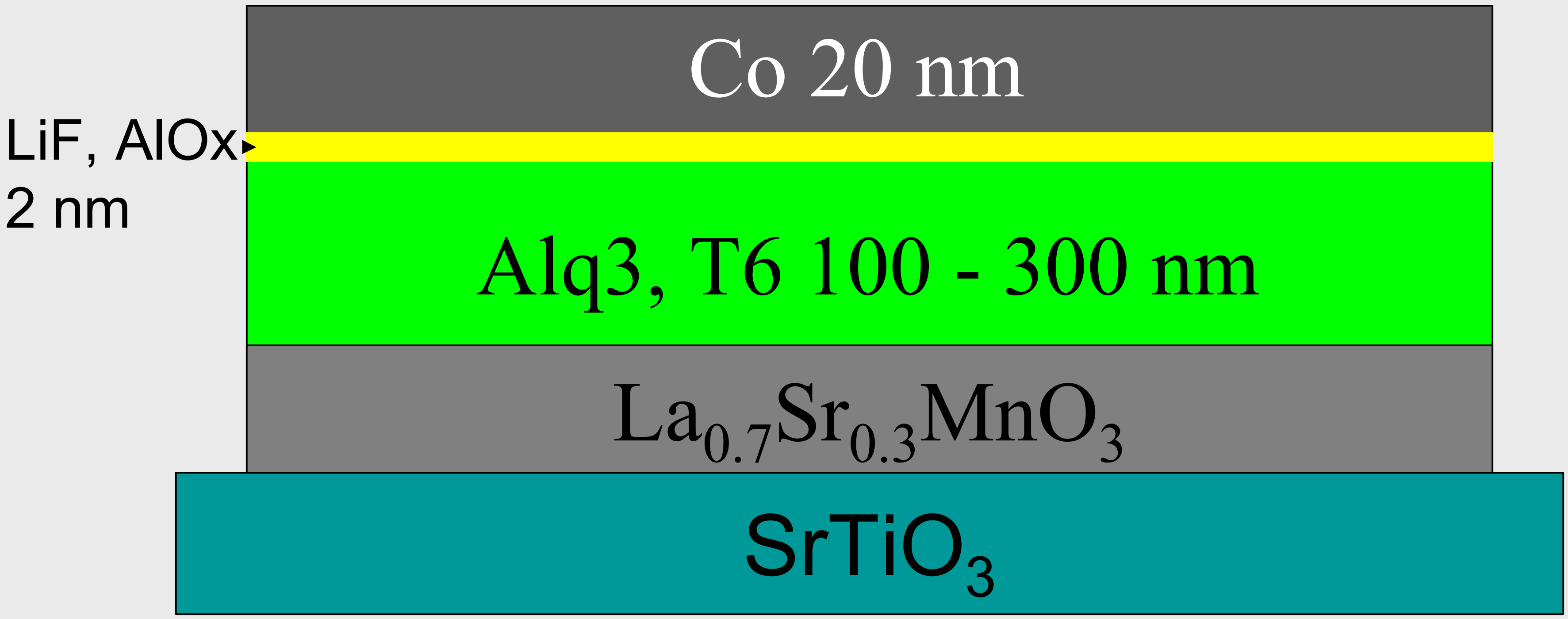

Tris(8-hydroxyquinoline)aluminium (Alq3)

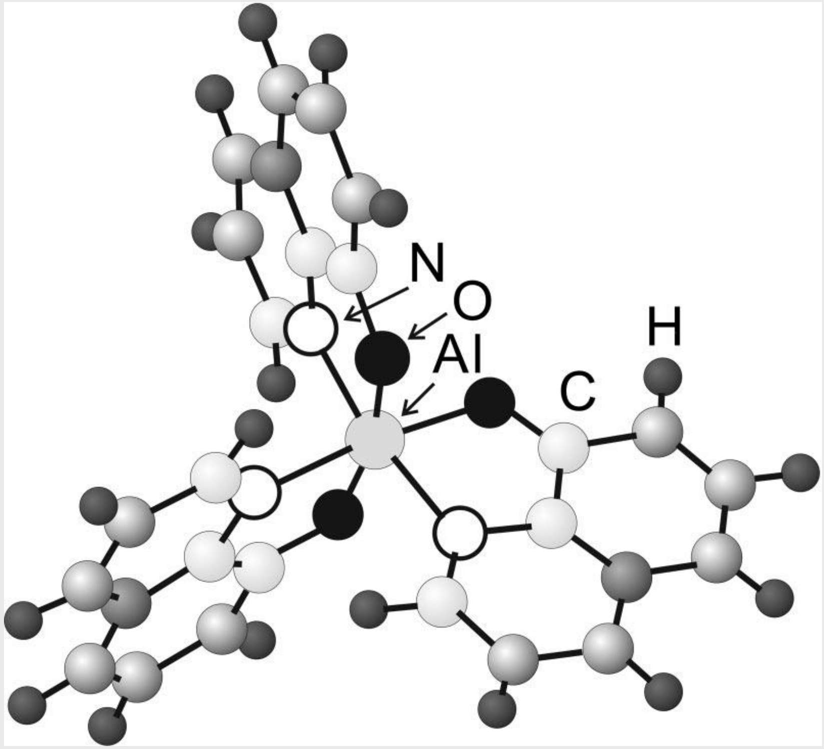

Material widely used in organic LEDs – UHV Molecular Beam Dep.

Forms ordered polycrystalline films at 120-150°C substrate T – rough surface

Forms amorphous films at room substrate T – smooth surface

Van der Waals interaction between molecules

LSMO/Alq3/TB/Co Spin Valve: IV curves

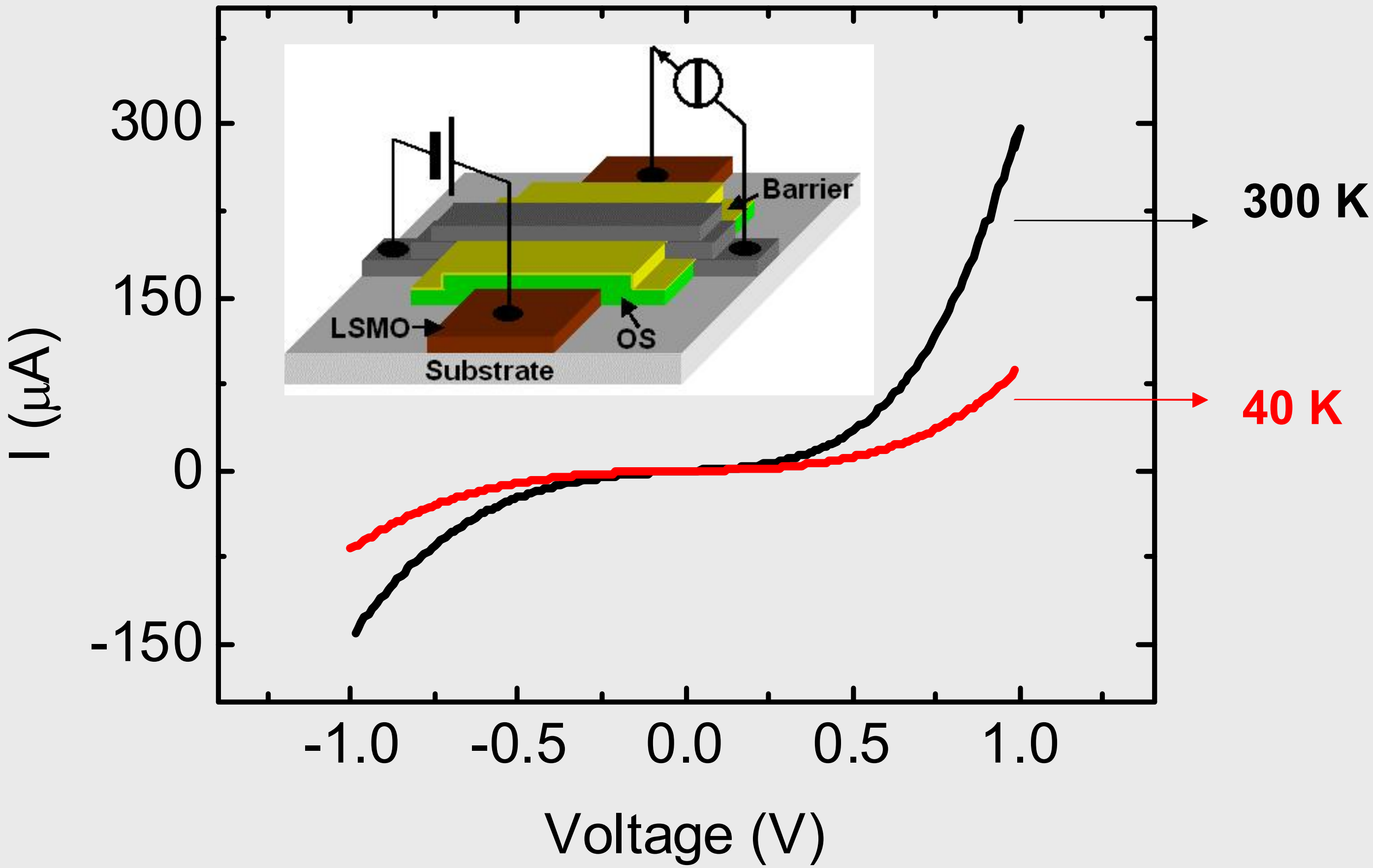

Insulating like behavior is typical for most spin valve devices

Immagazzinamento di informazioni e sensoristica nanomagnetica a base di dispisitivi spintronici ibridi

Dediu et al. Nature Mat. submitted

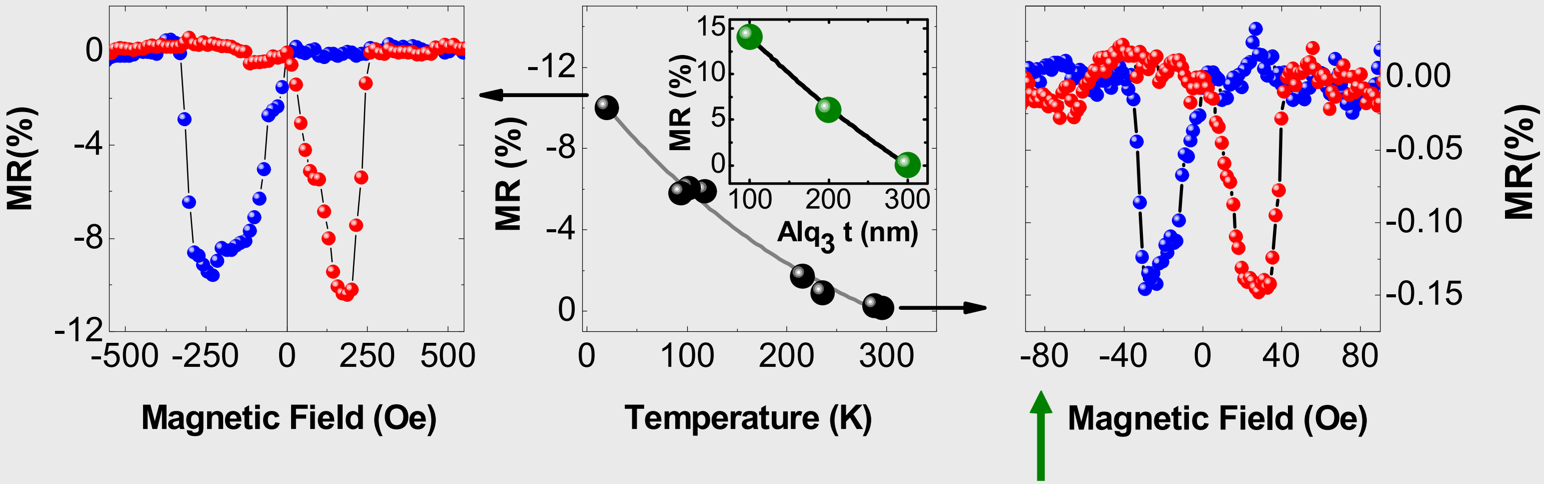

Raggiunto il funzionamento stabile a temperatura ambiente

Refflettometria raggi-X, MOKE

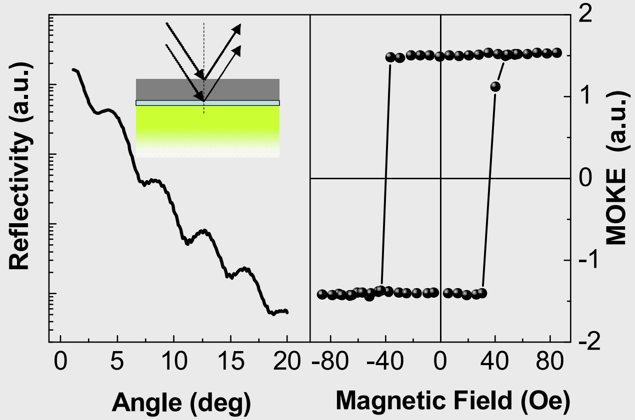

Sviluppati nuovi approcci di crescita dei metalli (magnetici) sopra i semiconduttori organici: raggiunte interfacce molto “sharp” e parametri magnetici di altissimo livello

a)

b)

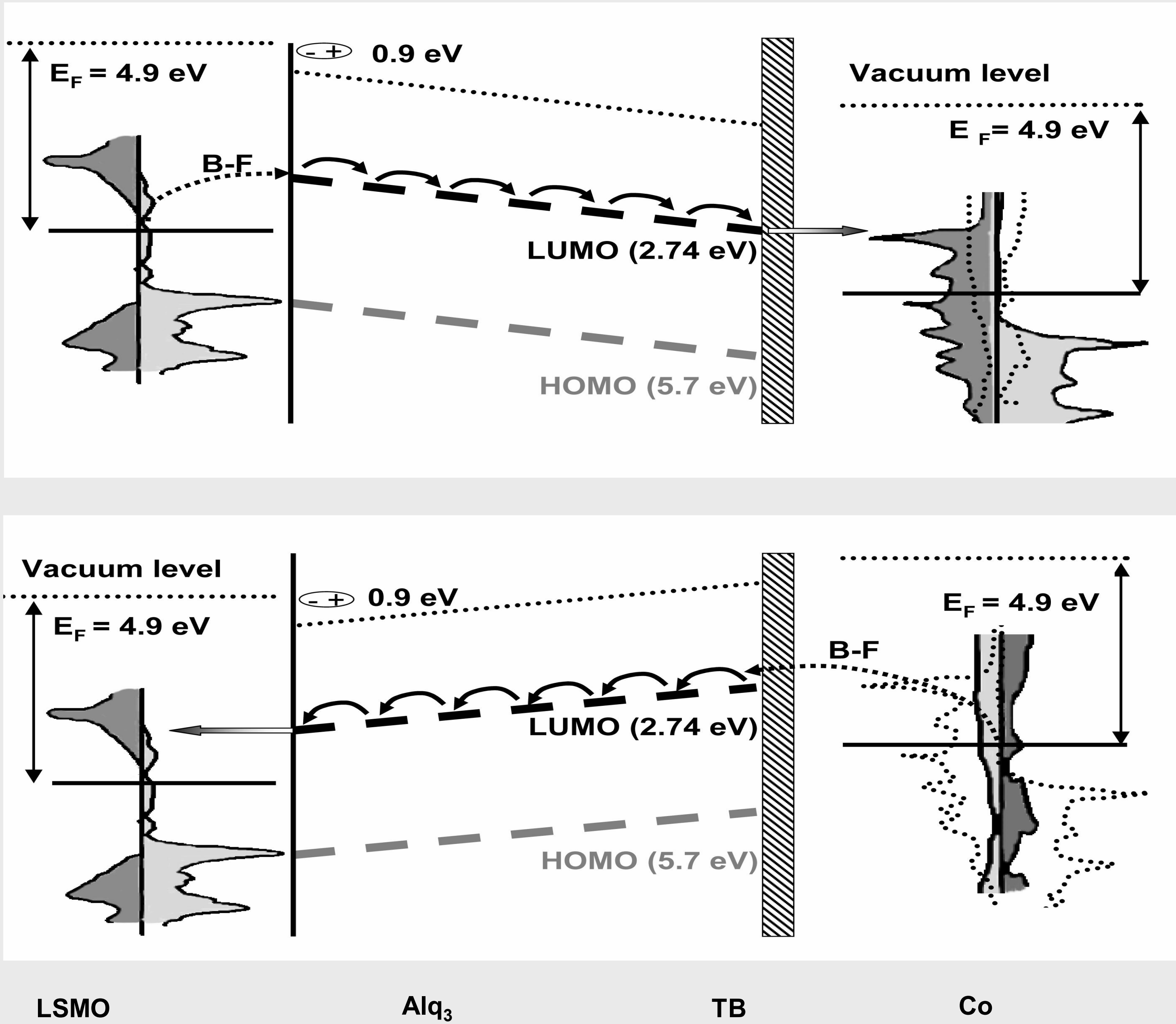

0.9 eV
E_F = 4.9 eV
Vacuum level
E_F = 4.9 eV
B-F
LUMO (2.74 eV)
HOMO (5.7 eV)
Vacuum level
0.9 eV
E_F = 4.9 eV
E_F = 4.9 eV
B-F
LUMO (2.74 eV)
HOMO (5.7 eV)
LSMO
Alq3
TB
Co

PLANAR DEVICES

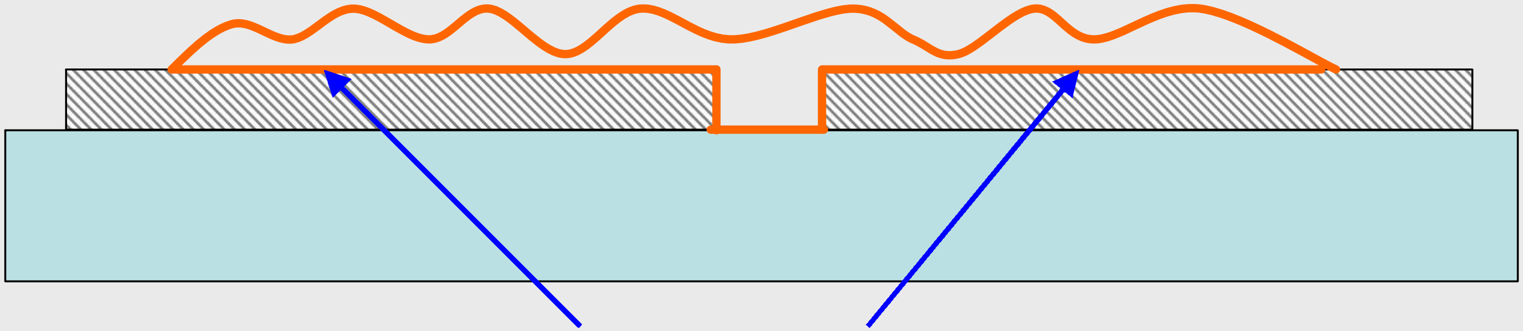

TWO “PERFECT” INTERFACES

VERTICAL DEVICES

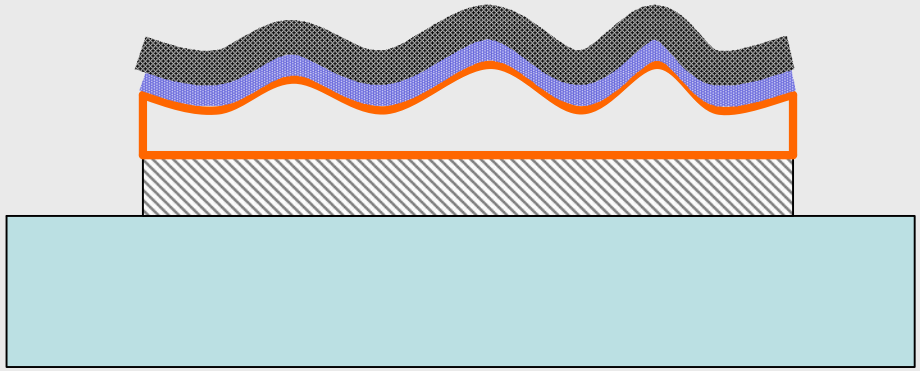

ONE “PERFECT” AND ONE “VERY BAD ”INTERFACE

Dimostrazione di memoria elettrica non-volatile in dispositivi spintronici ibridi: la possibilità di cambiare tra due stati di resistenza “scrivendo” con voltaggi positivi (1) e negativi (0)

Hueso, Dediu et al. Adv. Mat. 2007

up to room T

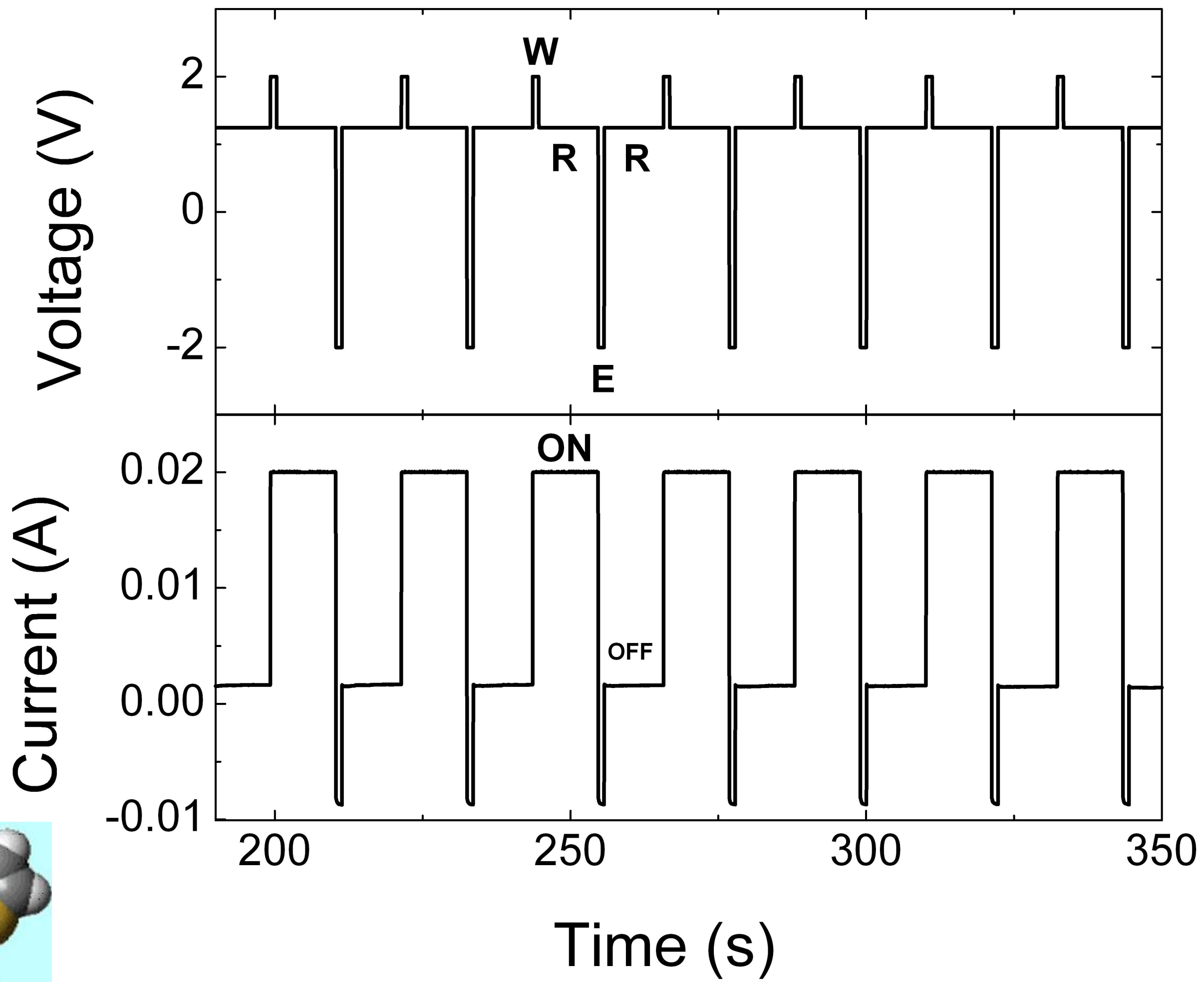

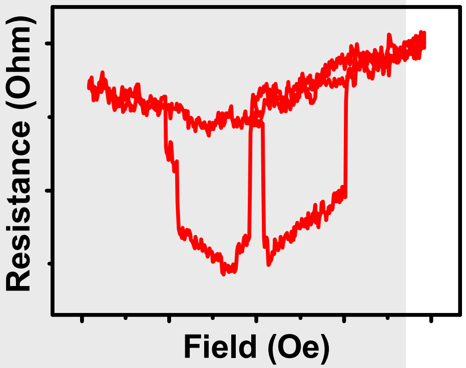

Principi della sensoristica magnetica a base dispositivi spintronici: nano-imaging

La resistenza del dispositivo cambia drasticamente tra gli stati di magnetizzazione parallela e antiparallela

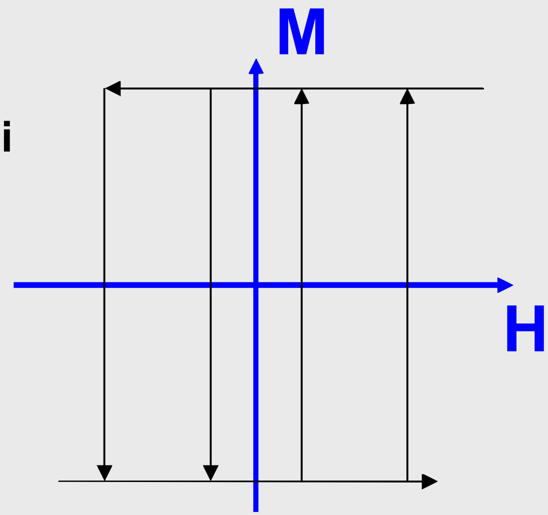

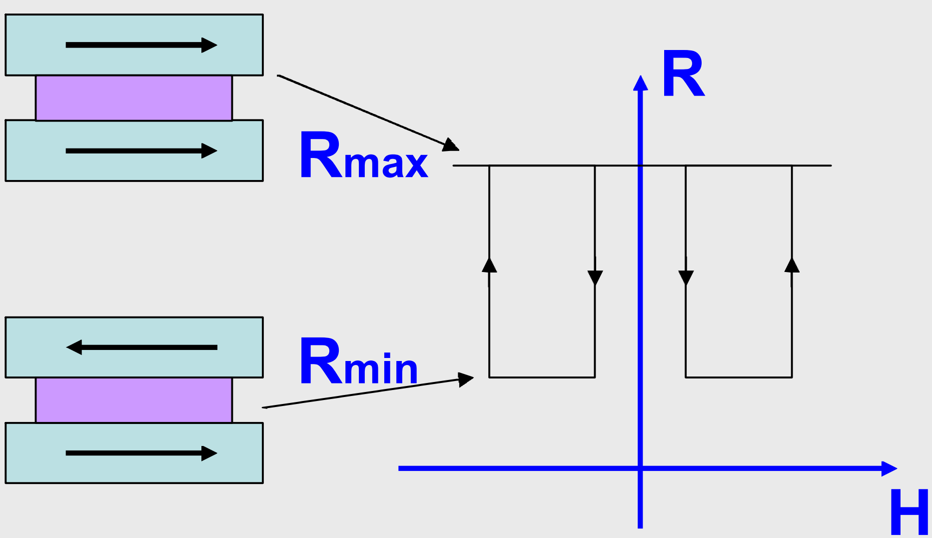

Il passaggio della nanoparticella magnetica inverte la magnetizzazione del elettrodo di sopra

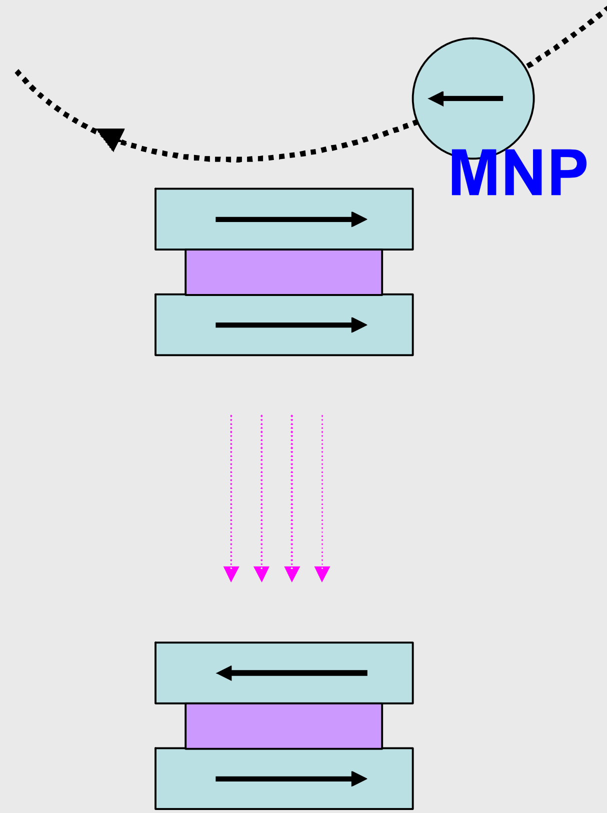

New EBL geometry: interdigitated strips

Au pads

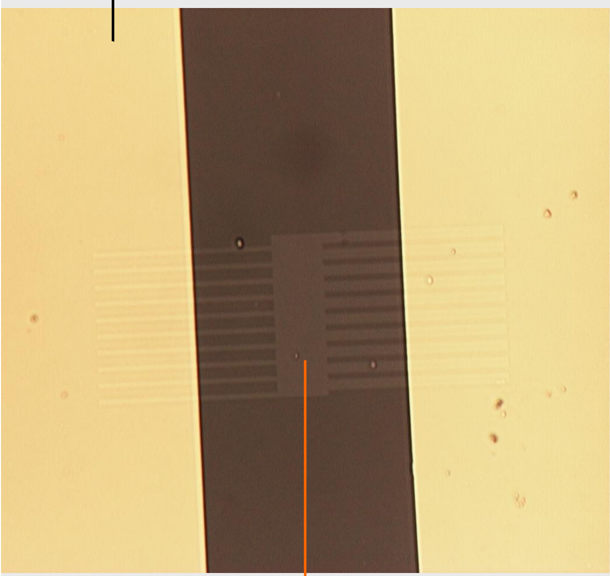

LSMO contacts

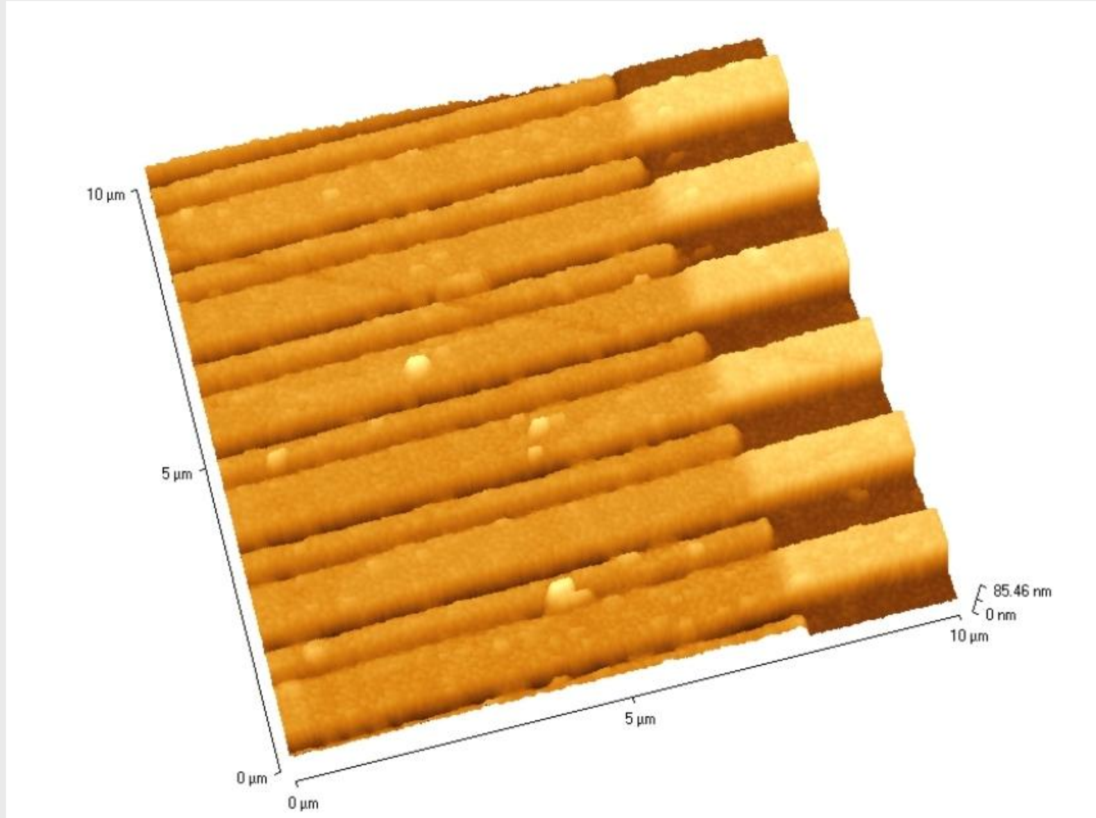

Alq3/LSMO

Manganite based OLEDs

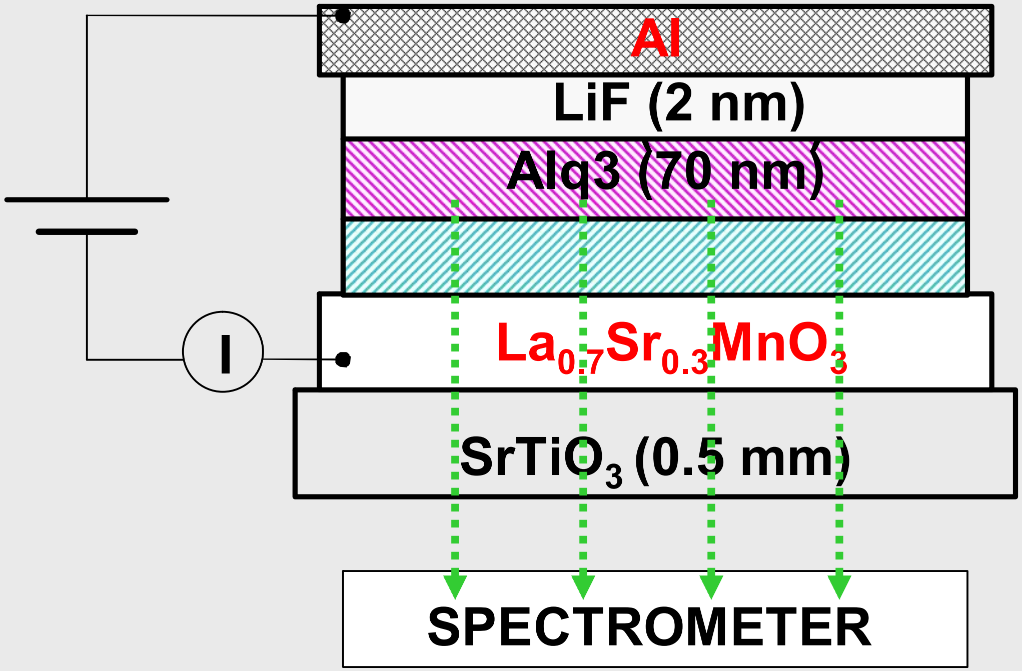

OLED off

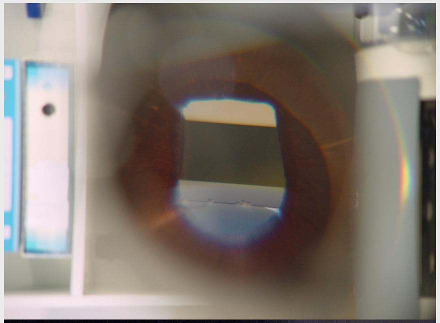

OLED on

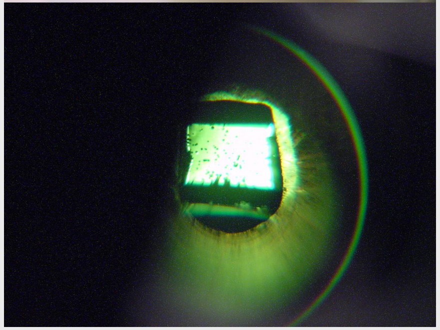

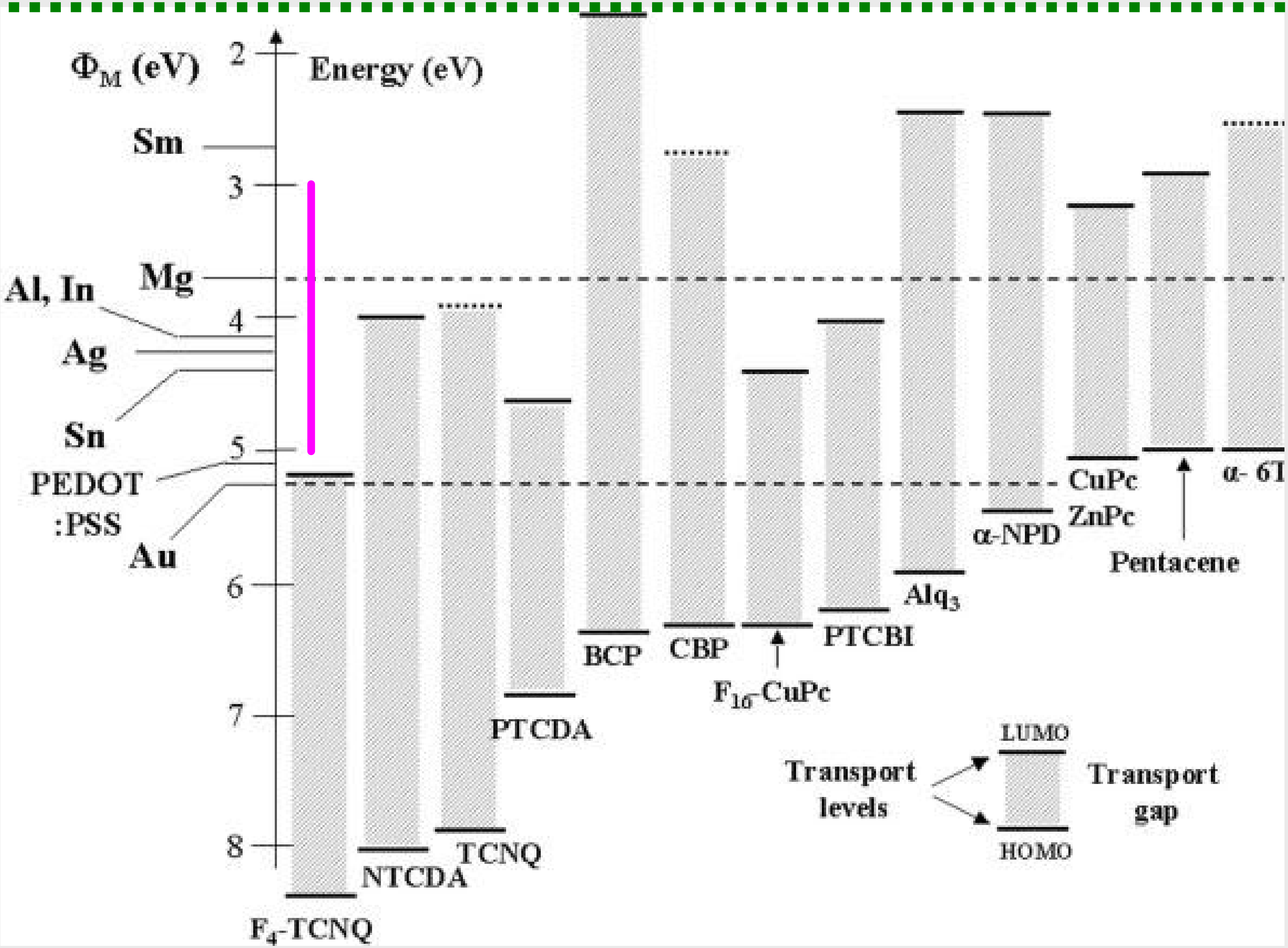

ANTOINE KAHN, NORBERT KOCH, WEIYING GAO

Optical transmission of $La_{0.7}Sr_{0.3}MnO_3$ ferromagnetic films at 300 K

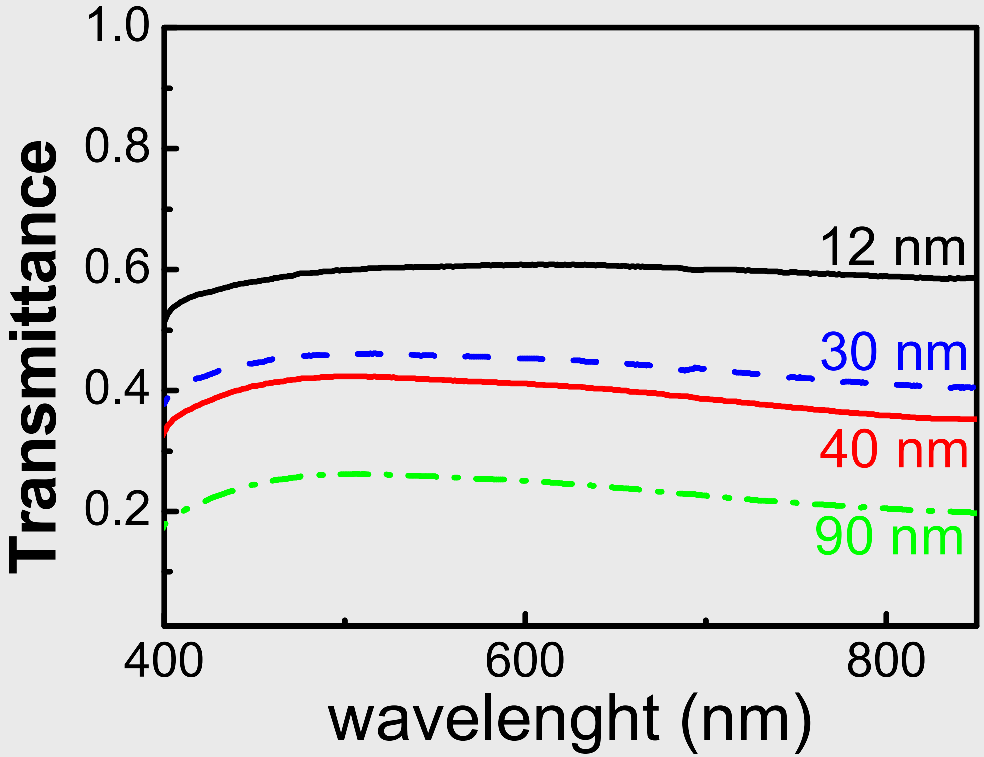

Single Spin Polarized Electrode AlQ_3 OLED (LSMO and Iron)

Electroluminescence

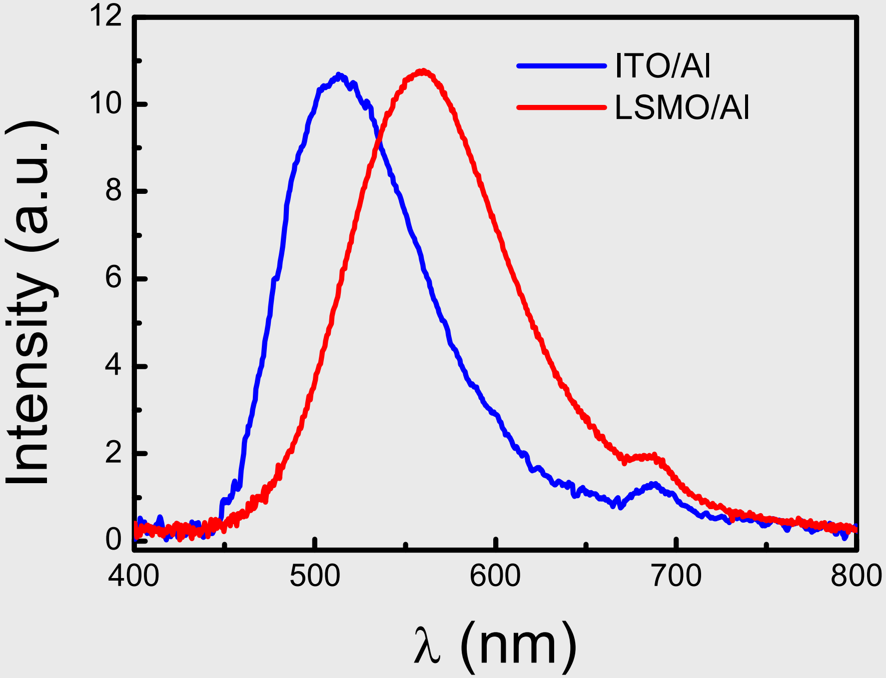

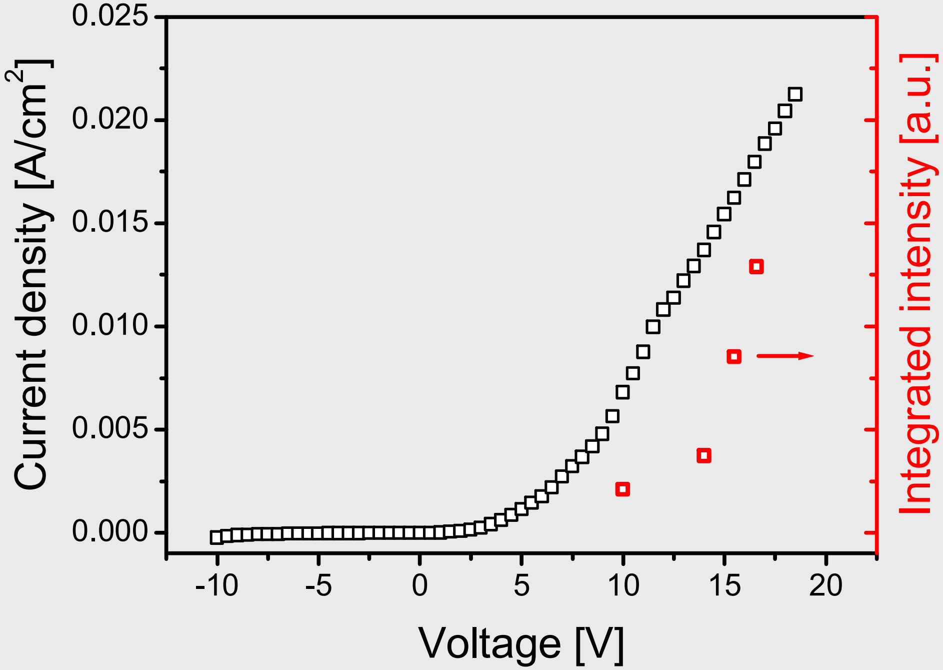

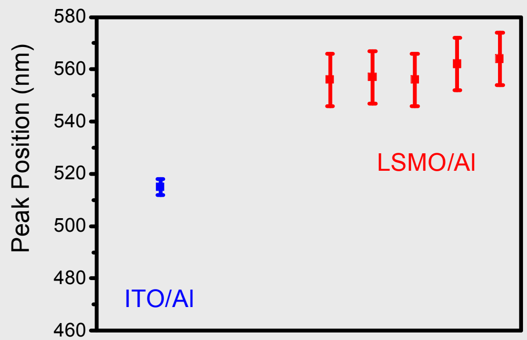

EL threshold at V_T= 6 V

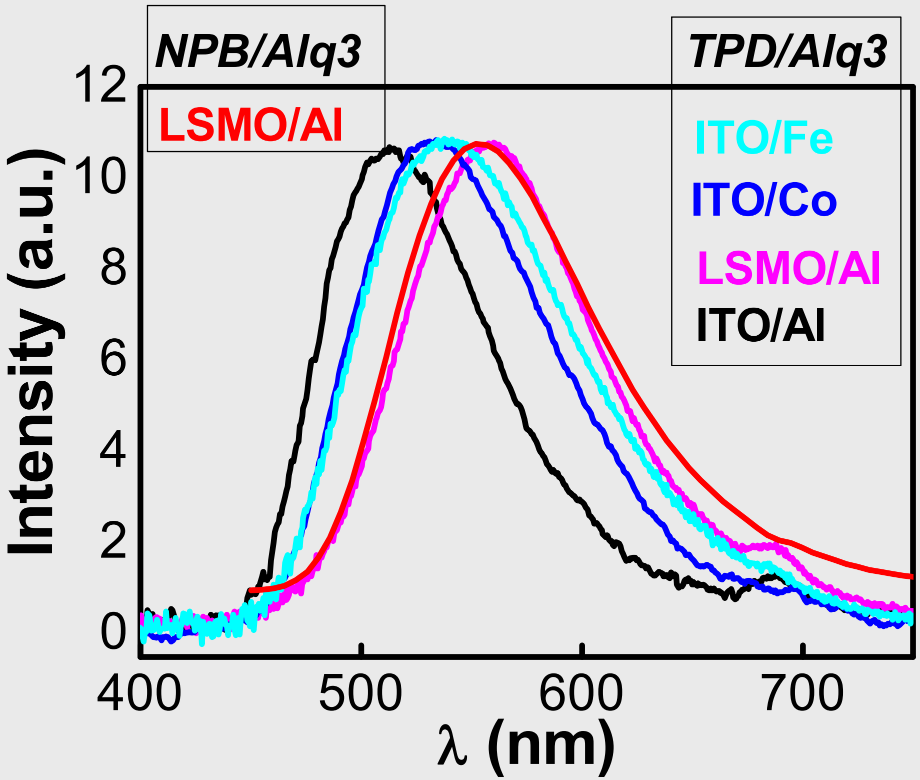
NPB/Alq3
LSMO/Al
TPD/Alq3
ITO/Fe
ITO/Co
LSMO/Al
ITO/Al
Intensity (a.u.)
λ (nm)
0
2
4
6
8
10
12
400
500
600
700

Tris(8-hydroxyquinoline)aluminium (Alq3)

Alek Dediu

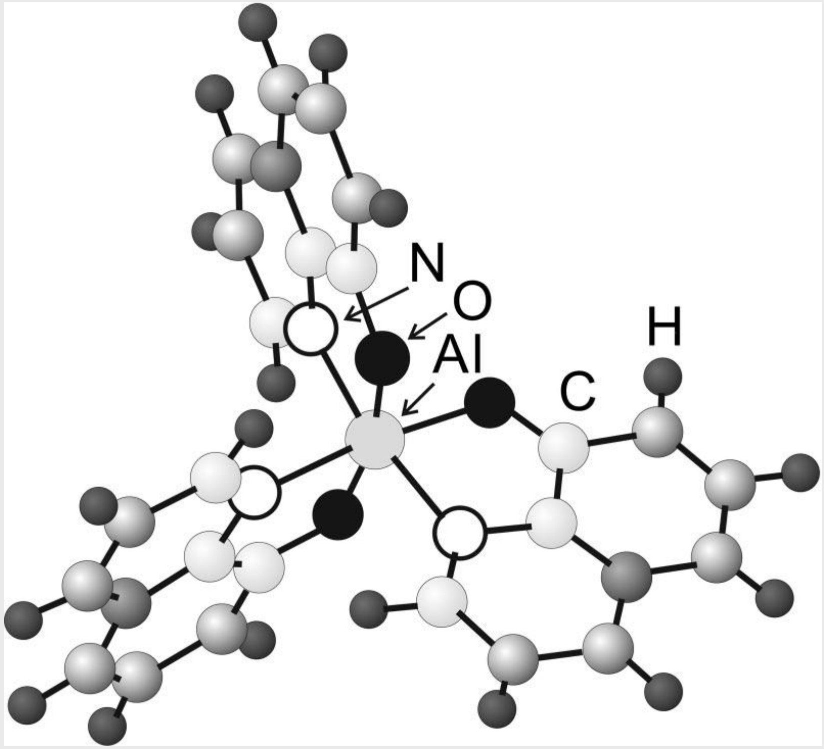

Material widely used in organic LEDs – UHV Molecular Beam Dep.

Forms ordered polycrystalline films at 120-150°C substrate T – rough surface

Forms amorphous films at room substrate T – smooth surface

Van der Waals interaction between molecules

Is the insulating/tunnel barrier needed?

Double role

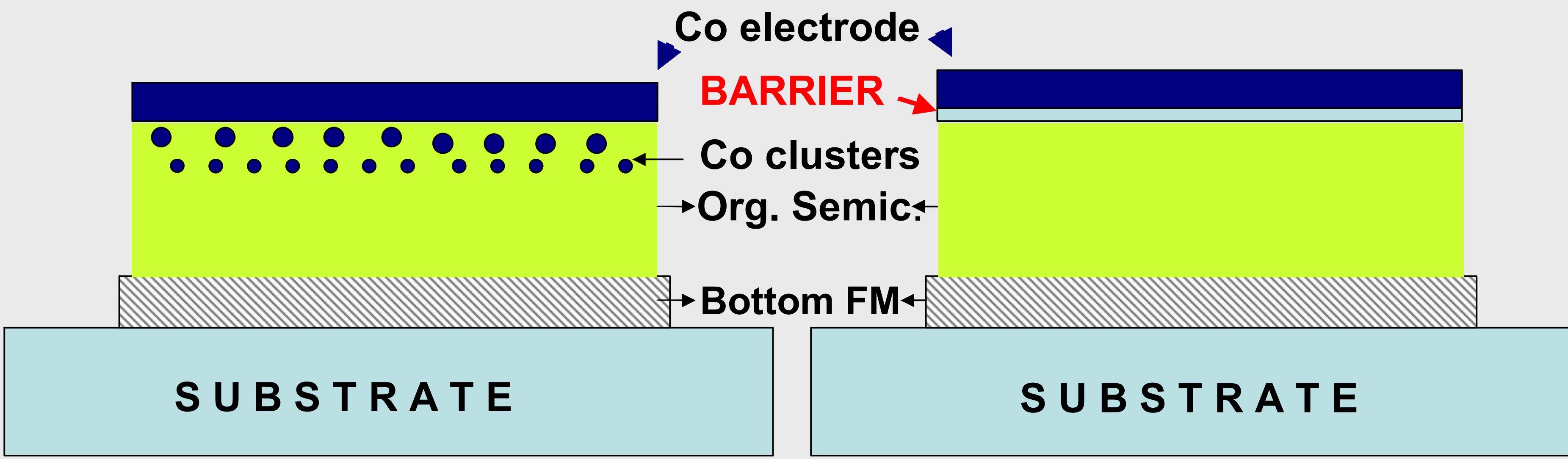

OUR OPINION!!!

??? The success of organic spintronics, at least for vertical devices, will be determined by the art of growing HIGH QUALITY TUNNEL BARRIERS on top of organic layers

??? Difficult or almost impossible to control and reproduce the quality of the top interface for direct deposition of metal on top of soft organic layer

PLANAR DEVICES

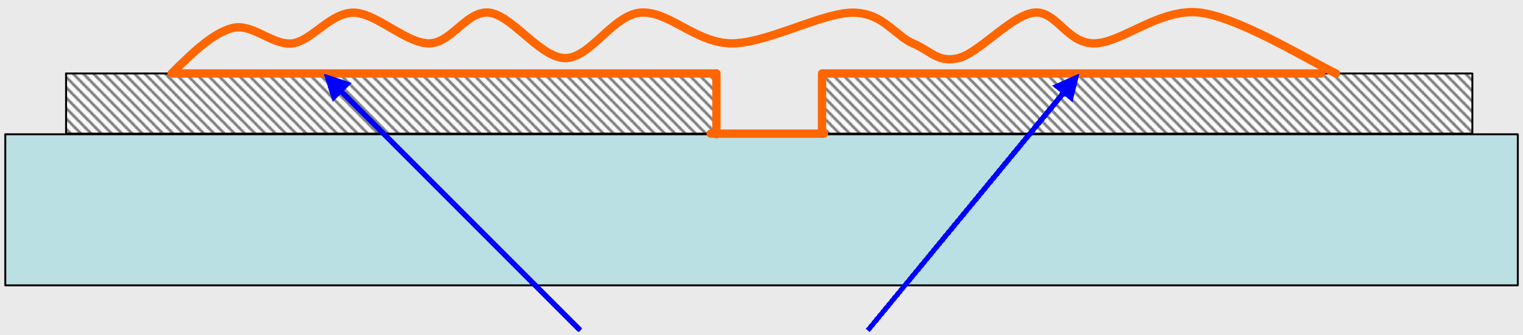

TWO “PERFECT” INTERFACES

VERTICAL DEVICES

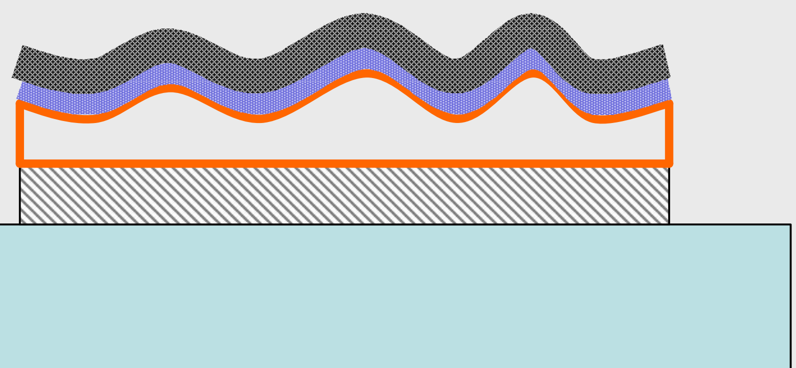

ONE “PERFECT” AND ONE “VERY BAD ”INTERFACE

Spintronics with carbon nanotubes

Exotic electrode materials. Highly spin polarized manganese oxides

Transformation of spin information into electrical signals

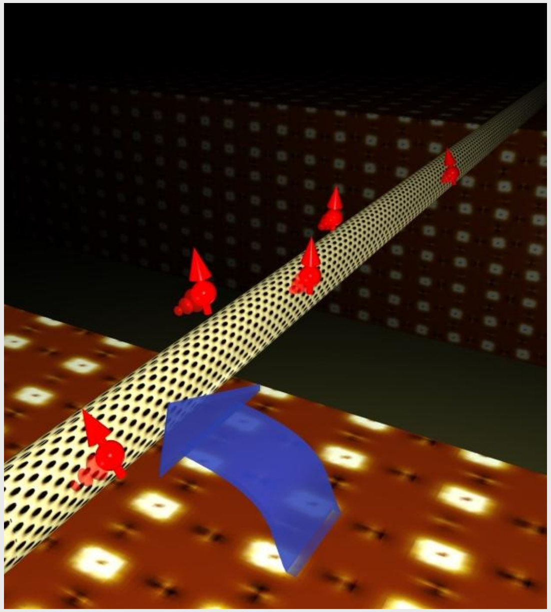

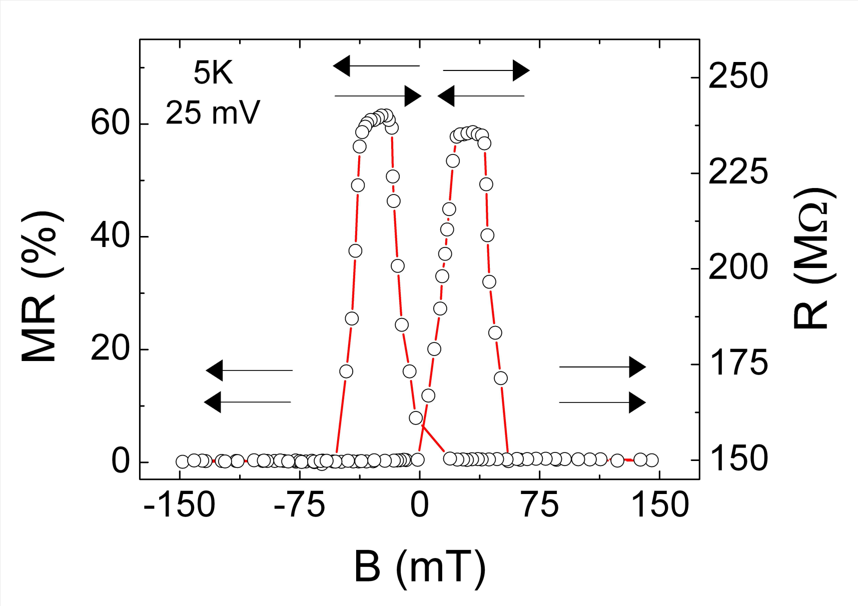

Long distance magnetoresistance as a proof of spin coherence

L.E. Hueso, A. Fert *et al.*, Nature 445, 410 (2007)

Will we, and how, combine various materials accepting spin injection?

Metals: Al, Au, …

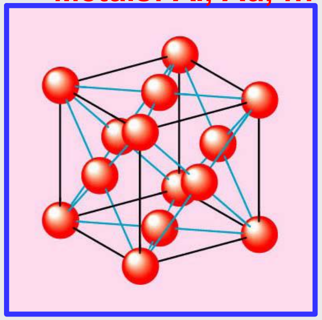

S/c: Si, GaAs, …

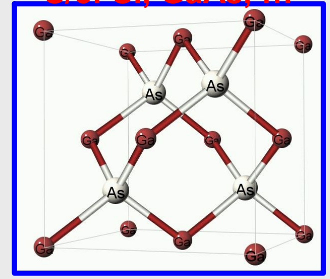

SP
injectors

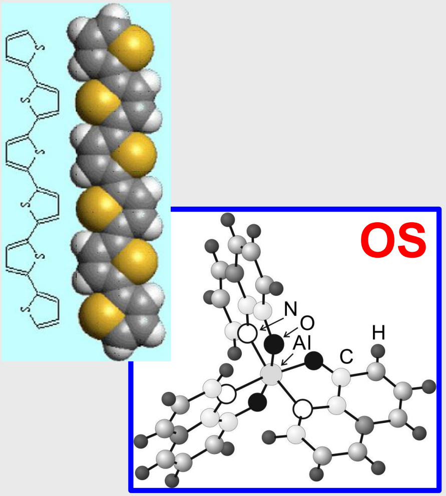

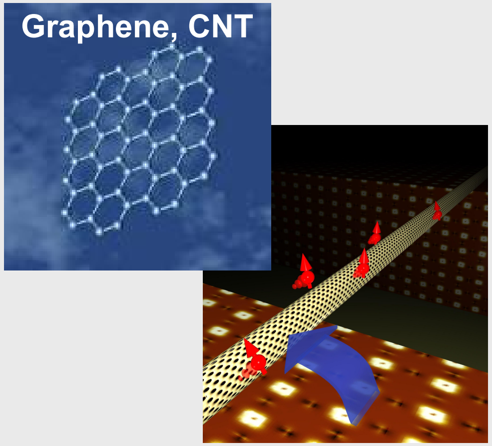

INTERFACES in Organic Spintronics – First EC project

Poster P22

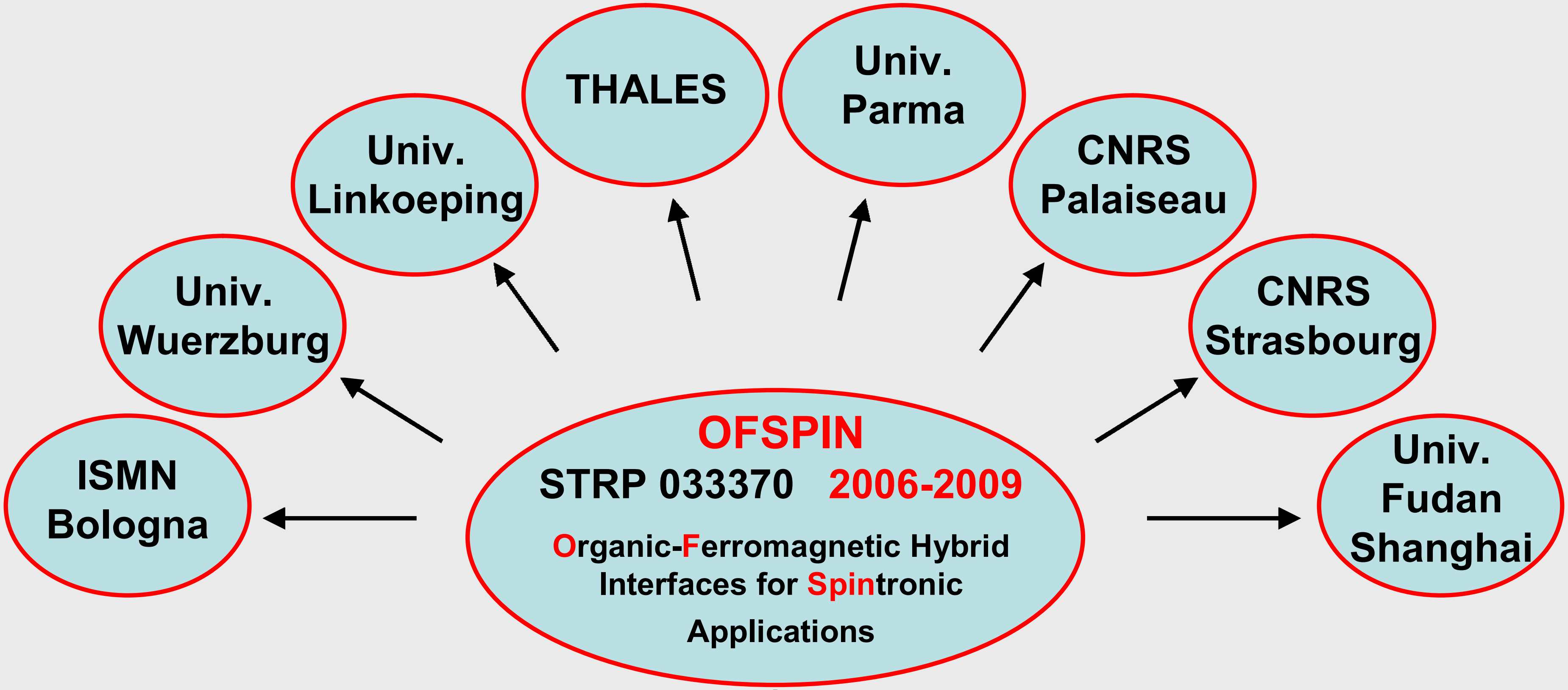

Knowledge of structural, electronic and magnetic properties of the new interfaces between organic and spin polarized magnetic materials

Improved charge and spin injection at such interfaces

and REPRODUCIBILITY!!!

SpinOS 2007

Workshop on Spintronic Effects in Organic Semiconductors
Bologna Italy 9 September - 11 September 2007

We are pleased to inform you of the Workshop on Spintronic Effects in Organic Semiconductors (**SpinOS 2007**) that will be held at the CNR Campus in **Bologna** from **9 to 11 September 2007**.

The main scope of the **SpinOS 2007** Workshop is to bring together for the first time the international community of scientists working in Organic Spintronics.

The organizers hope to start an intense dialog in the community and to lay the foundations for future regular meetings in the field of both basic research and applications of spin injection and transport in organic semiconductors.

The Conference will include presentations on recent experimental and theoretical results on various spintronic effects in organic semiconductors.

For more details, please visit our website at http://www.spinos.org

www.spinos.org

Conference chairman

C. Taliani. ISMN-CNR, Bologna

Scientific Advisory Committee (confirmed)

Martin Aeschlimann. Univ. Kaiserslautern
Sasha Alexandrov. Loughborough University
Arthur J. Epstein. Ohio State University
Albert Fert. Unité Mixte CNRS/THALES
Michel de Jong. Linkoping University
Bert Koopmans. Eindhoven UT
Jagadeesh S. Moodera. MIT
Laurens Molenkamp. University of Würzburg
Thom Palstra. University of Groningen
Stefano Sanvito. Trinity College Dublin
Darryl Smith. Los Alamos National Laboratory
Erio Tosatti. SISSA/ICTP
Evgeny Y. Tsymbal. University of Nebraska
Xin Sun. Fudan University
Z. Valy Vardeny. University of Utah
Markus Wohlgenannt. University of Iowa

Program committee

V. Alek Dediu. ISMN-CNR, Bologna
Georg Schmidt. University of Würzburg

We look forward to seeing you at the conference